

**Instituto Tecnológico de Costa Rica**  
**Área Académica Ingeniería Mecatrónica**



**Fraunhofer-Institut für Produktionstechnik und Automatisierung**  
**Bio-mechatronics Systems Department**



**“Bio-inspired Mechatronic Design for the Actuation of a  
Soft Orthosis for Rehabilitation and Assistance of Hands”**

**Project for obtaining the degree:**  
**Licentiate in Mechatronics Engineering**

**Jacob Hernández Sánchez**  
**Student ID: 201054413**

**Supervisors:**

**Dr.rer.nat. Oliver Schwarz MBA**

**Dipl. Ing. Conrad Hochberg.**

**Stuttgart, Germany**

**November, 2014**

**INSTITUTO TECNOLÓGICO DE COSTA RICA  
MECHATRONICS ENGINEERING PROGRAM  
GRADUATION PROJECT  
THESIS COMMITTEE MEMBERS**

Graduation Project argued before this committee as a requirement to qualify for the title of Mechatronics Engineer with Licentiate degree, issued by Instituto Tecnológico de Costa Rica.

Committee Members

  
\_\_\_\_\_  
Ing. Marvin Hernández Cisneros  
Reader Professor

  
\_\_\_\_\_  
Ing. Carlos Salazar García  
Reader Professor

**TEC** | Tecnológico de Costa Rica  
Ingeniería Mecatrónica

  
\_\_\_\_\_  
Ing. Arys Carrasquilla Batista  
Advisor Professor

The members of this committee attest that this graduate work has been approved and meets the standards set by Mechatronics Engineering Program

Cartago, November 14<sup>th</sup>, 2014

## Declaration of Authenticity

I, the undersigned Jacob Hernández Sánchez, declare that the project proposed was then raised entirely by my person using and applying literature, information and ideas of my own.

The sources consulted and quoted are properly attached within the references section.

So, I, in the most careful manner, take responsibility for the content and development of this project.

 Stuttgart 2011-11-18

**Jacob Hernández Sánchez**

**3 0463 0119**

## **Abstract**

It is described the design of a mechatronic system to actuate a hand soft orthotic device for rehabilitation and assistance purposes developed by the author of this thesis within the Bio Mechatronics Department of Fraunhofer Institute for Manufacturing Engineering and Automation (IPA) based in Stuttgart, Germany. The system mimics the musculoskeletal anatomy and kinesiology of the human body by resembling the bone-muscle-tendon configuration. A key feature of the orthosis is that allows the individual movement of the fingers. The actuation consists in the use of -high contraction- Festo Pneumatic Artificial Muscles (PAMs) within a 3D printed support structure which was designed using anthropometric data to aim to comfort and ergonomics. The PAMs are operated with piezoelectric -flow proportional- valves. The sensors mimic the human somatosensory system to control the motion and to confer a haptic nature to the human interface. The use of light indicators allows visual reinforcement during exercises. The final deliverable is a testing model that is going to be used for further experiments. Finally, this orthotic device is envisioned to become a mobile solution for self-aided rehabilitation.

**Keywords-** Bio-Inspired Mechatronics, Active Orthosis, Wearable Robotics, Pneumatic Artificial Muscles, Soft Robotics

## Dedication

*That every piece of my will, be given to God, my lord and guide, who knows me better than I do and uses me as his servant.*

*To María de los Ángeles Sánchez, Rodrigo Hernández and their beautiful daughter María de la Paz. All my hard work and dedication is attributed to your unconditional love and support.*

*To all my professors, guides and teachers since the elementary school, who always saw something in me that I'm just getting to realize...*

*And finally, to me, congratulations for your job Jacob.*

*“Feel free and have faith, let your efforts forge your future and your heart will never be defeated...”*

## **Acknowledgments**

To Dr.rer.nat Oliver Schwarz: I don't have enough words to say how much I appreciate what you have done for me, for giving me this opportunity, for having assigned me such an interesting project, and trust my desires to learn and grow as a professional. Perhaps a sincere and thoughtful thank you from the bottom of my heart would be the start.

Thanks to the Bio Mechatronics Department of Fraunhofer IPA, which I consider now a family; to all the support I received from you. You, such amazing professionals, who have given me a role model that I will pursue for the rest of my life.

Thanks to Luis Arturo Herrera, you are the living proof that there are Angels among us.

And finally, thanks to Arys Carrasquilla Batista, who trusted my capabilities to represent my country and my colleagues. Thank you for changing my present and future.

To all of you, blessings.

## GENERAL INDEX

Thesis Comitee Members .....	i
Declaration of Authenticity .....	ii
Abstract .....	iii
Dedication .....	iv
Acknowledgments .....	v
Chapter 1. Introduction .....	1
1.1. Context of the Project .....	1
1.2. Research Background .....	3
1.3. Problem Synthesis .....	5
1.4. Solution Approach .....	5
1.5. Objectives.....	7
1.5.1. General Objective .....	7
1.5.2. Specific Objectives .....	7
Chapter 2. Literature Review .....	8
2.1. Analysis of the Biomechanics and Functional Anatomy of the Hand. ....	8
2.1.1. Bones and Joints .....	8
2.1.2. Muscles .....	12
2.1.3. Tendons and Pulleys .....	15
2.2. State of the Art in Rehabilitation and Assistive Devices. ....	16
2.2.1. Rehabilitation Devices .....	18
2.2.2. Assistance Devices .....	19
2.3. Soft and Dexterous Structures. ....	23

2.4. Conclusions .....	25
Chapter 3. Requirements.....	27
3.1. Functional Requirements .....	27
3.2. Nonfunctional Requirements.....	29
Chapter 4. Design .....	30
4.1. Actuation .....	30
4.1.1. Mechanism .....	30
4.1.2. Active Actuators.....	36
4.1.3. Passive Actuators.....	45
4.1.4. Artificial Tendons.....	47
4.1.5. Actuators Layout .....	47
4.2. Pneumatics.....	48
4.2.1. Valve Selection.....	48
4.2.2. Overall Pneumatic Circuit Description.....	57
4.2.3. Air Consumption .....	57
4.3. Sensing .....	60
4.3.1. Physical Variables to Measure .....	60
4.3.2. Mimicking the Human Mechanoreceptors.....	63
4.3.3. Conclusion.....	67
4.4. Visual Feedback .....	67
4.5. Support Structure of the Actuators .....	68
4.5.1. Conception .....	68
4.5.2. Finite Element Analysis .....	77
4.6. Tendons Layout in the Glove .....	80

4.7. Electronics Design .....	84
4.7.1. Electrical Layout of the Glove .....	84
4.7.2. Controller .....	86
4.7.3. VEAA 3/3 Piezo Valves.....	87
4.7.4. Signal Conditioning .....	88
4.7.5. Power Supply .....	98
4.7.6. Overall Electronic Circuit .....	99
Chapter 5. Control Strategy.....	101
5.1. Inputs and Outputs .....	101
5.2. Concept 1. Feed Forward Control .....	102
5.3. Concept 2. Proportional (P) Feedback Control. ....	103
Chapter 6. Assembly.....	107
6.1. Methodology.....	107
6.2. Characterization.....	114
6.2.1. Actuation .....	114
6.2.2. Sensing Characterization.....	115
6.3. Findings.....	117
Chapter 7. Conclusions and Outlook.....	120
List of References .....	124
A. Appendixes .....	a
A.1. Glossary.....	a
A.2. Used Equations .....	b
B. Annexes .....	d
B.1. Electronic Control of the VEAA 3/3 Piezo-valves.....	d

B.2. Characterization of the Valve-Muscle System.....	f
B.3. Components Datasheets .....	g
B.3.1. Piezoelectric Flow Proportional Valve .....	g
B.3.2. Flex Sensor 5.9cm.....	i
B.3.3 Force Sensor .....	j
B.3.4 Lilypad Blue Pixel .....	l
B.3.5. Schematics of Arduino Micro.....	m
B.4. Project Datasheet .....	n

## FIGURES INDEX

Figure 1-1. Validated tendon driven mechanism. [8] .....	3
Figure 1-2. Documented Limitations of the Rudimentary Model. [8].....	4
Figure 1-3. Iterative development method in Concurrent Engineering. [9].....	5
Figure 1-4. Mechatronics design for the active wearable orthosis. ....	6
Figure 2-1. Bones and joints of human hand. [5] .....	9
Figure 2-2. Types of joints of the hand. [10].....	10
Figure 2-3. In (a) and (b) MCP joints motions are illustrated. Figures from (c)-(g) thumb motions are illustrated [13].....	11
Figure 2-4. Muscles for flexion of the fingers: From left to right: FDS, FPL, FDP. [15] .....	12
Figure 2-5. Muscles for extension of the fingers. From left to right and up to down: Extensor .Digiti Minimi, Extensor Indicis, Extensor Pollicis Longus, Extensor Digitorum, and Extensor Pollicis Brevis. [15].....	13
Figure 2-6. Schematic drawing of Extensor Apparatus. [13].....	14
Figure 2-7. Location of A1-A5 pulleys. [18] .....	15
Figure 2-8. Types of mechanisms for human finger's passive motion. [5] .....	16
Figure 2-9. Classification of hand exoskeletons according to various criteria. [5] .....	17
Figure 2-10. HandEXOS. [5].....	18
Figure 2-11. Device from Wege et al. [20] .....	19
Figure 2-12. Device from Hasegawa et al. [21] .....	20
Figure 2-13. Device from In et al. [22] .....	21

Figure 2-14. Device from Shields et al. [23] .....	22
Figure 2-15. Capabilities of hard and soft robots: (a) dexterity, (b) position sensing, (c) manipulation and (d) loading. [24] .....	24
Figure 4-1. Mechanical model of a human finger. [26] .....	30
Figure 4-2. Example of agonist-antagonist muscle principle. [32].....	33
Figure 4-3. Schematics of antagonist principle. [33].....	34
Figure 4-4. Selected tendons for the actuation. Highlighted are the tendons of the FDP and ED muscles. ....	34
Figure 4-5. Schematic representation of the shape memory effect and super elasticity. [35] .....	37
Figure 4-6. <i>Left:</i> Muscle configuration. <i>Right:</i> Tendon configuration. ....	38
Figure 4-7. Rudimentary pneumatic artificial muscles. [33].....	40
Figure 4-8. Second experiment for testing the functionality of PAM. [38] .....	41
Figure 4-9. Force (N) vs elongation (%) DSMP-5 MXAM 15°. Characteristic curve provided by Festo Co & AG. ....	43
Figure 4-10. Geometrical design of the DMSP-5-177N-RM-CM-CS-. [42].....	45
Figure 4-11. Geometry of the selected springs. D=6mm, L=60mm, d=0.7mm, F=50mm. [43]..	47
Figure 4-12. Sketch of first approach to the configuration of the actuation system with PAMs.	48
Figure 4-13. Two 2/2 valve configuration concept.....	49
Figure 4-14. 3/2 valve configuration of concept 2.....	51
Figure 4-15. Air Flow and the PWM Control Signal.....	51
Figure 4-16. Piezo-electric effect. [46] .....	53
Figure 4-17. Internal configuration of the 3/3 piezo valves. [46].....	54

Figure 4-18. Concept with 3/3 closed middle position piezoelectric valve. ....	55
Figure 4-19. VEAA 3/3 Closed middle position piezoelectric valve. [46] .....	56
Figure 4-20. Overall pneumatic design. ....	57
Figure 4-21. Contraction (%) and outer diameter (mm) vs pressure (bar). DSMP 5- MXAM 15°. ....	58
Figure 4-22. TSH sensor, Schdmith Control Instruments, Waldkraiburg, USA. ....	61
Figure 4-23. SD740 – Triaxial Gyroscope, Sensordynamics, 8403 Graz – Lebring, Austria.....	61
Figure 4-24. Mechanical compensation of the change of tension in the tendons.....	62
Figure 4-25. Resemblance Ruffini Endings → Flex Sensor.....	64
Figure 4-26. Resemblance Merkel Endings → Flex Sensor.....	66
Figure 4-27. Sketch of the layout of sensors and indicators on the orthosis. ....	67
Figure 4-28. Anthropometric data related to the design of the orthosis. The relevant numbers are explained in the text. [49].....	68
Figure 4-29. Rough sketches of concepts 1 and 2. ....	70
Figure 4-30. Rough sketch with some measurements for concept 3 of muscles’ support. ....	71
Figure 4-31. Part1. Final support structure for the actuators.....	72
Figure 4-32. Attachment of the springs and muscles.....	72
Figure 4-33. Inclusion of the fittings in the structure. ....	73
Figure 4-34. Concept 3. Muscles support structure. ....	73
Figure 4-35. Tendons slots. ....	74
Figure 4-36. Tendons attachment to the muscle.....	75
Figure 4-37. Exploded view of the actuators support structure.....	76

Figure 4-38. Mesh of the support structure of the actuators. ....	77
Figure 4-39. Von Mises stress study 1. ....	78
Figure 4-40. Factor of Safety study 1. ....	78
Figure 4-41. Von Mises stress study 2. ....	79
Figure 4-42. Factor of Safety study 2. ....	80
Figure 4-43. Dorsal side. Tendon-Pulleys layout of the glove. ....	81
Figure 4-44. Palmar side. Tendon-Pulleys layout of the glove. ....	82
Figure 4-45. “Tendon - Layer” of the glove. ....	83
Figure 4-46. Mechanical system of the project. ....	84
Figure 4-47. Electric layout of the glove. The connections are explained in Table 4-6. ....	85
Figure 4-48. Dimensions and Pin out of the Arduino Micro. [51] ....	87
Figure 4-49. Behavior of the Valve according to the Control signal and the Power conversion. ....	88
Figure 4-50. Basic configuration of the Flex Sensor measurement. ....	89
Figure 4-51. Span Width (Volts) vs Pull up Resistance (k $\Omega$ ) ....	91
Figure 4-52. Spans mismatch and level shifting correction. ....	92
Figure 4-53. Spans mismatch and required amplification. ....	93
Figure 4-54. Signal conditioning of the Flex Resistive Sensor ....	94
Figure 4-55. Simulation of the signal conditioning of the Flex Resistive Sensor ....	96
Figure 4-56. Application Information of the Force Resistive Sensor. [52] ....	97
Figure 4-57. Implemented configuration for conditioning of the Force Sensing Resistor. ....	98
Figure 4-58. Overall Electronic Design - Part 1. ....	99

Figure 4-59. Overall Electronic Design - Part 2. Signal conditioning per each pair of sensors (Flex-Force). .....	100
Figure 5-1. Inputs and Outputs of the System. ....	101
Figure 5-2. Feed-forward Controller.....	102
Figure 5-3. Feed-back P Controller .....	103
Figure 5-4. Flow Diagram of the Movement of One Finger in Rehabilitation .....	105
Figure 5-5. Control System Architecture .....	106
Figure 6-1. First Stage in the Assembly Process .....	107
Figure 6-2. Assembly of the Tendon Layout of the Glove .....	108
Figure 6-3. Assembly of the Electronic Layout of the Glove .....	109
Figure 6-4. Electronic Layer of the Glove .....	109
Figure 6-5. Mechanical Support of the Actuators .....	110
Figure 6-6. Glove-Support Interface.....	111
Figure 6-7. Breadboard Connections for the Testing with One Valve. ....	112
Figure 6-8. Assembly of the Testing Model.....	113
Figure 6-9. Test of inflation of the Muscles. ....	113
Figure 6-10. Final appearance of the Prototype.....	114
Figure 6-11. Characterization of the flex sensor .....	115
Figure 6-12. Characterization of the force sensor .....	116
Figure 6-13. High stability of the structure. ....	117
Figure 6-14. Bowstringing Effect in the orthosis. Right Image [18].....	118
Figure 6-15. Solution to Bowstringing Effect. Right Image [18].....	119

Figure 7-1. Conception, Design and Prototype of Bio-inspired Active Soft Orthotic Device. (a) Hand Muscle Anatomy. (b) Design Concept. (c) Actual Prototype. ....122

Figure B-1. VEAA 5 Way Control Circuit. Developed by Dipl. Ing. Hannes Wirtl. Festo Piezo Valves Division .....e

Figure B-2. Output Pressure ( $P_o$ ) and Muscle Stroke ( $S$ ) for Different Input Pressures ( $P_i$ ). Experiment conducted in Festo Ag & Co. .... f

## TABLES INDEX

Table 3-1. Experimental forces per each finger.....	28
Table 3-2. Experimental excursions per each finger [25] .....	28
Table 4-1. Ranges of Motion per each joint. [30].....	32
Table 4-2. List of suitable springs for the application. ....	46
Table 4-3. Dynamic behavior when using a PWM controlled 3/2 NC valve.....	52
Table 4-4. Description of the mechanoreceptors of the human somatosensory system. [47].....	63
Table 4-5. Relevant anthropometric data for the mechanical design of the actuation system. [49] .....	69
Table 4-6. List of electrical connections of the visual indicators and sensors in the glove .....	85
Table 4-7. List of relevant features of the Arduino Micro board. [51] .....	86

## **Chapter 1. Introduction**

This chapter aims to give an overview of the context of the project, the background of the research, the problem and how is it going to be addressed and finally concludes with the goal and objectives of the inquiry.

### **1.1. Context of the Project**

The hand is one of the most important parts of the human body. It is needed for almost all daily operations. It allows people modify their space while they are interacting with surrounding objects, i.e. grasping by applying certain force, execution of complex activities such as playing an instrument and most importantly touching and feeling.

Unfortunately, many diseases that affect the musculoskeletal system, such as cerebral palsy, amyotrophic lateral sclerosis, multiple sclerosis or strokes [1], have a very high influence in the partial or total loss of hands functions. The impact increases when both hands are affected. This translates into a strong dependency on others and in a highlighted necessity to take aided rehabilitation.

On a regular basis, the rehabilitation is lengthy, painful, difficult and not always marked by success. This is not uncommon given the lack of stamina and decreasing motivation of people during the whole process which certainly takes much time. This behavior is accented when the patient get used to need just their other healthy limb. [2]

It is shown that recovery from a brain injury is greatly influenced by the sensorimotor experience after the injury [3]. It is important for the patient to take intensive and continuous therapeutic exercise for successful rehabilitation, because the highly repetitive training help the brain to rebuild the lost connections. [3] , [4].

Nevertheless, a physical therapist has always been necessary for the execution of the relevant exercises with the patient, so that his disabled hand moves passively following up a certain strategy. Due to the increasing number of patients, there is not sufficient amount of physiotherapists for having an individual patient care. This fact turns out in long delays between sessions and ends up in decreasing the rehabilitation results.

The challenge in current researches lies in the necessary development of techniques and technologies for rehabilitation that result in a lesser dependence on a physiotherapist and more autonomy of the patient. Herein is the importance of designing individualized devices for the self-aided rehabilitation of patients. It has been shown that repetitive movement with the use of robotics might be a more effective treatment, especially for patients who have difficulty in performing unassisted repetitive motion [5].

Dr. Surjo Soekadar [2], a specialist from the Applied Neurotechnology Lab of University Hospital of Tübingen, Germany, highlights the necessity of a technology solution that leads the patients to restore motivation and trust in rehabilitation.

Correspondingly, this inquiry is aimed to the development of an orthosis whose main function is to rehabilitate the motion of the hands. An Orthosis is an external medical device that assists the function of a body part [6].

The project of this thesis took place in the Bio-mechatronics department of Fraunhofer-Institut für Produktionstechnik und Automatisierung (IPA), located in Stuttgart, Germany. The field of bio mechatronics includes all aspects of motion and bio signals detection, adaptive fusion algorithms, medical mechatronics, biomechanics and bionics, actuators, biomechanical simulations, and human-machine interfaces. [7]

## 1.2. Research Background

In an attempt to solve the problem stated before, a prior investigation was conducted by Eric Bojan. In his thesis<sup>1</sup>, Bojan validated a mechanism for the passive movement of the fingers using five pneumatic artificial muscles and five springs as actuators for respectively the bending and extension of each finger with the use of artificial tendons attached to a glove in a rudimentary model as it is illustrated in Figure 1-1

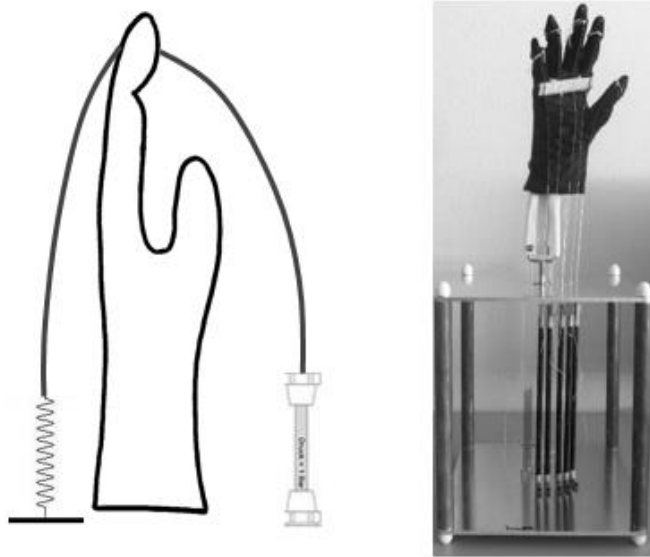


**Figure 1-1.** Validated tendon driven mechanism. [8]

The demonstrator consisted of a metal base with a model hand (resembling a paralyzed human hand) and a glove with tendons sewn on it.

---

<sup>1</sup> [25]

In his thesis, Bojan documented a limitation of the rudimentary model. When the wrist is moved the tension over the tendons is lost so as the control over the bending of the finger. As it can be appreciated in Figure 1-2, the glove has a metal part attempting to avoid the slack effect of the tendons.

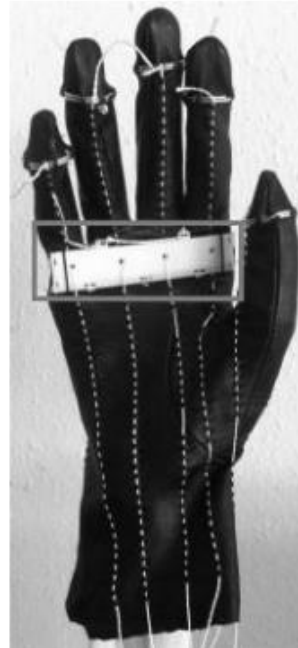


**Figure 1-2.** Documented Limitations of the Rudimentary Model. [8]

However, this solution compromises the comfort of wearing and therefore a new answer for that identified problem is required.

On the other hand, the FESTO Pneumatic Artificial Muscles used for the demonstrator, were too large for being ready to fit in a human forearm. That's why a proper actuation method had to be selected

### 1.3. Problem Synthesis

It is required to develop a bio inspired mechatronic system for the actuation and control of a glove that is aimed to be used as a soft wearable orthosis.

### 1.4. Solution Approach

The solution is intended to be found with the use of concurrent design methodology: Figure 1-3 illustrates the method.

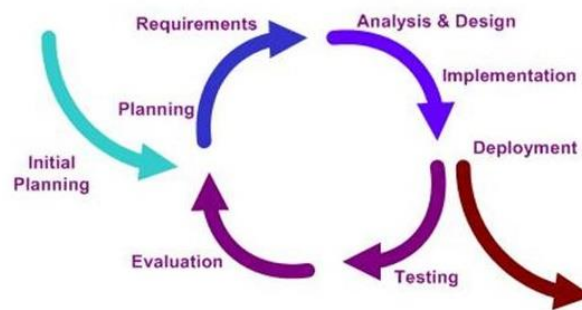


**Figure 1-3.** Iterative development method in Concurrent Engineering. [9]

It is important to clarify that since this is an iterative solution, the result can always be subject to modifications and upgrades until the requirements and specifications are fulfilled.

As can be appreciated from the research background, the preconceived model is purely mechanical. Thus, first the limitations are going to be addressed from the mechanical point of view and gradually integrate other fields of knowledge until the solutions are the most practical and innovative possible.

For the development of a cutting edge technological solution, the merging of knowledge from mechanical engineering, electrical engineering and control engineering is inherent in a multidisciplinary mechatronic environment.

Some identified systems to be designed are the following:

*Mechanical System*

It comprises anything about the physical part. The design must contemplate every aspect of the physics principles involved. Tools such as Computer Aided Design and Finite Element Analysis and Simulation are going to be used.

*Electrical System:*

It is foreseen that the system will require certain electronic aspects related to sensors/actuators, electrical control, signal conditioning and signal processing.

*Actuation System:*

The rudimentary model uses pneumatics. Within the analysis of the validation of the pneumatic system, other types of actuation must be studied (e.g. hydraulics, electronics, etc.)

*Software and Control System:*

There must be a system for the control of the device

All these subsystems would converge in a synergic mechatronic application as it can be seen in Figure 1-4.

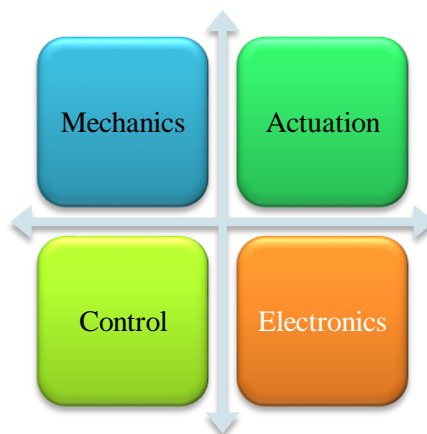


**Figure 1-4.** Mechatronics design for the active wearable orthosis.

## **1.5. Objectives**

### **1.5.1. General Objective**

Design a bio-inspired mechatronic system for the actuation and control of a tendon-driven glove that is aimed to become a hand orthosis for rehabilitation and assistive purposes.

### **1.5.2. Specific Objectives**

- a) Perform literature review and analysis regarding the biomechanics of the hand as well as the state of the art in rehabilitation and assistive devices.
- b) Select an actuation system for the orthosis based on bio-inspiration of human physiology.
- c) Design a housing for mechanical support of the actuators.
- d) Design the electronic system for the control and powering of the actuators.
- e) Assemble the subsystems in a testing model.
- f) Formulate a control strategy for the orthosis.

## Chapter 2. Literature Review

This chapter aims to serve as a starting point for the conception of the solution. The fundamentals of hand biomechanics are introduced with the objective of have a better understanding of hand motion. Also, the state of the art in rehabilitation and assistive devices as well as an introduction to soft structures are presented.

### 2.1. Analysis of the Biomechanics and Functional Anatomy of the Hand.

Because a hand orthosis is closely coupled with a hand when it is worn, it is necessary to explore a detailed explanation of the hand morphology. This is important to conceive and construct a mechanically safe and effective structure.

#### 2.1.1. Bones and Joints

The bones of the hand are grouped into the *carpus*<sup>2</sup>, comprising the eight bones which make up the wrist and root of the hands, and the digits, each of which is composed of its metacarpal and phalangeal segments [5]. The five digits are named as follows from the *radial* to the *ulnar* side: thumb, index finger, middle finger, ring finger, and little finger.

As it is illustrated in Figure 2-1 each finger has one metacarpal and three phalanges of different sizes, except for the thumb, which has just two phalanges.

There are 19 bones and 14 joints distal to the *carpals*. The carpals are arranged in two rows, and between the two of them is the intercarpal articulation.

---

<sup>2</sup> For medical terminology, consult the *Glossary*

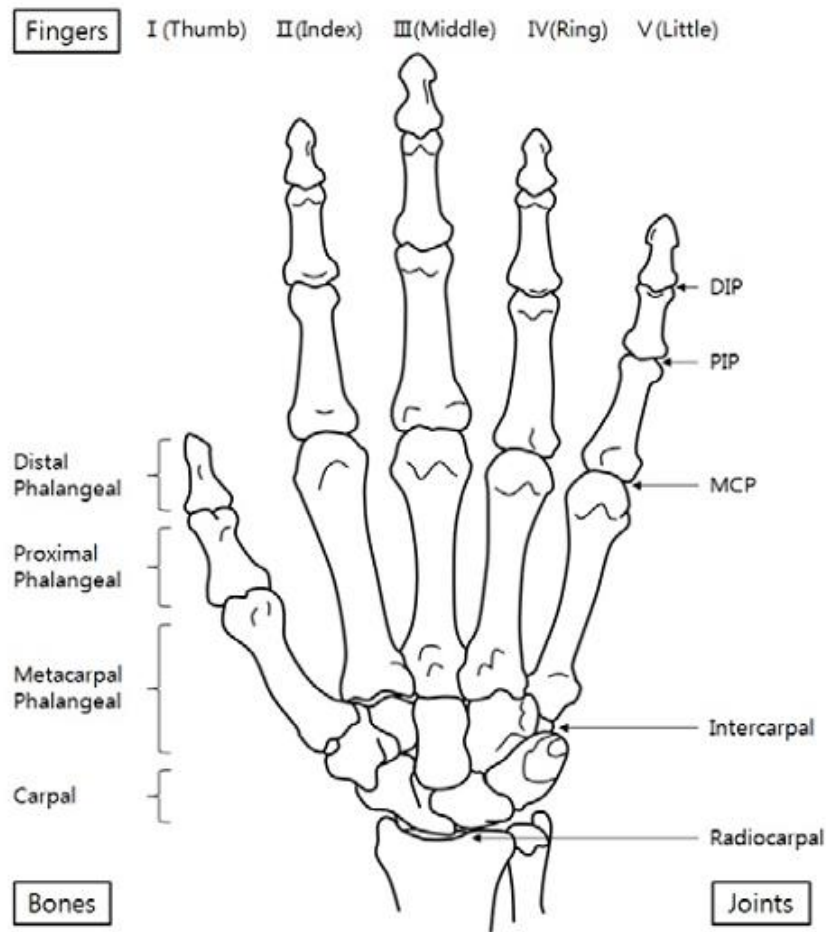


**Figure 2-1.** Bones and joints of human hand. [5]

### *Carpometacarpal (CMC) joint*

Each finger articulates proximally with a particular carpal at the carpometacarpal (CMC) joint [5]. The CMC joints of the fingers are classified as plane joints with one degree of freedom while the joint of the thumb is a seller or saddle joint, as it is illustrated in Figure 2-2 exhibiting two degrees of freedom: flexion and extension, and abduction and adduction<sup>3</sup>.

<sup>3</sup>For a better understanding of the type of movement see Figure 2-3

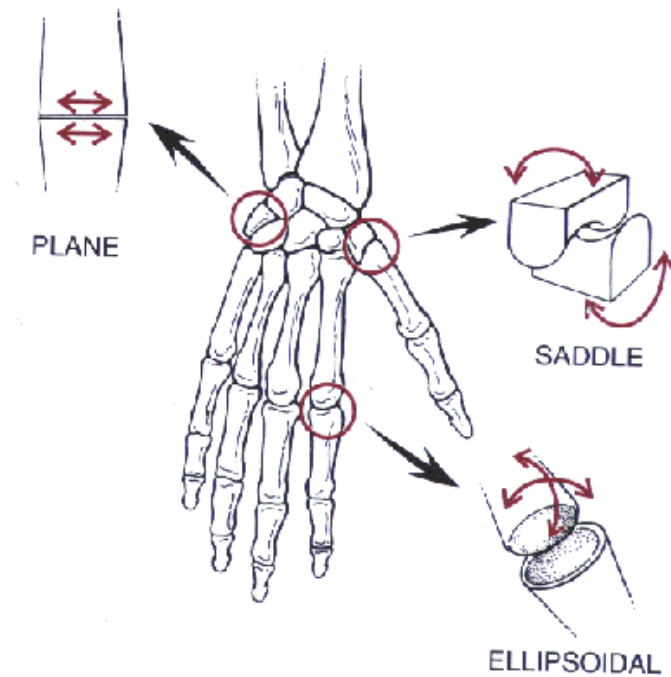


**Figure 2-2.** Types of joints of the hand. [10]

### *Metacarpophalangeal (MCP) joint*

The next joint of each finger links the metacarpal to the proximal phalanx at the metacarpophalangeal (MCP) joint. MCP joints are classified as ellipsoidal or condylar joints, illustrated in Figure 2-2 with two degrees of freedom, which again permit flexion, extension, abduction, and adduction movements. The types of movements are illustrated in Figure 2-3.

### *Interphalangeal (IP) joints*

The proximal interphalangeal (PIP) and distal interphalangeal (DIP) joints are found between the phalanges of the fingers; the thumb has only one interphalangeal (IP) joint [5]. They are both ellipsoidal joints but with one degree of freedom [11]

Although the IP joints are frequently modeled and assumed as having single axis of rotation for simplicity, in fact they don't remain constant during flexion and extension. [12].

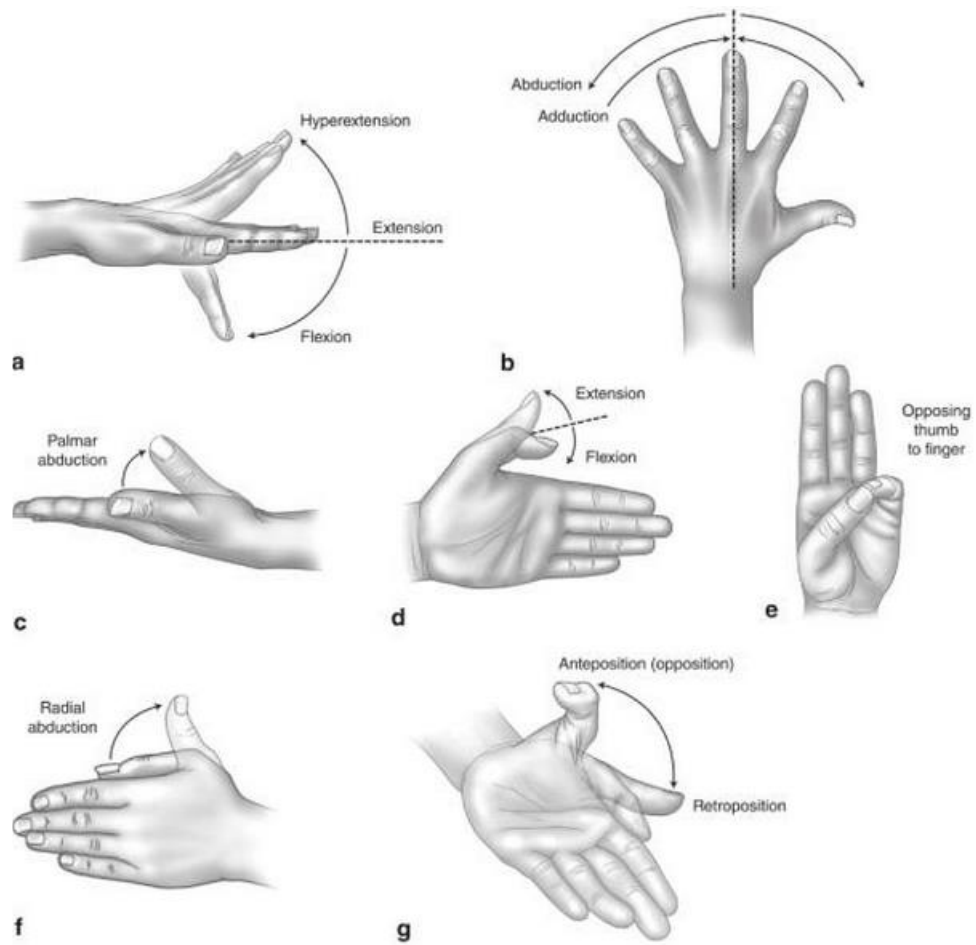


**Figure 2-3.** In (a) and (b) MCP joints motions are illustrated. Figures from (c)-(g) thumb motions are illustrated [13]

The PIP joint differs from the MCP in that the ligaments effectively restrict hyperextension. No ulnar or radial deviation is passively possible. [13]

*IP and MCP Interdependency*

In the extended finger it is impossible to flex the DIP without also flexing the PIP joint unless the PIP joint is blocked in extension. It has been calculated that on average, every degree of PIP joint flexion results in 0.67 degree of DIP joint flexion. [13]

### 2.1.2. Muscles

The hand movements involve two types of musculature: intrinsic and extrinsic. The extrinsic muscles originate from the arm and forearm, and they are responsible for flexion and extension of the digits. The intrinsic muscles are located entirely within the hand, and they permit the independent action of each digit (abduction and adduction) [14]. In this document, the interest would be specially focused in the muscles responsible for the flexion/extension.

There are nine extrinsic muscles. Three of them contribute with the flexion: the Flexor Digitorum Superficialis (connected to proximal phalanges), the Flexor Digitorum Profundus (connected to distal phalanges), and the Flexor Pollicis Longus (connected to the thumb) [5]. The Figure 2-4 illustrates the flexor musculature.

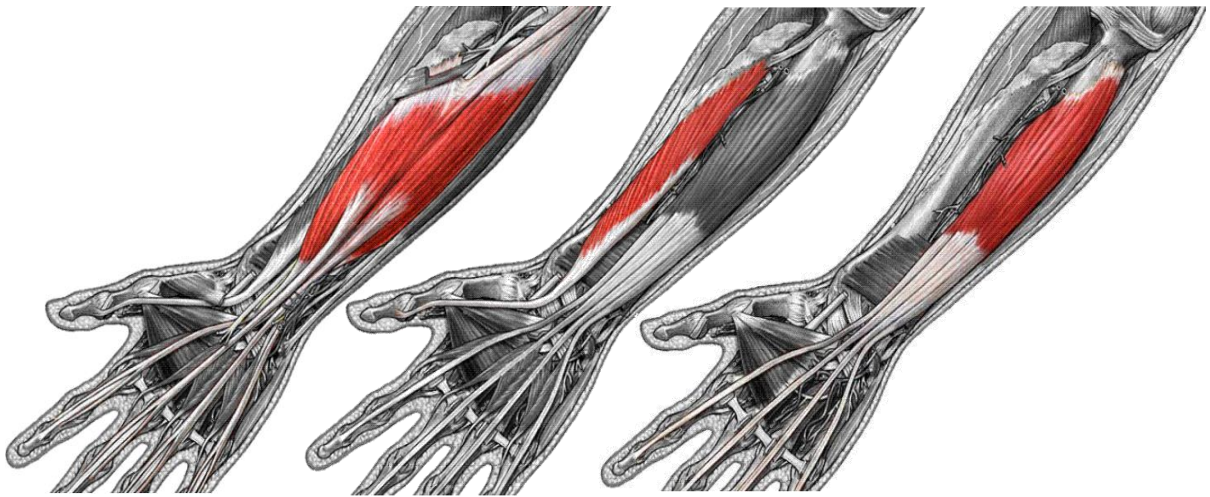


**Figure 2-4.** Muscles for flexion of the fingers: From left to right: FDS, FPL, FDP. [15]

Five extrinsic muscles contribute to the extension of the fingers. There are also extra muscles for the extension of the index and the little finger. Figure 2-5 illustrates the extensor muscles.

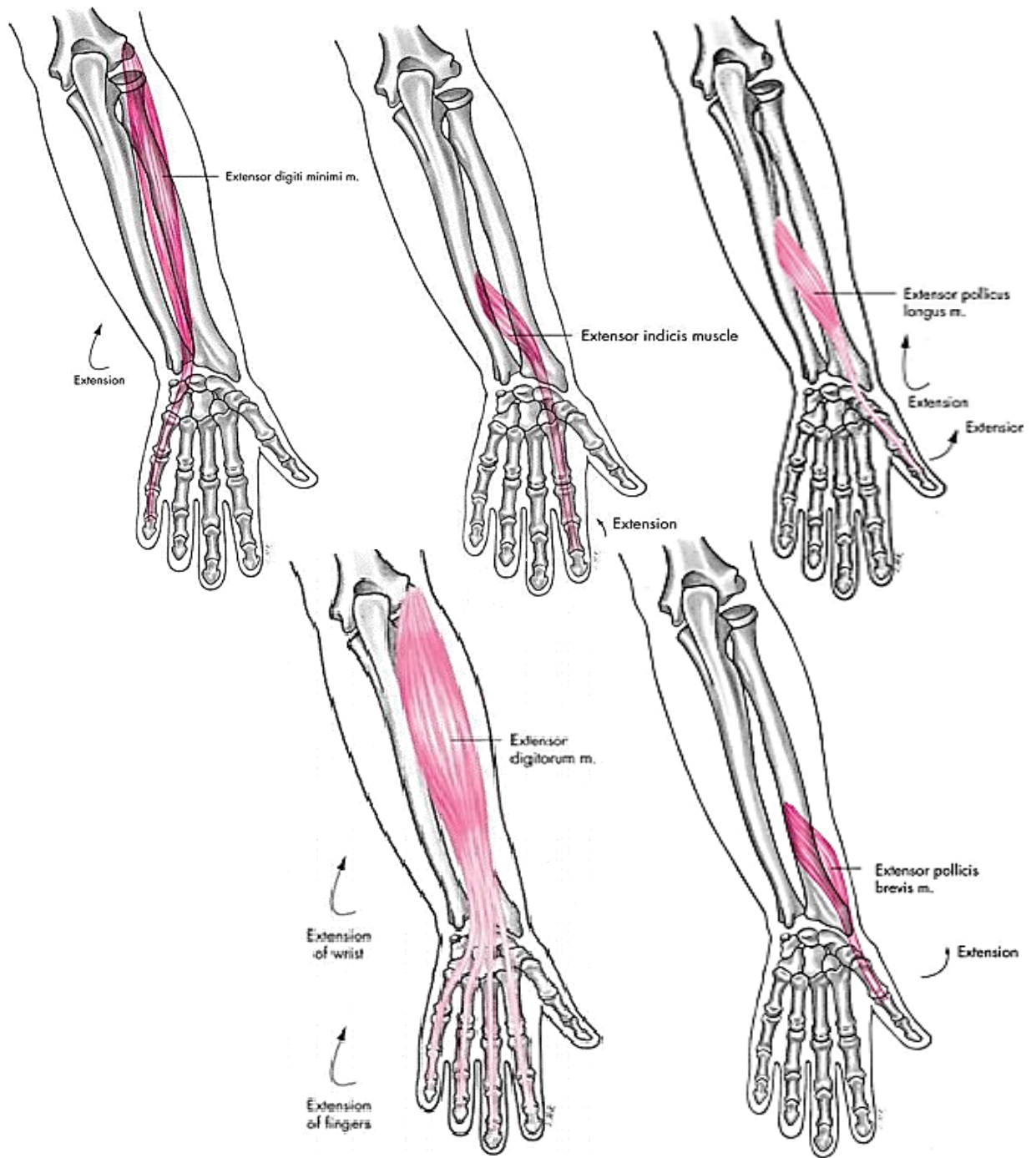


**Figure 2-5.** Muscles for extension of the fingers. From left to right and up to down: Extensor .Digiti Minimi, Extensor Indicis, Extensor Pollicis Longus, Extensor Digitorum, and Extensor Pollicis Brevis. [15]

Extensor Digiti Minimi is specific for the extension of the little finger, the Extensor Indicis is specific for the index extension, the Extensor Pollicis Longus and Brevis are in charge of the extension of the thumb. Finally, the Extensor Digitorum is in charge of the overall extension of the 5 fingers.

The dorsal interossei (DI) and palmar interossei (PI) are groups of intrinsic muscles arising between the metacarpals and attached to the base of the proximal phalanges or to the extensor apparatus.

The interossei flex the MCP joint and extend the PIP and DIP joints, as it can be appreciated in Figure 2-6. They are also effective abductors and adductors, and produce rotation of the MCP joint. [14]. Because of this interaction between the extrinsic and intrinsic musculature, the actions of the PIP and DIP joints are functionally coupled.

The lumbrical muscles have several unique characteristics. They connect two antagonistic muscles. Proximally, they are connected to the Flexor Digitorum Profundus and distally they are inserted into the lateral band of the extensor tendon. [13]

The lumbrical muscles permits stability on the MCP joints while the PIP and the DIP joints are extending.

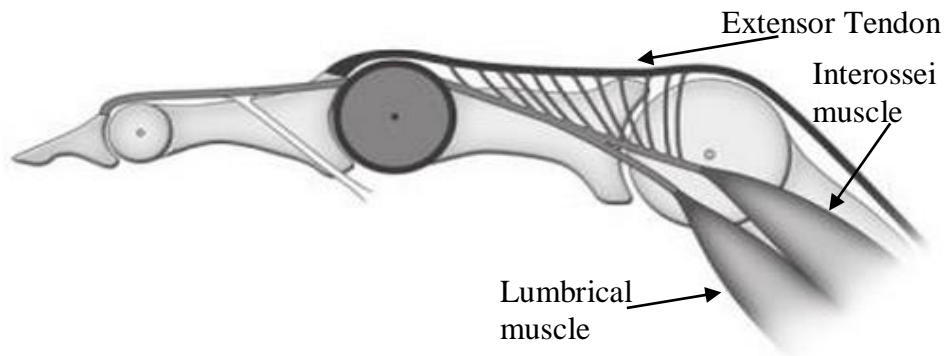


**Figure 2-6.** Schematic drawing of Extensor Apparatus. [13]

### 2.1.3. Tendons and Pulleys

#### *Tendons*

Tendons are the type of tissue that connects muscle to bone. As a digit moves, each tendon slides a certain distance. This displacement takes place simultaneously in the flexor and extensor tendons. [16]

The relationships between the linear displacements of the finger tendons and the angular displacement of the different joints have been studied and they seem to be both linear and nonlinear. [5]

The excursions are larger in the more proximal joints. Also, the excursion of the flexor tendon is larger than the extensor tendon, and the excursion of the extrinsic muscle tendons is larger than the intrinsic muscle tendons [17].

#### *Pulleys*

Flexor tendon is covered with four annular and three cruciate pulleys. They give protection to the tendons and also provide gliding surface and an efficient restraint system that holds the tendons close to the bones and joints.

There are five pulleys in the fingers, called annular pulleys, and they are named A1 through A5. As it is illustrated in Figure 2-7 the A1, A3, and A5 pulleys are smaller and considered minor pulleys [18]. The A2 and A4 pulleys are larger and are called the major pulleys. The A1, A3, and A5 pulleys are located at the MCP, PIP and DIP joints respectively. The A2 and A4 pulleys are located in the middle of the proximal and middle phalanx respectively.

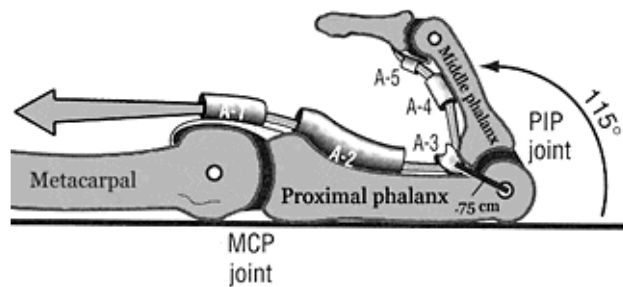


**Figure 2-7.** Location of A1-A5 pulleys. [18]

## 2.2. State of the Art in Rehabilitation and Assistive Devices.

The problem that is trying to be solved has been treated by other researchers and scientists around the world. Because the human hand is a very complex part of the body, with inherent motor and sensory requirements, the technologies such as hand exoskeletons or hand orthoses, for rehabilitation and assistive engineering have not progressed as rapidly as the devices for lower and upper limbs

Most assistive or rehab devices perform their motions by enabling one degree of freedom per each joint, which in most cases allow extension and flexion of them.

As an essential requirement for the hand assistive and rehabilitation structures, the rotation of each part must be always aligned with rotation centers of the joints of the fingers. Figure 2-8 is a representation of some methods that satisfied the requirement of matching the center of rotation. This is important because if the exo-device performs any motion out of this axis, it would cause unnecessary shear stress on the patient's hand articulations.

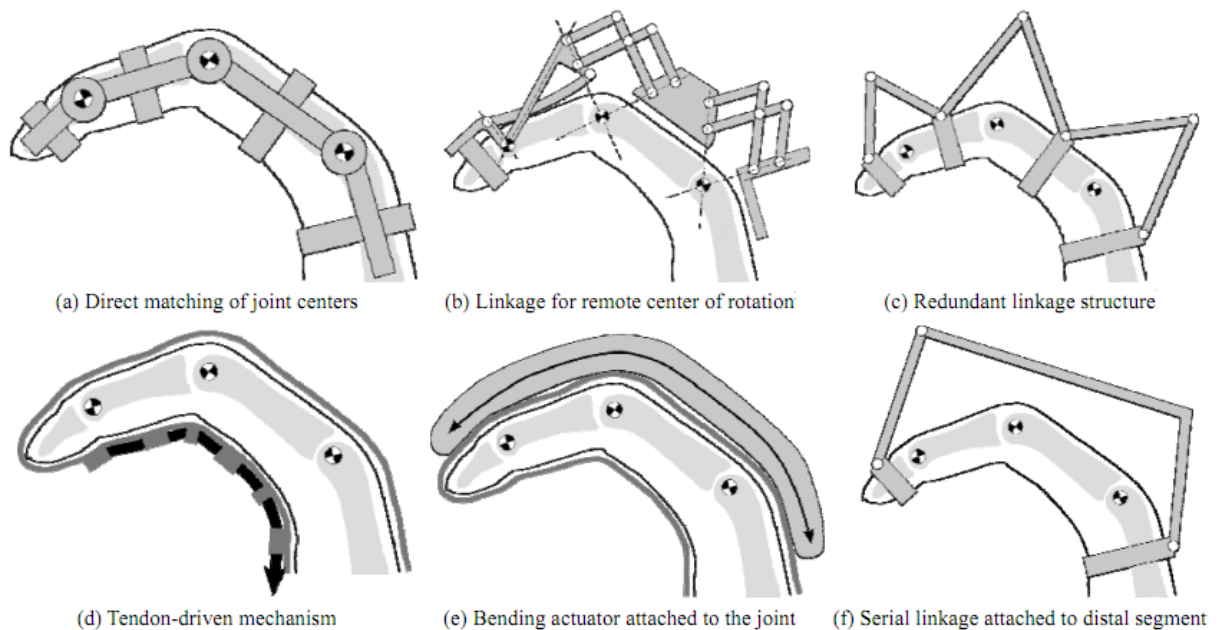


**Figure 2-8.** Types of mechanisms for human finger's passive motion. [5]

According to the picture showed above, the type of mechanism that fulfills the profile of bio-inspiration is shown in Figure 2-8(d), which will be referred from now on as “tendon-driven mechanism”

Most devices for rehabilitation and assistance have been developed as exoskeletons, and which according to Pilwon et al [5] can be addressed according to its type of actuation, power transmission, sensing method and purpose. This classification is illustrated in Figure 2-9.

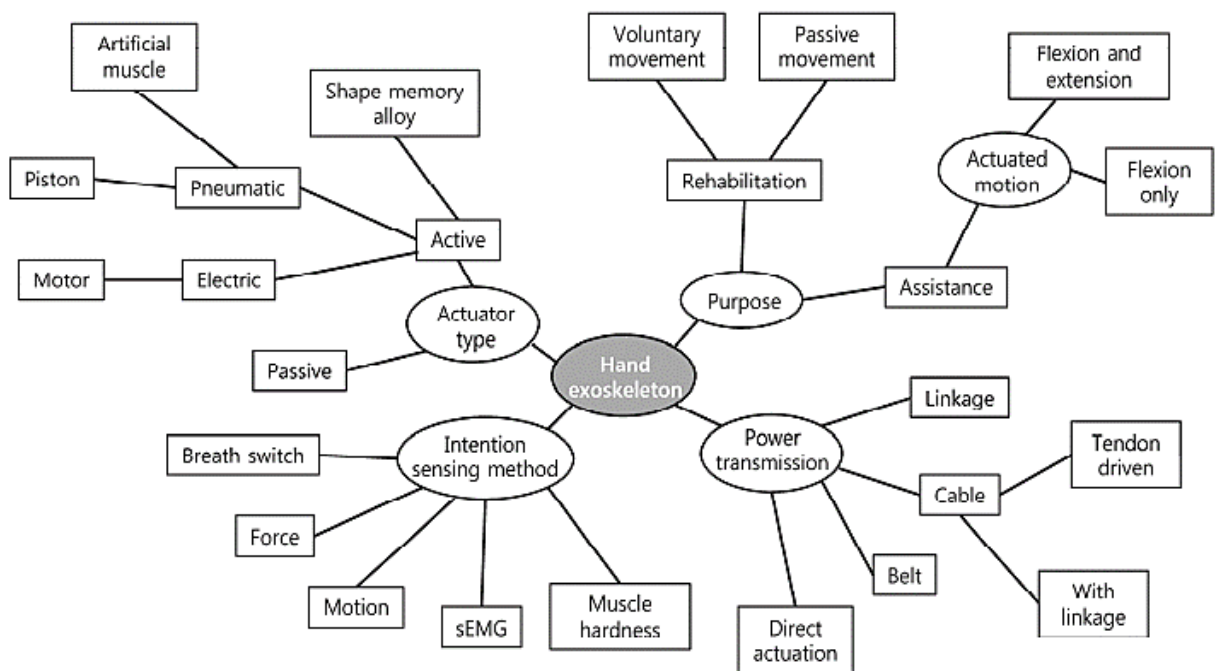


**Figure 2-9.** Classification of hand exoskeletons according to various criteria. [5]

### 2.2.1. Rehabilitation Devices

Some representative devices that have been tailored for rehabilitation are presented.

#### HandEXOS

This is a hand exoskeleton developed by Chiri et al [19] with one independent module per each finger. It is composed of 3 links for the phalanges, where the center of rotation matches with the corresponding joint of the digit. The flexion and extension of the MCP joint is driven by a slider-crank mechanism, while Interphalangeal are driven by Bowden cable transmissions.

It can be said that the joints of the fingers are under actuated, because in their movement, they use a single actuation unit. The system is provided with interaction force sensing.

The linear slider for MCP rotation is equipped with strain gauges to measure the force transmitted by the driving cable. Figure 2-10 illustrates HandEXOS.

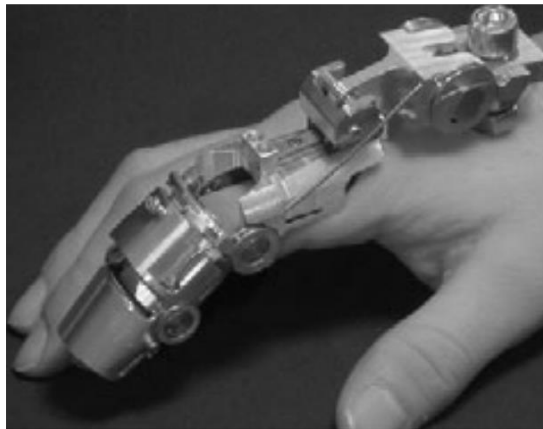


**Figure 2-10.** HandEXOS. [5]

Wege et al.:

The hand exoskeleton developed by Wege et al. [20], and illustrated in Figure 2-11, uses a Bowden cable for each joint with an electric motor. It uses two pull cables for each joint for supporting the bidirectional movement. Only one motor is used for each joint. The motion is applied through a leverage construction on each finger attachment. [5]

This device is controlled by EMG signals. Each finger rests in its relaxed position when no muscle activation is measured. Depending on the muscle activation, a linear force is calculated and the fingers are moved as if acting against a constant friction. The movements of the MCP, PIP, and DIP joints are performed in a coupled motion. [5]

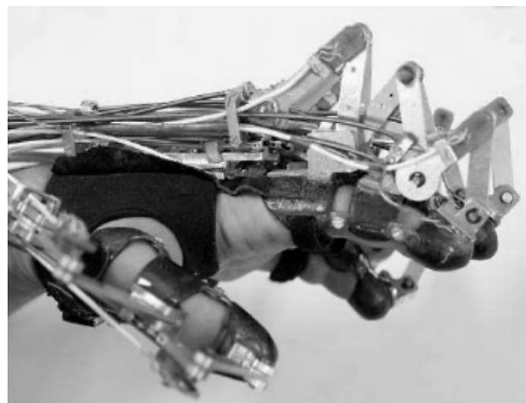


**Figure 2-11.** Device from Wege et al. [20]

### **2.2.2. Assistance Devices**

There have also been developments for the assistance of hands motion, which are particularly useful in cases of weakness or fatigue. Some of them are presented as follow:

*Hasegawa et al.*

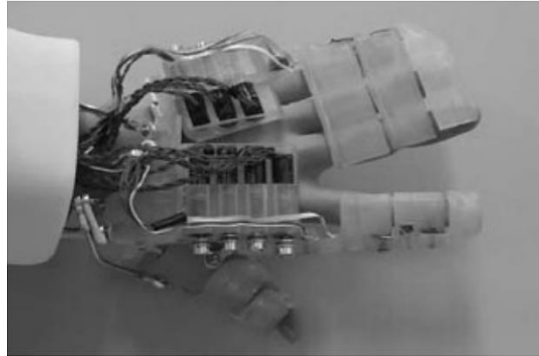


**Figure 2-12.** Device from Hasegawa et al. [21]

As Figure 2-12 shows, Hasegawa et al [21], have developed an exoskeleton to assist with hand and wrist functions. There are 11 active DOF: three for the index finger, three for the middle-ring-small fingers combined, two for the thumb, and three for the wrist.

A tendon-driven mechanism is used, but the control of each joint is independent. This method is used to have an exact control of the force of each finger in the action of grasping, to maintain grasping stability. The grasping force is measured indirectly using electrodes on the lumbrical muscles. When the estimated grasping force is below a certain threshold, meaning that the force assistance is not required, the device controls the motors to keep the wires slightly relaxed, regardless of the finger posture.

The motor control commands are generated by calculation of the required wire lengths based on the joint angles measured from the exoskeleton.

When finger assistance is unnecessary the resistance is low, but if the determined grasping force is greater than certain threshold indicating that the user needs force assistance, the control mode of the exoskeleton is switched to the other mode, which controls the grasping force. [5].

*In et al*

Figure 2-13 illustrates a hand exoskeleton from In et al. [22]. It uses a differential mechanism (commonly used in grippers) for multi-finger under actuation

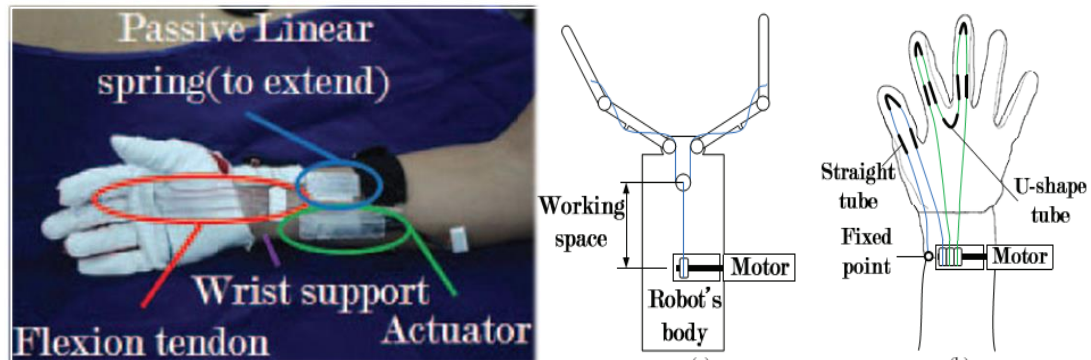


**Figure 2-13.** Device from In et al. [22]

This device uses the patient's own hand as a supporting structure for finger movement, because there are no rigid linkages.

The flexion motions of the three actuated fingers are performed using a motor, and the extension motions are performed using extension springs. The differential mechanism enables the device to grasp an object with a three-dimensional surface securely with only one actuator by adjusting the movement of the fingers. The key parts of the proposed differential mechanism are U-shaped tubes located at the fingertips and between the fingers. The tubes at the fingertips move with the fingers, while the tube between the fingers maintains its position.

The flexion of the fingers is due to the pulling of the tensor cables from a spooler attached to a motor, when the total length of the tensors is shortened, then the finger moves. When there is no external resistance, the actuated fingers are flexed almost evenly, and when there is an object, the differential mechanism provokes that the unobstructed finger approaches rapidly to the opposite one.

*Shields et al*

This device was developed by Shields et al [23] and it is conceived as a solution for increased fatigue and dexterity loss of astronauts during extravehicular activities, given the stiffness of gloves and spacesuits when they have to perform such activities. Figure 2-14 illustrates the device.

It has three actuated fingers (index, middle, ring-small), with one DOF per each finger. [5]

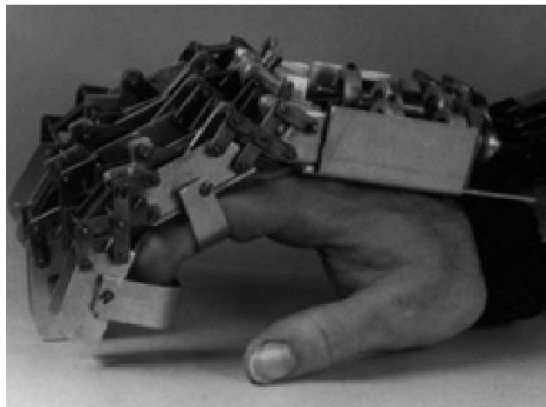


**Figure 2-14.** Device from Shields et al. [23]

Each finger has a 4-bar mechanism to allow the joints to rotate about remote centers (see Figure 2-8 (b)) that are coincident with the joints of the wearer's fingers. The motions of the two joints for each finger are synced. This device exerts a flexion force with a cable mechanism driven by a motor, while the extension occurs with the passive force provided by the stiffness of the space suit glove and the inactivity of the flexion actuator.

### **2.3. Soft and Dexterous Structures.**

The device that is subject of this document is planned to be bio-inspired (since the mechanism will resemble the musculoskeletal *kinesiology* of the human hand). This feature confers to the orthosis the epithet of “soft robotic” as far as the design regarding the interaction with the hand is planned to be devoid of rigid components.

The importance of the incursion into the field of soft robotics lie on the need for manufacturing a flexible device not just as an intrinsic feature of its components but in the flexibility of use regarding shapes and sizes of hands that will wear it.

A robot is classified as hard or soft, on the basis of the compliance of its materials [24]. A hard robot is typically used in well-defined environments in which they repetitively perform a motion with great precision. These robots are designed to be stiff so that vibration and deformation of the structure don't affect the accuracy of movement. In general, hard robots have multiple flexible joints connected by rigid links. Each joint moves in one rotary or translational direction to provide a degree of freedom (DOF) of robot motion and all of them combined comprise the robot workspace.

Soft robots and traditional hard robots use different mechanisms to enable dexterous mobility. As it can be seen in Figure 2-15, soft robots have distributed deformation with theoretically an infinite number of DOF.

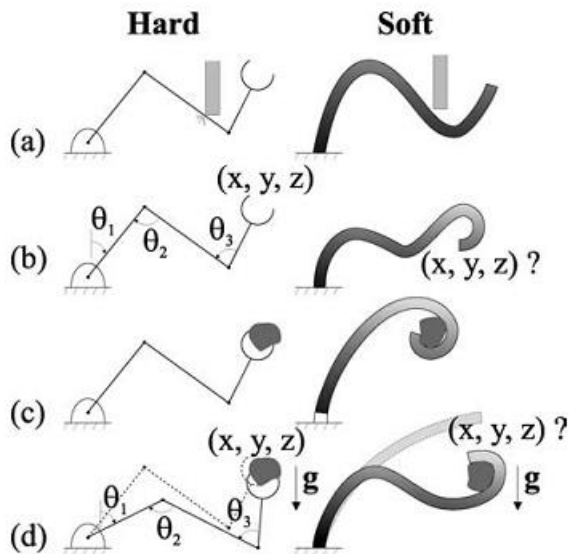


**Figure 2-15.** Capabilities of hard and soft robots: (a) dexterity, (b) position sensing, (c) manipulation and (d) loading. [24]

As it is stated by D. Trivedi et al [24], the soft structures have the following advantages:

- Infinite Degrees of Freedom (DOF)
- Continuous actuation
- Large strains
- High safety
- Variable size of manipulation
- Highest conformability to obstacles

It is also important to mention the following disadvantages:

- Low accuracy
- Low controllability
- Difficult Path Planning

- Difficult position sensing
- They have less actuators than DOF (underactuation).

Hence, the scenario for the development is, that to be able to increase comfort and wearability of the Orthosis, accuracy in position and controllability of every DOF have to be compromised.

A hard structure linked to the fingers, would limit the diversity of shapes and sizes of hands. Since there are many variables, starting with bones sizes and morphology of the joints, a rigid device would require tailor made solutions.

In summary, a rigid exoskeleton is being confronted with a soft Orthosis (glove), which given the nature of the application, has important advantages that are ideal for the interaction with humans' limbs.

#### **2.4. Conclusions**

The hand possesses very complex mechanisms for having complete dexterity; regarding the actuation, most of extrinsic muscles are in charge of the flexion/extension of both the fingers and the wrist. On the other hand, most of intrinsic muscles are in charge of the abduction/adduction of the fingers.

The entire hand kinesiology involves a large amount of muscles to manage 21 degrees of freedom (4 DOF per each finger, except from the thumb which has 5 DOF). This situation certainly increases the difficulty for mimicking the musculoskeletal system.

From this point, the Orthosis has to consider just the most important hand movements, so that the solution is the most practical possible. These critical motions of interest seem to be the flexion and extension, which is reflected in most current developments studied from the state of the art.

Nevertheless, even if focusing just in flexion and extension, there are 8 extrinsic muscles involved in the flexion/extension movements ensuring stability under different scenarios.

Fortunately, the flexion seems to be more important than extension because it is the base of grasping, which is one of the most important functions of the hand.

As a consequence, for rehab devices as well as assistance devices, the grasping motion is a desirable characteristic. It is performed by the opposition of the thumb to another finger, generally the index. Here is also worth to mention that Soekadar [2] highlights the importance of being able to grasp for performing most of the daily activities. And as a conclusion, the crucial role of the flexion is confirmed.

Every single bone-muscle-connective tissue has an important role in the kinesiology of the hand. Along with the tendons, the pulleys are pieces of connective tissue that any tendon driven mechanism has to consider to assure the force transmission to the mechanical linkages (bones).

Most developments have used rigid components for a strict control over the position of the fingers, however, most of them are under actuated. That means that even if they measure the rotational coordinates of every joint, there is always a restriction over the number of possible degrees of freedom.

Regarding the control signals, most of assistive devices have used the applied force or EMG signals as the physical variables to drive the behavior of the devices.

Finally, a soft robotic hand Orthosis that resembles the musculoskeletal system of the human body would be the first in his type, according to the presented research. Herein is the importance of this research.

## **Chapter 3. Requirements**

There are several design characteristics that need to be addressed in order to develop a wearable device that can successfully help patients with hand rehabilitation exercises. Those characteristics can be classified as ‘functional’, when they are related to what the Orthosis have to do and ‘nonfunctional’ regarding of how the Orthosis have to be.

### **3.1. Functional Requirements**

#### *FR.1. Type of motion.*

The system has to allow the flexion/extension of the finger under the principles of human kinesiology. The flexion has to be performed with active actuators, so that the foreseen final product could be used for grasping assistance. On the other hand, the extension can be either active or passive.

#### *FR.2. Individual movement of the fingers*

The actuation system has to be designed to allow the independent movement of each of finger.

#### *FR.3. Frequency of movement*

Experts recommend [2] to limit the maximum allowable speed up to open-close 10 cycles/min. This requirement lies on the fact that as a rehabilitation device, the system shouldn’t act abruptly mainly because of user’s safety, but also because the patient needs to mentally process the movement by becoming aware of its disabled limb and then try to relearn how to use it.

#### *FR.4. Finger intention of movement*

The system should allow the user to select which finger should move in an intuitive way.

*FR.5. Visual feedback*

The system should indicate which finger is moving in an intuitive way. The intention is to give a positive visual reinforcement to the finger's intention of movement.

*FR.6. Estimated forces*

According to the findings of the prior study [25], the necessary forces, basis for choosing the appropriate actuation method, are presented in Table 3 1.

**Table 3-1.** Experimental forces per each finger.

Finger	Forces (N)
<b>Thumb</b>	10,8
<b>Index</b>	8,8
<b>Middle</b>	9,8
<b>Ring</b>	11,8
<b>Little</b>	9,4

As it can be seen in the Table presented above, the actuation method has to be able to exert forces up to 12N.

*FR.7. Estimated strokes for the flexor tendons*

According to the findings of the prior study [25] and borne out again in the laboratory during this research, the actuation method over the tendons has to be able to contract/extend the following estimated distances shown in Table 3-2

**Table 3-2.** Experimental excursions per each finger [25]

Finger	Strokes (mm)
<b>Thumb</b>	30
<b>Index<sup>4</sup></b>	50 (52)
<b>Middle</b>	50
<b>Ring</b>	43
<b>Little</b>	40

<sup>4</sup> The prior work [25] suggests using 50mm instead of 52mm.

As it is shown in Table 3-2, the actuation method has to be able to achieve excursions of the tendons up to 50 mm.

### **3.2. Nonfunctional Requirements**

#### *NFR.1. Bio inspiration*

The orthosis is planned to be a bio inspired device, so it should consider human hands' anatomy. The fundamental configuration is muscle-tendon-pulley.

#### *NFR.2. Low mass/inertia*

The mass of the orthosis must be kept to a minimum, as it interferes with the forces transmitted from the actuators to the human. A device with large mass requires excessive use of the actuator power to counterbalance gravity effects.

According to Soekadar [2], the device shouldn't weight more than 500 grams.

#### *NFR.3. Comfort of wearing*

As the prolonged use of such a device has to be possible and probably necessary, the device must be as comfortable as possible, causing no fatigue to the user even after long periods of use. This should include easiness of adjustment and removal.

#### *NFR.4. Safety*

As the system is in direct contact with the human operator the safety requirement is paramount for a rehabilitation device. It must be designed not only to be safe but also to seem safe to operator.

#### *NFR.5. Versatility*

As with all systems, user acceptance is dependent to a large extent on how versatile is the device as well as how ease is to get it on the market. It is therefore vital that appropriate design concerns are given to versatility regarding different sizes and shapes of hands.

## Chapter 4. Design

This chapter is aimed to describe deeply the design process of the mechatronic system by showing the important considerations regarding the study and selection of the actuators, the sensors, the components needed for human interaction, the mechanical design of the support structure for the actuators and the modification of the glove for suiting the application.

### 4.1. Actuation

This section is aimed to explain the selection process of both active and passive actuators.

#### 4.1.1. Mechanism

As it was studied in the previous chapters, each human finger requires the synergic movement of several muscles to complete its ranges of motion.

For understanding the necessary mechanism for the movement of a human finger, a mechanical model of a human hand was studied [26] and it is illustrated in Figure 4-1.

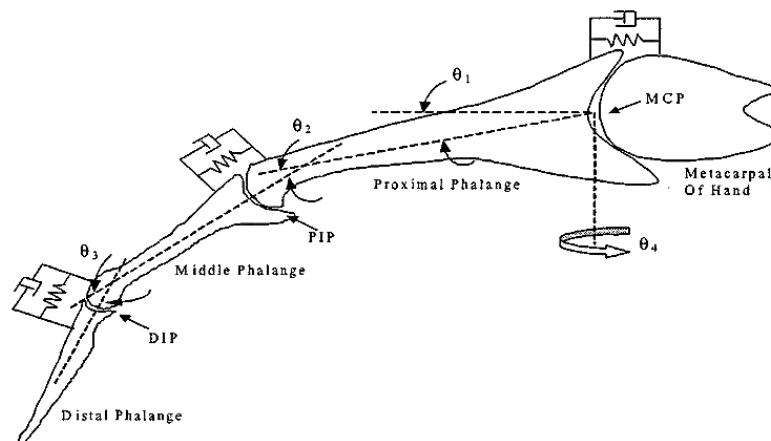


Figure 4-1. Mechanical model of a human finger. [26]

The finger can be represented as a three links kinematic chain with four DOF. Also, each union is modeled with a damper – spring configuration that regulates the speed of motion of the condylar joints.  $\theta_1$ ,  $\theta_2$  and  $\theta_3$  represent the angles for the flexion/extension of the MCP, PIP and DIP respectively and  $\theta_4$  is the second rotational DOF of the MCP joint for abduction/adduction.

Given the required versatility of the orthosis (*NFR.5*), and given that the inertias, lengths and spring/dampers coefficients would differ among individuals, as well as that the forces are going to be exerted via soft structure with high parametrical uncertainties, it is worthless to derive a dynamic model to calculate the forces. Thus, the only important data that needs consideration for selecting the necessary mechanism is the study of the ranges of motion of every rotational degree of freedom.

The different shapes in the finger joint, result in different types of DOF at each joint. Also, the orientation of the thumb and its particular configuration of its CMC joint increase its range of motion and give it greater flexibility. [27], [28]

The resting posture is a position of equilibrium without active muscle contraction. In this position, the wrist is extended  $20^\circ$  in neutral *radial/ulnar* position, the MCP joints are flexed approximately  $45^\circ$ , the PIP joints are flexed between  $30^\circ$  and  $45^\circ$ , and the DIP joints are flexed between  $10^\circ$  and  $20^\circ$ . [29].

Now, regarding the documented ranges of motion, the flexion of the MCP joints represent a rotation of about  $90^\circ$ , except in case of the little finger, which is around  $95^\circ$ , and the index finger, which is around  $70^\circ$ . For PIP and DIP joints, the flexion is about  $110^\circ$  and  $90^\circ$  respectively. [5]. The extension behavior varies among individuals.

Finally, in abduction/adduction, the angle is usually  $15^\circ$ .

Constraints mentioned before are summarized in Table 4-1.

**Table 4-1.** Ranges of Motion per each joint. [30]

Rotational Parameter	ROM (°)
$\Theta_{\text{MCP-Flexion}} (\Theta_1)$	90
$\Theta_{\text{PIP}} (\Theta_2)$	110
$\Theta_{\text{DIP}} (\Theta_2)$	90
$\Theta_{\text{MCP-A-A}} (\Theta_4)$	$\pm 15$

As it was studied in the literature review, both interphalangeal joints have different mechanisms for completing the flexion/extension, than the metacarpophalangeal joint. Because for stability reasons, the *extensor apparatus* provokes the flexion of the MCP while the DIP and the PIP are extending. Regarding that, it would be necessary to resemble the interossei and the lumbrical muscle for performing a simultaneous flexion of the three joints.

Fortunately, there is a paramount inner constrain that can be analyzed from the study of the biomechanics of the hand. The internal ligaments that connect the phalanges enable a functional coupling between to the DIP and the PIP as it is stated in Equation (4-1).

$$\theta_{DIP} = \frac{2}{3} \cdot \theta_{PIP} \quad (4-1)$$

In other words, the model can be simplified regarding the interphalangeal joints because one joint indirectly determines the rotation of the other.

For this reason, given that the implementation of the *extensor apparatus* mechanism would augment the amount of required actuators as well as the mass of the orthosis compromising *NFR.2 (Low mass/inertia)*, and also that most important movement is the flexion *FR.1 (Type of motion)*, the most practical solution would be to develop an under actuated mechanism for the flexion of the coupled DOF from the DIP and the PIP joints.

There is a mechanism that resembles the human kinesiology for the rotational movement of a single DOF that is the antagonistic muscle pair.

The agonist is the muscle that provokes the motion by its own contraction, while the antagonist is the one who opposes the movement and supports it by slowing it down and also restores the position of the limb. Antagonism is a role depending on which of both muscles is contracting. [31]. Figure 4-2 shows this principle in the movement of the human elbow, using the Triceps and the Biceps as a reference.

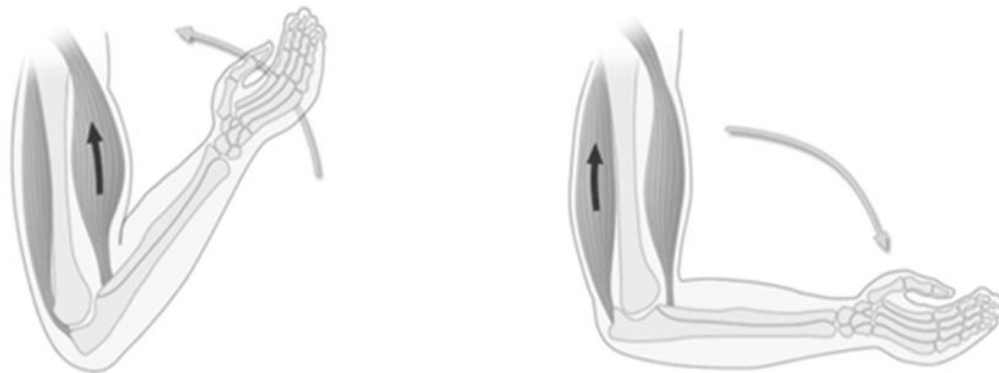


**Figure 4-2.** Example of agonist-antagonist muscle principle. [32]

In the figure above, when the flexor contracts, which in the case of the forearm is the Biceps, then the extensor (Triceps) gives stability to the movement through its gradual relaxation. Conversely, in the extension of the forearm, the flexor became the antagonist.

As it can be appreciated from part 1 and 4 from The Figure 4-3, in the case of a single DOF joint, the antagonistic pair is aimed to achieve certain a controlled bi-directional change in a rotational parameter ( $\theta$ ) of the joint.

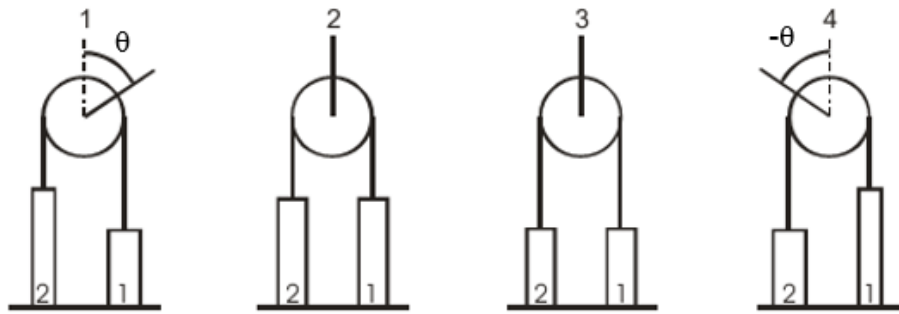


**Figure 4-3.** Schematics of antagonist principle. [33]

The idea is to use springs as passive actuators for the extensor antagonist muscle, correspondingly with the prior model. [25].

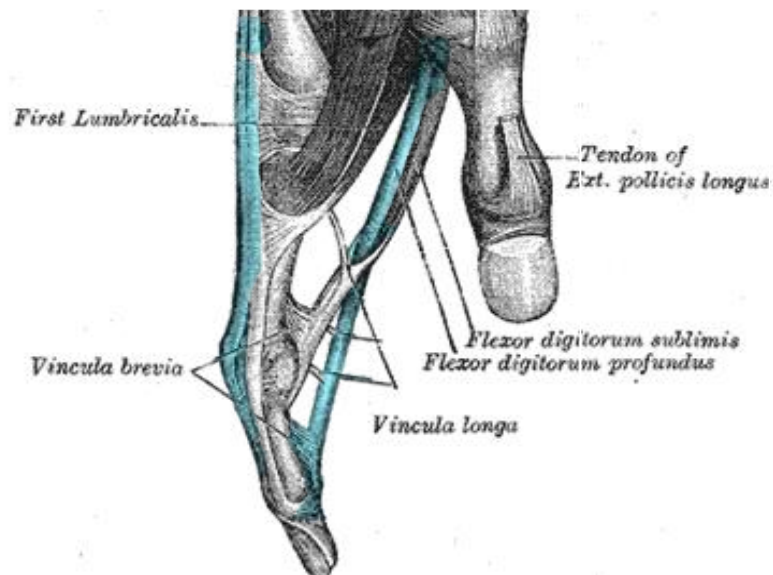


**Figure 4-4.** Selected tendons for the actuation<sup>5</sup>. Highlighted are the tendons of the FDP and ED muscles.

Moreover, the antagonist pair would involve as depicted in Figure 4-4, the main flexors and tensors tendons mechanically attached to the distal phalanx.

<sup>5</sup> Original image taken from [69]

By using antagonistic pairs for the movement of each finger, the number of actuators is reduced to ten, where five of them are active and five of them passive.

*Finger flexion (active muscles):*

1. Flexor Pollicis Longus – Thumb
2. Flexor Digitorum Profundus- Index Finger
3. Flexor Digitorum Profundus- Middle Finger
4. Flexor Digitorum Profundus- Ring Finger
5. Flexor Digitorum Profundus- Little Finger

*Finger extension (passive muscles)*

1. Extensor Pollicis Longus – Thumb
2. Extensor Digitorum- Index Finger
3. Extensor Digitorum- Middle Finger
4. Extensor Digitorum- Ring Finger
5. Extensor Digitorum- Little Finger

By doing this, the functional requirement *FR2 (Individual movement of the fingers)* is fulfilled.

### **4.1.2. Active Actuators**

According to the *NFR.1*, the system should be bio-inspired. Thus, the actuators were found to behave as artificial muscles.

Artificial muscle is a generic term used for materials or devices that can reversibly contract, expand, or rotate within one component due to an external stimulus (such as voltage, current, pressure or temperature). [34] The actuation response is provoked by a single component, thus, conventional motors and pneumatic linear or rotary actuators do not qualify as artificial muscles, because there is more than one component involved in their actuation.

Artificial muscles can be divided into four major groups based on their actuation mechanism: Electro active polymers (EAPs), Ion-based actuators, Pneumatic actuators, and Thermal actuators. [34]

This research is focused in studying two types of artificial muscles. The first one is the Nitinol as a Thermal artificial muscle and the second one is the Festo Pneumatic Artificial Muscles with a modified membrane.

#### ***4.1.2.1. Concept 1: Nitinol***

This section explores the concept of Nitinol as a Thermal Artificial Muscle.

##### ***4.1.2.1.1. Generalities***

Nitinol is a metal alloy of nickel and titanium (Ni-Ti system). This material has the characteristic of having a shape memory behavior. It stands for ‘Niquel Titanium Naval Ordnance Laboratory’ and it is also known as TINEL, the brand name of a family of Ni-Ti alloys from Raychem Corp. who pioneered the shape memory technology in California. [35]

“Shape Memory” describes the effect of restoring the original shape of a plastically deformed sample by heating it. [36] This phenomenon results from a crystalline phase change known as “thermo elastic martensitic transformation” at a controllable temperature. The shape memory effect combined with the property of super elasticity (more than 10 times the elasticity of structural steel) and high biocompatibility, confers the Nitinol a huge potential application in designing and implementing medical devices. [35]

The Figure 4-5 can illustrate the transformation. At values below the transformation temperature, Nitinol alloys are martensitic. In this condition, they are very soft and can be deformed easily. Heating above the transformation temperature, recovers the original shape and converts back the material to its high strength austenitic condition. [35]

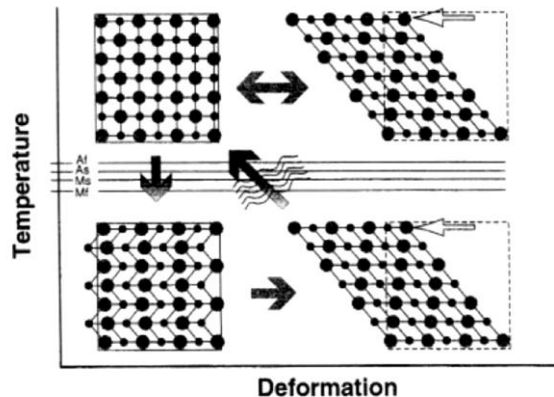


**Figure 4-5.** Schematic representation of the shape memory effect and super elasticity. [35]

#### **4.1.2.1.2.      *Applicability in this Project***

In this project, a shape memory effect material would be very convenient because the mechanical design of the Orthotic device would be incredibly simplified.

There are two possible configurations:

1. Use Ni-Ti as an artificial muscle wire.
2. Use Ni-Ti as tendons.

The Figure 4-6 describes graphically both configurations.

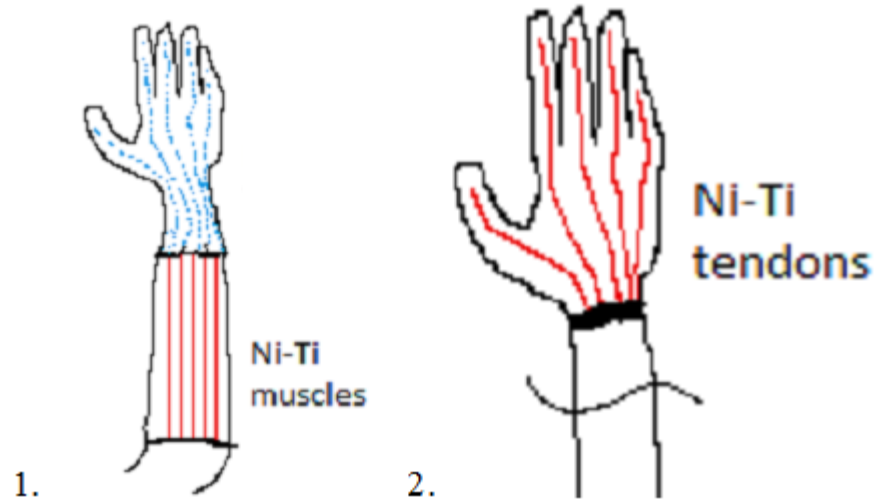


**Figure 4-6.** *Left:* Muscle configuration. *Right:* Tendon configuration.

As mentioned before, the use of Ni-Ti would deplete the mechanical complexity of the current Pneumatic Rudimentary Model, in terms of weight, overall geometrical dimensions, portability and flexibility to wear.

Nevertheless, to be completely feasible to implement, the material must adapt to the final requirements.

#### **4.1.2.1.3. Analysis of Required Forces and Strokes:**

Based on Table 3-1 and Table 3-2 from the *FR.6* and *FR.7*, regarding the estimated forces and strokes in a SOMSO Model hand, it is required a force of 11,8 N max to move a finger, and it is required to pull the rope a distance of 50mm max.

Regarding those features, the technical information of the Nitinol was consulted online [37]

### *Required force*

Given the value of 11.8 N (1203 g.f.), it should be required a wire of 0,31 mm in diameter, which performs a heating pull force of 1280 g. But unfortunately, it requires a current of 1500 mA for the movement and it takes a recovery cooling time of 8,1 seconds. [37] Another possible solution would be to use two 0,20 mm diameter in a parallel configuration to perform a heating pull force of 1140 g.f (11% less than required), with a current withdrawal of 660 mA per each one and a recovery time of 3.2 seconds. In any case, to perform a total force needed for the movement of the ring finger it is necessary to have an electrical power supply for 1,5 A.

### *Required stroke*

Unfortunately, under optimal conditions, the Nitinol contracts a maximum of 4% of its nominal length when heated [35]. Thus, correspondingly with the values of Table 3-2, the required length of Nitinol for completing movement of the index finger is  $50/0,04 = 1250$  mm. That represents a big amount of material to use if it is applied in the configuration illustrated in picture 1 of Figure 4-6. For that reason, it would be required to think about a new configuration to achieve the required movement of the tendons.

On the other hand, for the second configuration shown in Figure 4-6, it is required to know first the size of the human hand before programming the desired movement with the Nitinol. This is not feasible because the glove should be flexible for the use in different patients.

### *Required cycle time*

The contraction of the Nitinol actuator wire is due solely to heating and the relaxation solely to cooling. [36] Both contraction and relaxation are virtually instantaneous with the temperature of the wire. As a result, the mechanical cycle speed is dependent on and directly related to temperature changes. Applying high currents for short periods of time can quickly heat the wire. In fact, it can be heated so fast, that the limiting factor is not the rate at which heating can occur but rather the stress created by such rapid movement. If the wire is made to contract too fast with a load, the inertia of the load can cause over stress to the wire.

To have a control over the cycle time, a proper cooling control should be implemented. The relaxation time is the same as cooling time. Cooling is greatly affected by heat sinking and design features. The simplest way to improve the speed of cooling is to use smaller diameter wires. The smaller is the diameter, the more surface and mass the wire has and the faster it can cool down.

The next possibility for improving the relaxation or cooling time, is to use wires that can change its shape at higher temperatures. Accordingly, the temperature differential between ambient temperature and the wire temperature is greater and correspondingly the wire's temperature will drop below the transition temperature faster in response to the faster rate of heat loss.

#### **4.1.2.2. Concept 2: Pneumatic Artificial Muscles**

This concept explores the use of a new type of Festo Pneumatic Artificial Muscle which has a modified membrane that allows more contraction with lesser overall dimensions.

##### **4.1.2.2.1. Generalities**

Pneumatic Artificial Muscles (PAMs) are contractile and linear motion engines operated by gas pressure [38]. They are comprised by a reinforced fiber membrane attached to a couple of fittings that transmit a linear and unidirectional force. The membrane expands radially and contracts at the same time when a gas, usually air, is forced into it. The fibers create a rhomboidal pattern with a three- dimensional grid structure [39] (See first image of Figure 4-7).

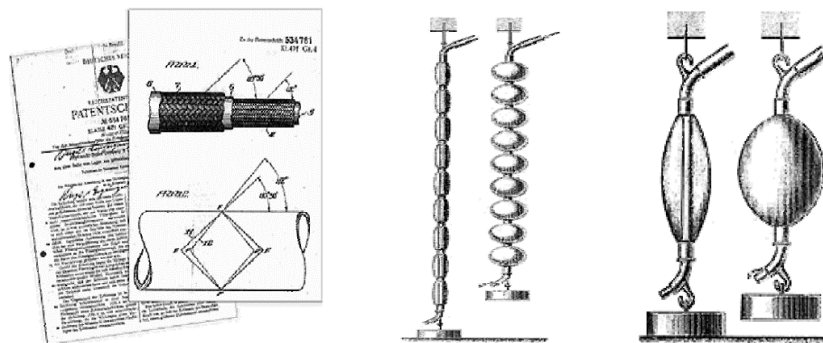


**Figure 4-7.** Rudimentary pneumatic artificial muscles. [33]

The first PAM was the McKibben muscle. It was first developed in the 1950's by the American physician Joseph L. McKibben with the intention to actuate artificial limbs for amputees [40]. It consisted in an internal bladder covered with a braided mesh shell. As the volume of the bladder increases due to the increase in pressure, the actuator shortens and produces tension.

To test the operation of a PAM, a common experiment is usually set up as shown in the last image of Figure 4-7, where a load is placed in one side of the muscle hanging over a hook. The muscle is gradually inflated with gas, acquiring certain pressure, until its pulling force reaches the weight of the load placed aside and it starts to contract. From this experiment, two basic actuator behavior rules can be deduced: (1) a PAM shortens by increasing its enclosed volume, and (2) it will contract against a constant load if the pneumatic pressure is increased. [38].

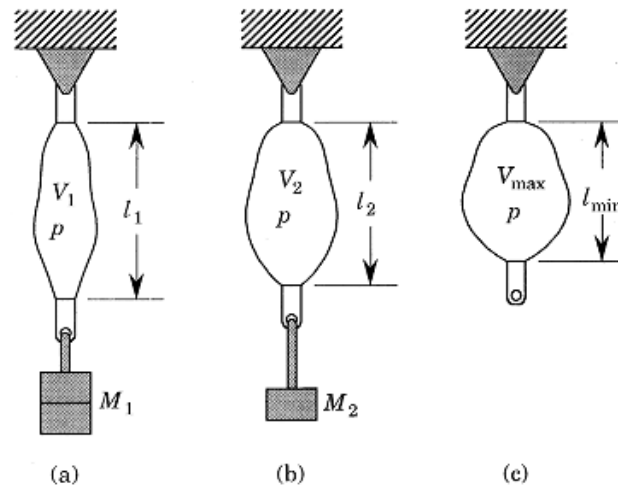


**Figure 4-8.** Second experiment for testing the functionality of PAM. [38]

There is a second experiment, where a mass is placed on a PAM and it is changed while the gauge pressure is kept constant. In this case, if the load is completely removed, as depicted by Figure 4-8 (c), the volume will reach its maximum value. ( $V_{max}$ ), and the length reaches its minimum value. ( $L_{min}$ ). However, the pulling force drops to zero.

The conclusions for the second experiment are, first, that a PAM will shorten at a constant pressure if the load is decreased and, secondly, that its contraction has an upper limit at which it will develop no force and its enclosed volume is maximal.

#### **4.1.2.2.2. Advantages of the use of PAM:**

The PAMs can be very useful to this project since they have a lot of important features described below:

- These actuators have high power and force to weight/volume ratios  $>1$  kW/kg. [41]
- Being pneumatic in nature, confers the muscle high flexibility, softness in contact and excellent safety potential.
- Pneumatic muscles systems have seemed to be controllable with an accuracy of better than 1% of displacement [41]
- Bandwidths for antagonistic pairs of muscles of up to 5 Hz can be achieved. [41].
- When compared directly with human muscle, the contractile force for a given cross-sectional area of actuator can be over  $300$  N/cm<sup>2</sup> for the PMA compared to  $20$ – $40$  N/cm<sup>2</sup> for natural muscle. [41].
- The actuators can operate safely in aquatic, dusty or other liquid environments.
- The actuators are highly tolerant to mechanical (rotational and translational) misalignment, reducing the engineering complexity.

#### **4.1.2.2.3. Analysis of Required Forces and Strokes:**

The rudimentary model uses Festo Standard Pneumatic Artificial Muscles type DSMP 5-200 (Press Fitted Connection,  $\phi$  5mm and 200mm long). However, for completing the required strokes (*FR.7*), those muscles had to have very big overall geometrical dimensions, since they could contract only up to 15% of their original length with a 6 bar pressure [25].

In that matter, it was necessary to use a muscle of 334mm (50 mm/0,15) for completing a stroke of 50 mm (value of excursion for the index finger's flexor tendon - *FR.7*). This length value, is greater than the average size of the forearm (230 mm long according to NASA's anthropometric data, see Figure 4-28) and therefore, those muscles weren't suitable for a translation to a wearable orthosis.

However, Festo Membrane technologies offered a new prototype membrane as a solution: MXAM 15°. The new angle of the membrane fibers, confers it more capacity of contraction up to 30% at 6 bar (See Figure 4-9).

With that level of contraction, it would be required a 167 mm (50mm/0,30) muscle to fulfill the functional requirements of excursions for the flexor tendons.

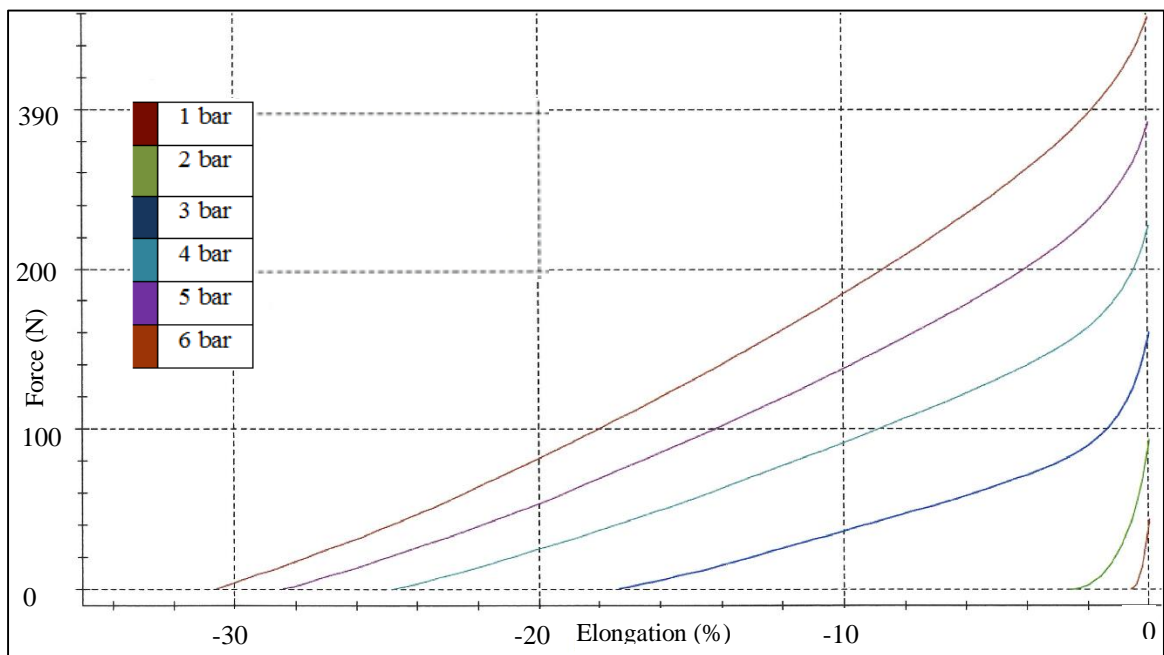


**Figure 4-9.** Force (N) vs elongation (%) DSMP-5 MXAM 15°. Characteristic curve provided by Festo Co & AG.

On the other hand, regarding the required forces from *FR.6*, as it is depicted in Figure 4-9, with a pressure of 6 bar (*brown line*), the muscle would exert an initial pulling force of more than 300N and it would stabilize in the necessary force to hold the load. For example, it exerts 20N when reaches 29% of contraction which overcomes the upper limit of required forces (11.8N according to *Table 3-1*). Hence, this pneumatic actuator seems to be ideal for this application.

#### **4.1.2.3. Conclusions**

In spite of the possibility of a proper selection of Ni-Ti wires for the required force, a high current electrical supply must be used, which can be dangerous for humans.

In spite of the high potential features of Nitinol, such as super elasticity and shape memory effect, the use of it as an actuator is limited by the range of strain, up to 4% of the nominal length. For this application, that fact represents the use of high amounts of material.

Despite theoretically the speed of motion could be very high, a proper and controlled temperature change should occur in order to maintain the stability of the system.

The pneumatic artificial muscle with the MXAM 15° membrane is the best choice for the application, because it can achieve the necessary strokes with nominal dimensions that match the forearm's anthropometry.

On the other hand, regarding the forces, the PAM's extraordinary power can amply fulfill the requirements and overcome any extra demand of pulling force.

Moreover, its minimum weight and soft muscle-like actuation, satisfies the requirement of bio-inspiration while its high force to volume rate satisfies the specified necessary forces and contractions of the tendons.

The PAM was tailor made for the application by Festo Co& AG as DMSP-5-177N-RM-CM-CS-Ø1,5, which means a press fitted connection muscle of 5mm diameter and a nominal length of 177 mm, with pneumatic connection, radial at one side (RM-CM) and a final connector with a 1,5 mm hole that is going to be used for the attachment of the tendons. The 177 mm dimension (6% longer than required) was selected to achieve more stroke while it still fits in the forearm.

Figure 4-10 illustrates the geometrical configuration described above. All the features including the final connector and the selected nominal length were conceived within the design process of the mechanical support of the actuators<sup>6</sup>.

DMSP-5-177N-RM-CM-CS-Ø1,5

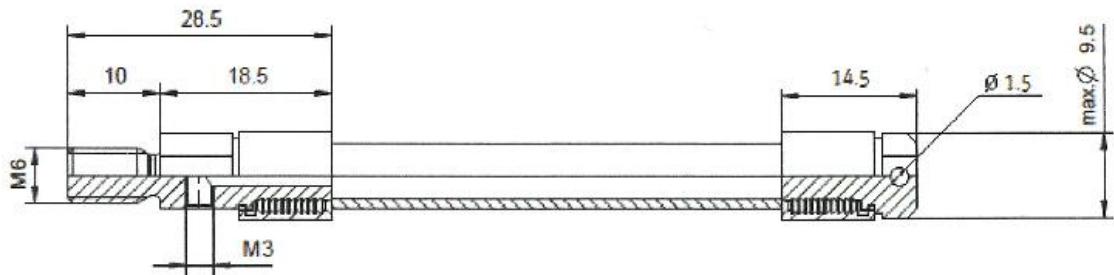


**Figure 4-10.** Geometrical design of the DMSP-5-177N-RM-CM-CS-. [42]

### 4.1.3. Passive Actuators

For this application, the passive actuators in charge of performing as antagonist muscles which regulate the motion and support the extension of the fingers, were chosen to be tension springs.

Five springs were selected on an online catalogue from MISOUMI [43]. The selection criteria was a cross reference between the maximum values of load and deflection.

<sup>6</sup> See Chapter 4 Section 5.

The springs needed to be designed for tension. Taking into account the maximum values from Table 3-1 and Table 3-2, it results in the need of a spring that can stand 11,8 N and extend 50mm. The only limitation is that an application like this, of a considerably required load with a big deflection is very rare, since most springs are specifically designed either for load or extension.

Using this information, there were three important factors to take into account: outer diameter, the maximum deflection and the maximum load, being the first factor the most important (for compactness reasons). In a combination of these three values, among the whole catalogue, just three types of springs were found out as it can be stated in Table 4-2, and for each of them a security factor for the load was calculated.

**Table 4-2.** List of suitable springs for the application<sup>7</sup>.

Load Type	Part Number		Wire Diameter (d) [mm]	Dynamic Load		Initial Tension [N]	Spring's Constant [N/mm]	Security Factor
	Type	D-L [mm]		Max. Deflection (F) [mm]	Max. Load [N]			
<b>Ultra-light load</b>	AUA	12-60	1,1	51,5	19,6	2,94	0,32	1,66
<b>Light Load</b>	AUY	8-65	0,8	58,8	12,75	2,35	0,2	1,08
<b>Light to Medium Load</b>	AWU	6-60	0,7	50	12,94	1,67	0,23	1,10

A Light to Medium Load Ø6 mm spring (AWU 6-60) was selected with a security factor of 1,10, mainly considering its final geometry as explained before, which can be illustrated in Figure 4-11.

<sup>7</sup> Extracted form MISUMI Catalog [43]

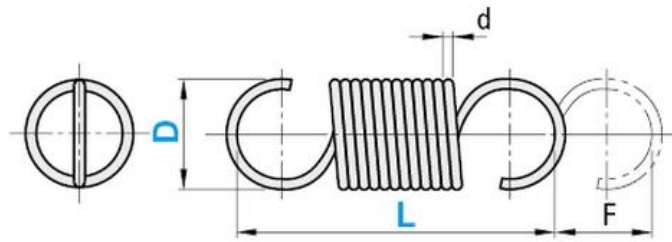


**Figure 4-11.** Geometry of the selected springs.  $D=6\text{mm}$ ,  $L=60\text{mm}$ ,  $d=0.7\text{mm}$ ,  $F=50\text{mm}$ . [43]

It is important to outline, that as in the case of the active actuators, the selection was based in the higher requirement for only one type of passive actuator for every finger. This would be helpful to increase the maintainability of the system.

#### 4.1.4. Artificial Tendons

The artificial tendons were chosen to be made of Dyneema®. Dyneema® is a super-strong fiber made from Ultra-High Molecular Weight Polyethylene (UHMwPE) [44]. It is characterized because of its extreme strength and low weight. Dyneema turns out to be 15 times strongest than steel on a like to like basis. [44].

For this application, a cord of  $\text{Ø}0,4$  mm and a maximum load of 50 daN, code SK-75 cord was used. Because of its minimum size, it could be easily threaded in a needle. Moreover, it fulfilled the forces requirements.

#### 4.1.5. Actuators Layout

Finally, a sketch for a first approach of an arrangement of the actuation system, into the body was developed and it is presented in Figure 4-12. As it can be seen, the first conception placed the pneumatic muscles in the underside of the forearm and the springs in the dorsal side of the hand. This idea is going to be assessed in the *Section 5* of this Chapter.

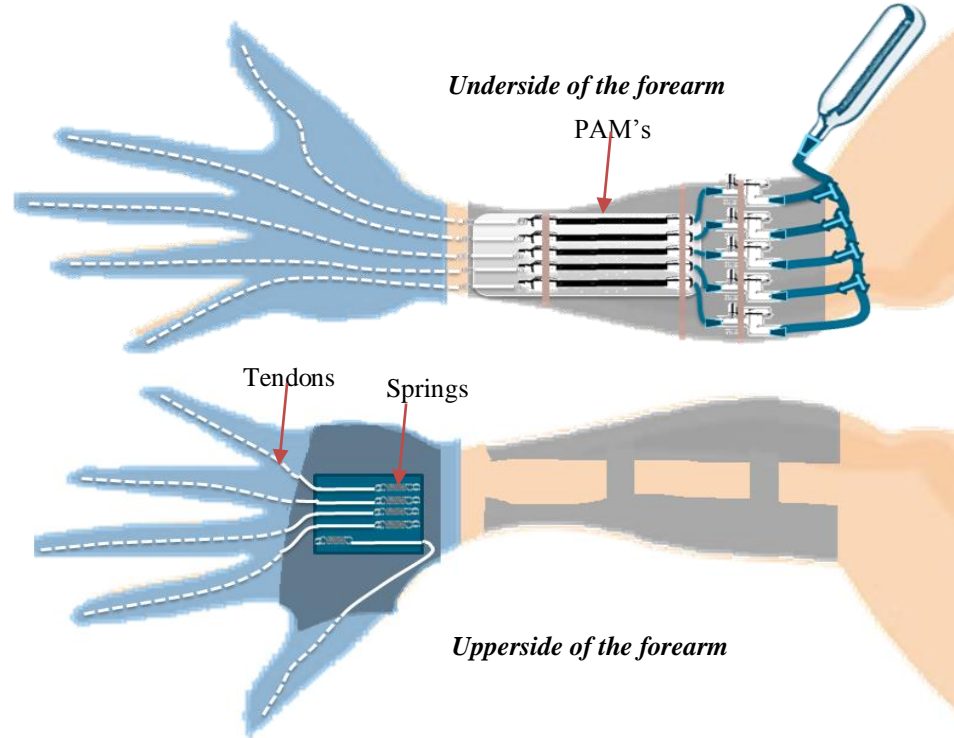


**Figure 4-12.** Sketch of first approach to the configuration of the actuation system with PAMs.

## 4.2. Pneumatics

In this section the pneumatic design process is going to be described, starting with the selection of the type of valve, a description of the overall pneumatic circuit and air consumption calculations.

### 4.2.1. Valve Selection

A desired characteristic in the actuation system, is to achieve a proportional manipulation of the muscle's contraction by regulating the air flow and pressure. Unfortunately, the nonlinearity of the Pneumatic Artificial Muscles, makes that a proportional control of the actuators is not as straightforward as it would be in DC Electric Actuators. For that reason, three different valve configurations are discussed as concepts for approaching the proportional desired behavior.

#### 4.2.1.1. Concept 1: 2/2 Solenoid Valves

The first possible solution for controlling the air flow and therefore the speed of contraction of the muscles, would be to use two 2/2 NC (2 positions 2 ways - Normally Closed) Solenoid Valves.

These are binary on/off valves would serve for inflation and deflation of the muscle respectively. This concept is depicted in Figure 4-13.

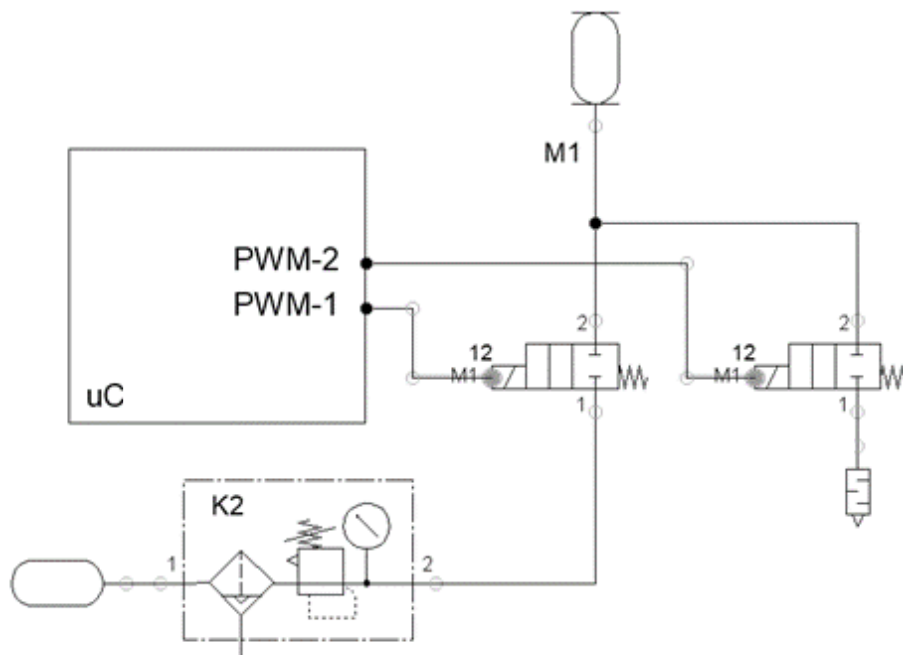


**Figure 4-13.** Two 2/2 valve configuration concept.

The valves would be individually controlled by PWM (Pulse -Width-Modulated) signals from a microcontroller. The variation of the duty cycles would regulate the air flow that is released or pumped into the muscle.

The main advantage of this concept is that the off-the-shelf binary solenoid valves available in the market, are very small and therefore this benefits the desired compactness of the final device. Moreover, a separate control over the air flow for inflation and deflation is possible

The obvious disadvantage regarding the amount of actuators (1 each finger - *FR2* ), is that it would be necessary to have 2 valves for each muscle, and therefore 10 valves in total are required. This situation would have a direct impact in the amount of control signals required from the process unit.

A second disadvantage would be that since they are solenoid valves with a binary behavior, the frequency of operation would be limited to the valve response time for switching. Most commercial valves have a response time of 20 ms [45], this means that the PWM frequency should be of about 50 Hz. This would slow down the behavior of the system as well as the control loop run time.

#### ***4.2.1.2. Concept 2: 3/2 Solenoid Valves***

This second concept would be about the use of a single 3/2 NC (3 ways 2 positions – Normally Closed) valve, that either inflate or deflate the artificial muscle according to the duty cycle of a single PWM signal. The schematics in Figure 4-14 illustrates the concept.

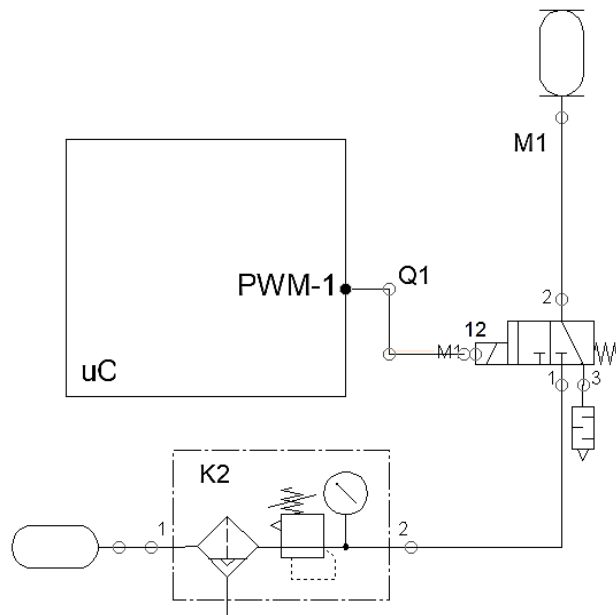


**Figure 4-14.** 3/2 valve configuration of concept 2.

This solution is aimed to decrease the amount of valves needed for each muscle. The idea is to change the behavior of the muscle depending on the relation between the amount of injected air and the amount of air that is released, as it is illustrated in Figure 4-15

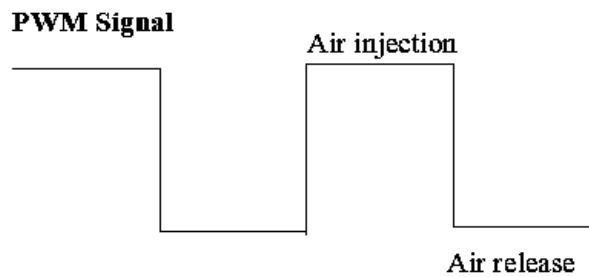


**Figure 4-15.** Air Flow and the PWM Control Signal.

The behavior is summarized in Table 4-3.

**Table 4-3.** Dynamic behavior when using a PWM controlled 3/2 NC valve.

Duty Cycle	Muscle Action
<50%	Extension
50%	Holding
>50%	Contraction

Then, when the duty cycle of the PWM signal is less than 50%, the amount of air exhausted from the muscle is greater than the amount of air pumped into it and as a consequence, the muscle relaxes. The speed of relaxation is controlled by the pulse width, reaching the maximum relaxation speed at 0%

On the other hand, a similar but opposite case would happen if the duty cycle is greater than 50%. In that case, the muscle would receive more air than the amount that is released from it and therefore it contracts. The maximum contraction speed occurs at 100% duty cycle.

When the duty cycle is 50%, and therefore the times of air injection and air exhaustion are even, the muscle holds its position.

The only disadvantage is that there would always be an air flow consumed from the air reservoir. This would compromise the time of operation of the Orthosis and demands a bigger air reservoir.

To overcome this issue, it is necessary to increase the frequency of the PWM signal, so that the differential of air volume per injection or release is very small in every period. However, the dynamic behavior would be ruled for the valve response time, since it is still a solenoid valve. This type of valves has response times of about 5ms [45].

#### **4.2.1.3. Concept 3: Piezoelectric Flow Proportional Valves**

The third concept is to use a 3/3 (3 ways / 3 Positions) closed middle position flow proportional valve. This concept was developed after these valves were presented in a meeting with Festo Med Lab, Piezoelectric Valves Development.

Festo has a new division of Piezoelectric Valves that have been used specially in medical applications. They are characterized for being miniature valves with low electrical power consumption.

Piezoelectric materials transform applied stress into electrical energy and conversely [46]. In this case a beam of piezoceramic material in combination with a passive conductive substrate, are mechanically actuated when a voltage is applied, as it can be shown in Figure 4-16.

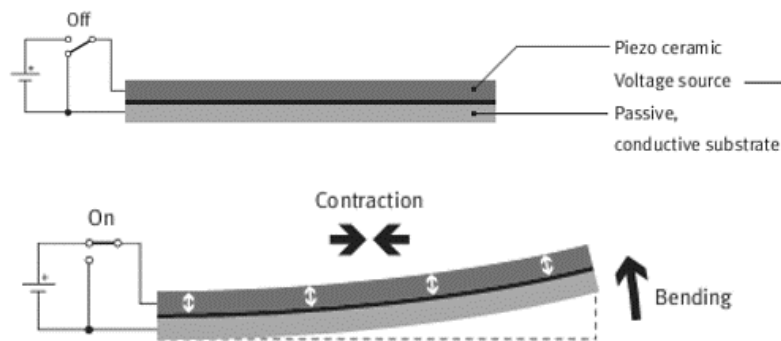


**Figure 4-16.** Piezo-electric effect. [46]

The main advantage of the piezoelectric materials is that despite they need high voltages, the current they draw is very low, and therefore the electrical power they need for actuation is very small. Also, no magnetic field is needed to keep the valve actuated. This means no heat build-up in the device. It also enables a more compact design. [46]

Piezo valves consume up to 95% less energy than solenoid valves [46]. Their capacitive properties enable the operating status to be maintained without power. Piezo valves also offer the option of energy recovery, enabling up to 50% of the switch-on energy to be recycled. [46]

Moreover, piezo valves are quieter than solenoid valves: the free movement of the bending actuator takes place without any stop noises [46].

There is a very convenient configuration for the piezo electric valves, which is the 3/3 closed middle position flow proportional valves. The middle position enables air saving during the desired hold position, as it is depicted in Figure 4-17

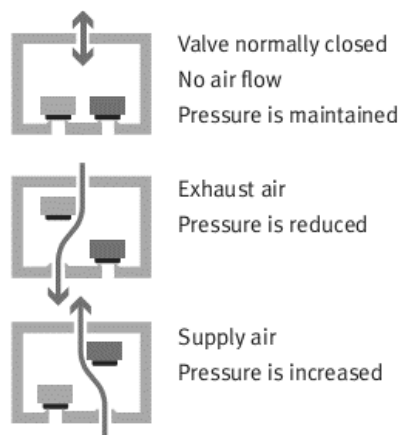


**Figure 4-17.** Internal configuration of the 3/3 piezo valves. [46].

An important implication about using piezo electric valves is that they operate with 300V, and for that reason they require a step-up DC-DC converter for its operation, as well as a power driver interface for the electrical control.

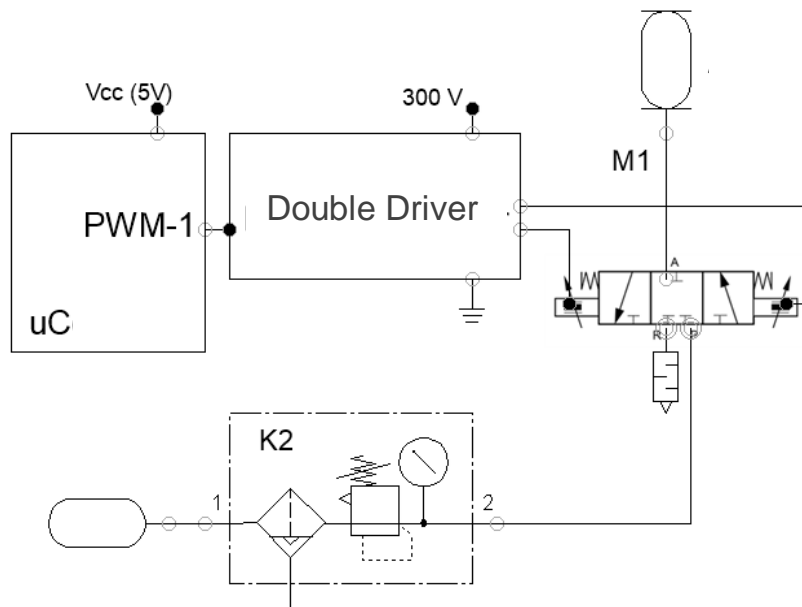


**Figure 4-18.** Concept with 3/3 closed middle position piezoelectric valve.

Figure 4-18 illustrates the concept with the 3/3 Piezo Valve. Since they are high voltage controlled proportional valves, they required an analog signal from 0 to 300V for their operation.

The control signal is a high frequency PWM signal which after being low pass filtered and therefore converted in an analog signal, can control a double driver for the high power regulation of both sides of the valve.

Since the first and last position of the valve are complementary, they can be operated with just one control signal.

#### 4.2.1.4. Conclusion

For all the reasons mentioned above, a VEAA 3/3 piezoelectric valve (See *B.3.1*).was selected for the operation of the pneumatic artificial muscle. This type of valves has a service life of more than  $10^6$  cycles and it can works with pressures up to 12 bar [46], which fulfills the necessary 6 bar of the pneumatic muscle operation for the required contraction. Moreover they consume less than 4 mW. Finally, the size of the VEAA piezo valves satisfies the desired compactness, since they are very small (7 mm x 14,4 mm x 35 mm) and they weight about 60 g. An illustration of the selected valve is found in Figure 4-19.

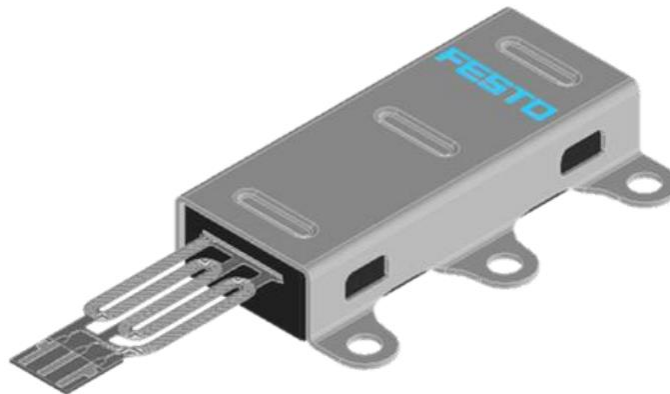


**Figure 4-19.** VEAA 3/3 Closed middle position piezoelectric valve. [46]

### 4.2.2. Overall Pneumatic Circuit Description

Figure 4-20 illustrates the overall pneumatic design. It consists in a reservoir of air (1), a service unit comprised by a filter and a pressure regulator (2), four branching units to split the air connection (3), five VEAA 3/3 closed middle position valves with mufflers (4), and five artificial muscles type DSMP-5-177-15°-Ø1.5<sup>8</sup> (5).

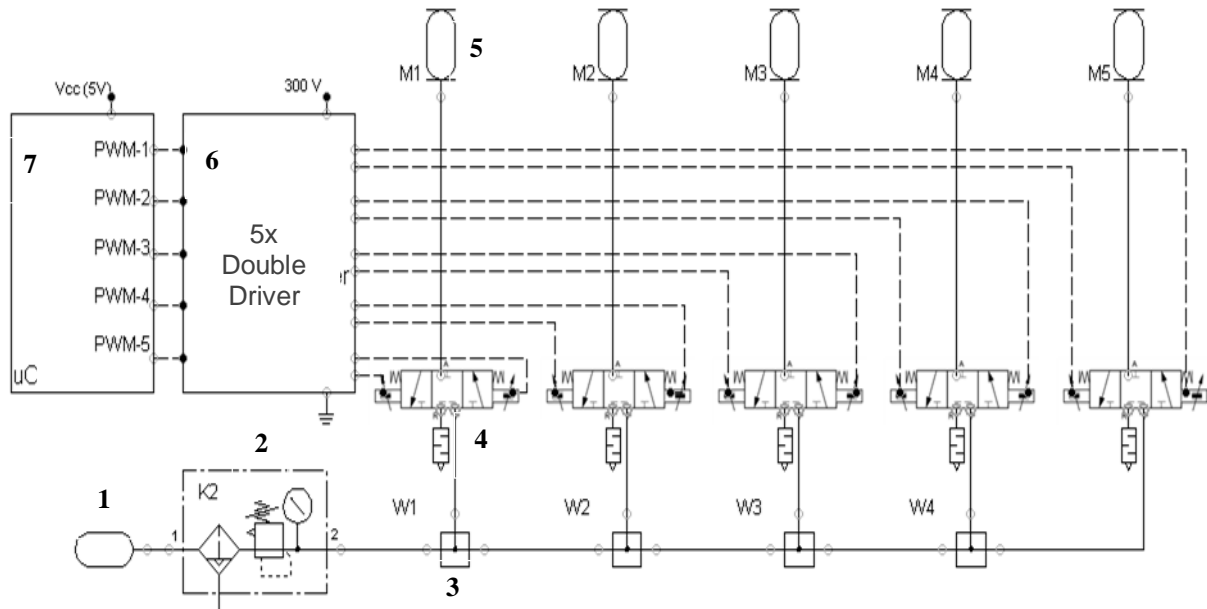


Figure 4-20. Overall pneumatic design.

On the other hand, the design includes the required electronic interfaces such as the 5 channel double driver fed with 300V (6) and the microcontroller fed with 5V (7).

### 4.2.3. Air Consumption

For calculating the amount of air consumed by each pneumatic muscle, the geometry of its maximum contraction at 6 bar has to be taken into account.

<sup>8</sup> See Figure 4-10

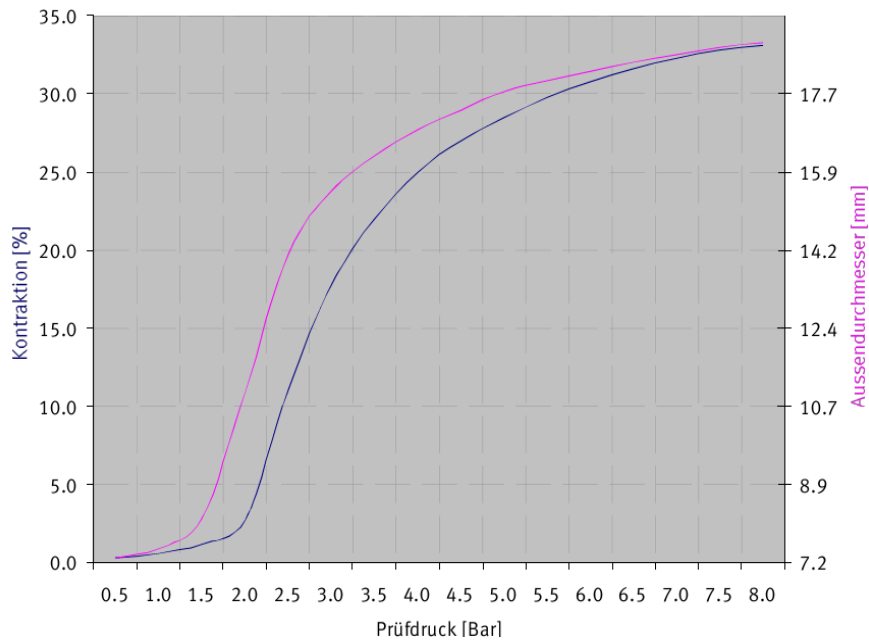


**Figure 4-21.** Contraction (%) and outer diameter (mm) vs pressure (bar). DSMP 5- MXAM 15<sup>09</sup>.

As it is depicted in Figure 4-21, the outer diameter of the muscle for the selected pressure (6 bar) is nearly 18mm. Therefore, the maximum volume of air that the muscle draws from the source during contraction is calculated in Equation (4-2) approaching the shape of an inflated muscle to a perfect cylinder.

$$V = \frac{\pi}{4} (18\text{mm})^2 \cdot 177\text{mm} = 4,5041 \times 10^{-5} \text{m}^3$$

(4-2)

---

<sup>9</sup> Characteristic Curve Provided By Festo

Assuming that the muscle contracts isothermally at certain temperature (20° C for example), using the ideal gas law with a constant of  $R=8,3144621(75) \times 10^{-5} \text{ m}^3 \cdot \text{bar} \cdot \text{K} \cdot \text{mol}^{-1}$ , the number of moles  $n$  of air consumed in such contraction is calculated in Equation (4-3).

$$n = \frac{6 \text{ bar} \cdot [4,5041 \times 10^{-5} \text{ m}^3]}{(273,15 + 20) \text{ K} \cdot 8,3144621(75) \times 10^{-5} \text{ m}^3 \cdot \text{bar} \cdot \text{K} \cdot \text{mol}^{-1}} = 1,10875 \times 10^{-2} \text{ mol} \quad (4-3)$$

Using a molar mass of 44,01 g/mol for CO<sub>2</sub>, and 28,9645 g/mol for common air, the masses are calculated in Equations (4-4) and (4-5) respectively.

$$m_{\text{CO}_2} = 1,10875 \times 10^{-2} \text{ mol} \cdot \frac{44,01 \text{ g}}{\text{mol}} = 0,4880 \text{ g} \quad (4-4)$$

$$m_{\text{air}} = 1,10875 \times 10^{-2} \text{ mol} \cdot \frac{28,9645 \text{ g}}{\text{mol}} = 0,32114 \text{ g} \quad (4-5)$$

Thus, the five muscles would consume either 2,44 g of CO<sub>2</sub> or 1,61 g of air in one full actuation. For portability reasons, a commercial liquid 20 oz. CO<sub>2</sub> reservoir<sup>10</sup> can be used for this matter. This cylinder would allow the system to perform **232** full actuation cycles of all fingers assuming isothermal gas consumption.

---

<sup>10</sup> Such as 5GAR9, W. W. Grainger Inc., Lake Forest, IL 60045, USA

### **4.3. Sensing**

After the actuation system was fully defined, was time to overcome the limitations from the previous rudimentary model. The main identified limitation [25] as stated in the *research background*, was about the tendons lack of tension when the wrist was extended or flexed and therefore the hand orientation changes, because there was no longer control over the movement of the fingers.

For that reason, instead of thinking about a complex hard mechanism, a practical solution was explored by the incursion in the field of sensing.

The incorporation of soft sensors not only reduces mechanical complexity, but also, it opens a path for controllability over the performance of the Orthosis. It will also represent a plurality of advantages that could fulfill other requirements such as *FR.4*.

Another potential application of the sensors is the possibility of remotely keeping record over the recovery progress of the patient. This would enable a physician to assess the patient without the need of a face meeting.

In the following sections, the selection process of the sensors is presented.

#### **4.3.1. Physical Variables to Measure**

To overcome the problem of the controllability of the fingers position, several concepts of variables to measure were developed. The first concept is related to a direct measurement of the tension of the strands, the second one is about determining the orientation of the hand, and the last one is about determining the position by resembling the human physiology.

##### **4.3.1.1. Concept 1: Tension of the Tendons**

The first concept consisted in measuring the tension of the ropes that resemble artificial tendons, using a sensor as depicted in Figure 4-22, and then use that value for mechanically compensate the lack of tension

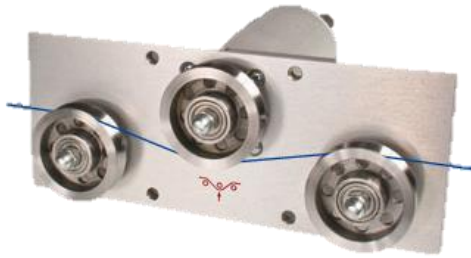


**Figure 4-22.** TSH sensor, Schdmith Control Instruments, Waldkraiburg, USA.

The obvious advantage is that there would be a closer control over the force exerted along the tendons, so these values could indirectly determine the exerted force in the movement.

However, a big implication about this concept is that there has to be one sensor per each rope, and given the size of them, the portability and overall geometry of the orthosis is compromised. Besides, since the measurement is performed per each tendon, the demand of inputs from the microcontroller is higher.

#### **4.3.1.2. Concept 2: Angle of the Wrist**

The second concept consisted in the use of integrated triaxial gyroscope (Figure 4-23) that would allow to measure the change in the hand orientation to a forward mechanical compensation of that disturbance.

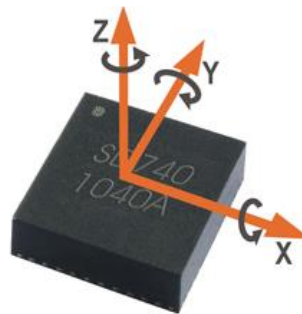


**Figure 4-23.** SD740 – Triaxial Gyroscope, Sensordynamics, 8403 Graz – Lebring, Austria.

The advantage of this concept is the portability. The minimum size of the electronic gyroscope and its low weight, make it ideal for incorporation in the same soft glove Orthosis.

The disadvantage is that for having good repeatability there has to be a fixed rigid reference point within the glove for measuring the angle and then relates it to the tension of the strands.

#### 4.3.1.3. *Mechanical Compensation for the First and Second Concepts.*

For the first and second concepts, there were thought two ways for mechanical compensation of the tendons lack of tension by applying changes on the actuation system.

The first way, as it is depicted in Figure 4-24 A. is about modifying the relative linear position of the actuation set according to the position of the wrist, in this way, the tension of the ropes would be adapted to the orientation of the hand. This of course would imply the use of an extra actuator for the linear displacement of the support structure.

The second way, as it is illustrated in Figure 4-24 B, is to ‘pre’contract the muscles, in order to overcome the lost tension of the tendons. The advantage in comparison with A. is that there’s no need of an extra linear-displacement actuator.

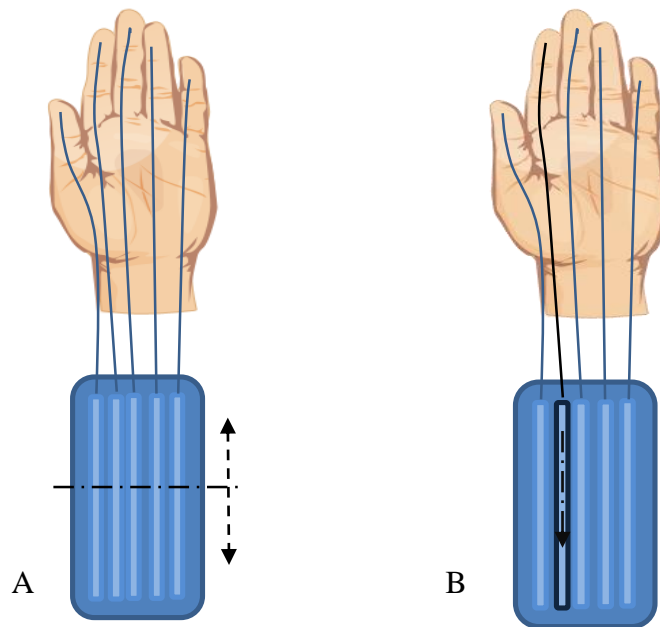


**Figure 4-24.** Mechanical compensation of the change of tension in the tendons.

### 4.3.2. Mimicking the Human Mechanoreceptors.

Regarding the physical variables to measure, it is inevitable to wonder how the human body senses the external environment in order to perform complex manipulation tasks with the fingers. For that reason, the human somatosensory system is being considered and studied.

The human body uses the skin as a transducer. Regarding manipulation tasks, certain innervated neurons within the hand allow the brain to perceive and plan the actuation of the muscles for fulfilling the desired motions. The mechanoreceptors are encapsulated nerve endings that send most of the tactile information [47]. They are sensitive to mechanical pressure or deformation of the skin.

There are four types of mechanoreceptors: Meissner’s corpuscles, Pacinian corpuscles, Merkel’s disks and Ruffini endings.

The mechanoreceptors are classified according to the rate of adaptation and frequency of stimulus. Table 4-4 shows the classification.

**Table 4-4.** Description of the mechanoreceptors of the human somatosensory system. [47]

<b>Receptor</b>	<b>Rate of adaptation</b>	<b>Stimulus frequency</b>	<b>Function</b>
<i>Merkel’s Disks</i>	SA-I (Slow adapting type I)	0—30 Hz	Pressure; edges and intensity
<i>Ruffini Endings</i>	SA-II (Slow adapting type II)	0—15 Hz	Directional skin stretch, tension
<i>Meissner’s corpuscles</i>	RA-I (Rapid adapting type I)	10—60 Hz	Local skin deformation, low frequency vibratory sensations
<i>Pacinian corpuscles</i>	RA-II (Rapid adapting type II)	80—400 Hz	Unlocalized high frequency vibration; tool use

From Table 4-4 can be inferred that:

- ✓ Contact forces and low frequency movements are detected by Merkel's discs and Ruffini endings. These two receptors are responsible for rough manipulation and force detection.
- ✓ Vibration primarily stimulates the Meissner's corpuscles and Pacinian corpuscles. Those receptors augment the sensitivity of the hand.

Sensors that resemble slow adapting mechanoreceptors would be good for the application, and for that reason, a new concept was developed and it is presented below.

#### 4.3.2.1. *Concept 3 Position of the fingers by resembling the Ruffini endings.*

This concept would overcome the disadvantages of the previous concepts. It consists in a flex resistive sensor that can be easily adapted to the orthosis. The main characteristic is that the measurement is aimed to be taken right over the finger. The resemblance idea is depicted in Figure 4-25.

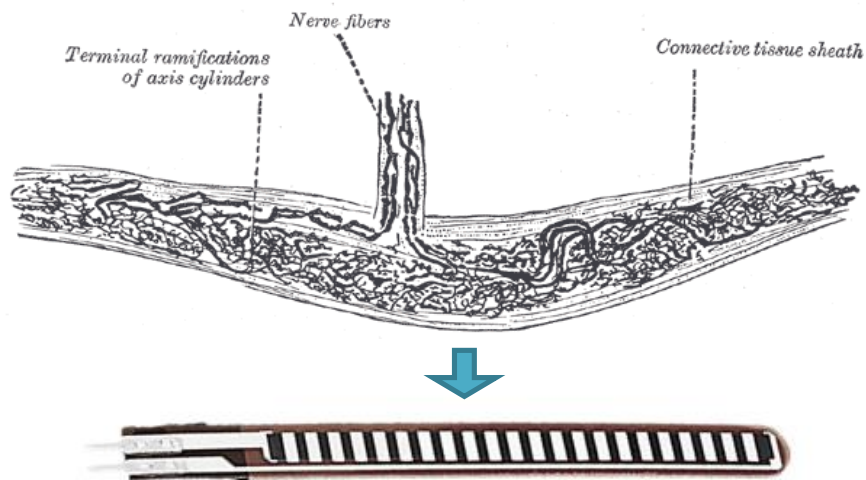


**Figure 4-25.** Resemblance Ruffini Endings → Flex Sensor<sup>11</sup>

<sup>11</sup> Image above taken from: [70]. The image down is Flex Sensor 5.9 cm, Tinker Soup, Berlin, Germany.

The flex resistive sensor is printed with a polymer ink that has conductive particles embedded in it. [48] The resistance changes while the sensor is bending and the particles are moving further apart. By measuring the resistance of a sensor placed in each finger, it is possible to determine how much it is bent.

The main advantage of performing the measurement directly over the fingers, is that then it doesn't matter whether the tendons have lost tension or not, because the system would just exert the required force and stroke until the finger completes its preprogrammed bending path.

Also, this concept wouldn't be affected by the tenodesis effect. The tenodesis effect is a phenomenon of passive grasping or extension that occurs when the wrist is moved due to the inner musculoskeletal configuration of the hand [13].

Thus, the tenodesis effect can be either complemented or compensated, because at the end what matters is that the users move their fingers to a desired position.

In summary, given that the relevant unknown is the final position of the finger relative to the resting position, the most practical solution would be to use a flex sensor for transduction.

### *Important Considerations*

Since there is not a known linear relationship between the excursion of the tendons and the position of the fingers, it will represent a huge and unpractical effort, to try to parameterize the rotational coordinate of each joint according to the displacement of the muscle. Thus, solely the fact of knowing when the finger is bend (with the help of the selected sensor) to a certain empirically determined position, with a repetitive and precise pattern, is good enough for the required application.

**4.3.2.2. *New variable to measure: force exerted over the finger by resembling Merkel Endings.***

Taking advantage of the previous study of the somatosensory system and regarding the *FR4 (Finger Intention of Movement)*, a new variable was taken into account. A FSR (Force Sensing Resistor) placed on the finger, would resemble the action of the slow adapting mechanoreceptor known as Merkel Endings.

For this application, the force determination would be aimed to serve as an intuitive indicator of selecting which finger should move, which is particularly convenient for people who can still use their other hand. The idea is that the sensing area would be located in the finger tips, where, in fact, the Merkel Endings have been found to be denser, such as depicted in Figure 4-26.

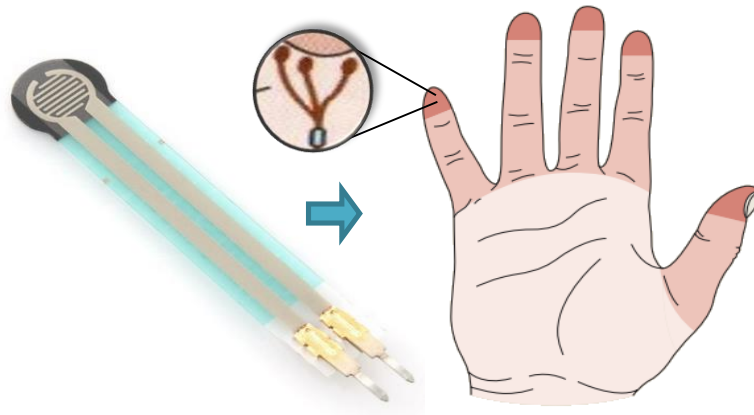


**Figure 4-26.** Resemblance Merkel Endings → Flex Sensor<sup>12</sup>

Even though the FSR would just serve as bi-state on/off switch ruled by a force threshold, it can easily be used in further developments for having real control over the pressure exerted in manipulation and grasping tasks.

---

<sup>12</sup> Right image taken from: [71]. The left image is a Force Sensing Resistor – 4 mm, Tinker Soup, Berlin, Germany.

### 4.3.3. Conclusion

The best concept to overcome the identified limitation of the rudimentary model was the Concept 3 that control de position of the fingers by measuring their flexion, in order to avoid any mechanical compensation. Also, this concept is not affected by the tenodesis phenomenon.

### 4.4. Visual Feedback

In this step, the *FR.4 Visual Feedback* is aimed to be fulfilled. Among several visual ways to indicate that the finger is moving (computer interface, display, etc.) a simple but effective way was chosen to do so: the use of LED's as visual indicators. The sketch of the first conception of the LED's and Sensors Layout is depicted in Figure 4-27. From now on, this part of the glove is going to be referred as an electronic layer of the glove.

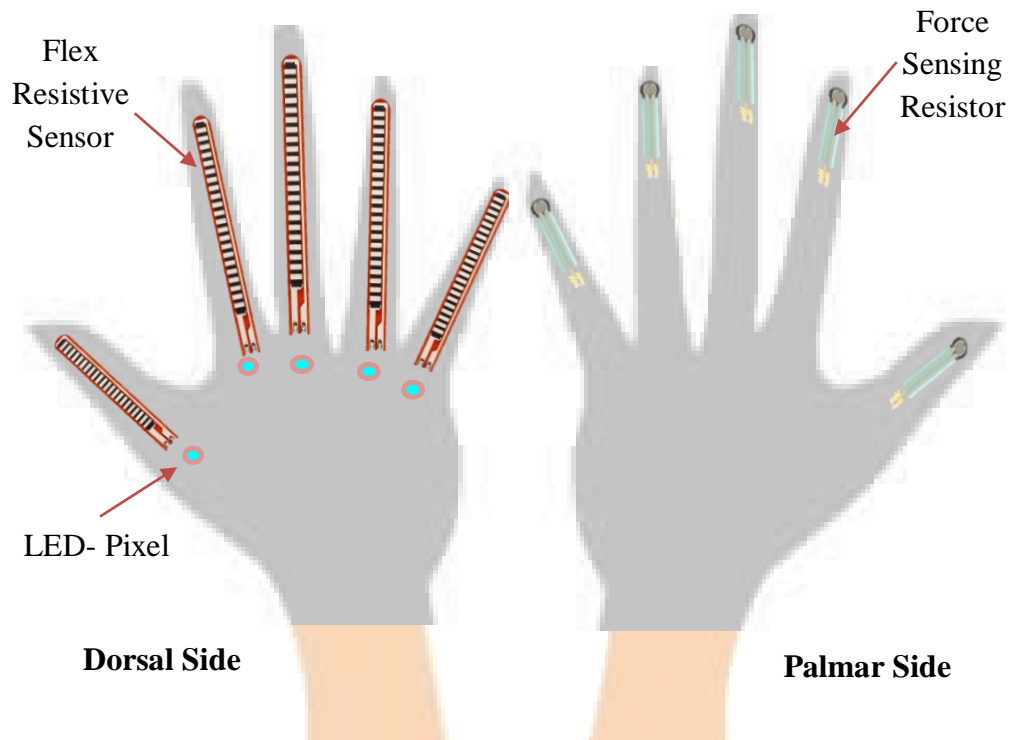


**Figure 4-27.** Sketch of the layout of sensors and indicators on the orthosis.

This represents an “electronic layer” of the glove that in combination with the “tendon - mechanical layer” will constitute the soft orthosis.

#### 4.5. Support Structure of the Actuators

In this section, the conception and development of the support structure for the actuators is going to be presented, including the mechanical -computer aided- design, and finite element analysis. From now on, the support structure of the actuators is also going to be referred as the frame of the actuators.

The support is supposed to be a rigid structure that contains the muscles that will actuate the soft orthosis (glove), it is planned to be worn in the forearm with a simple attachment method, so that hand disable people can easily use it.

##### 4.5.1. Conception

The first step in the conception was to take a look at the available anthropometric data, to have a clear idea of the magnitude of size of the required actuators’ support. An extract of relevant measurements from NASA’s anthropometric data is presented in Figure 4-28.

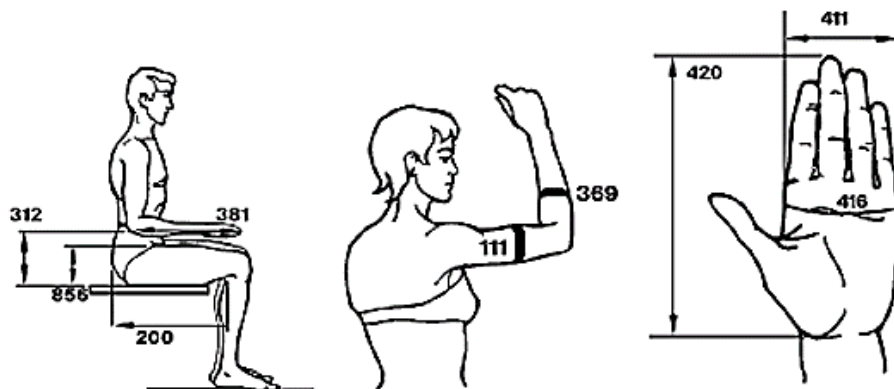


**Figure 4-28.** Anthropometric data related to the design of the orthosis. The relevant numbers are explained in the text. [49]

From the information presented above, the relevant features to consider for the actuators support design are: **369** (forearm circumference), **381**(forearm hand length) and **420** (hand Length). These dimensions are detailed for both men and women in Table 4-5.

**Table 4-5.** Relevant anthropometric data for the mechanical design of the actuation system. [49]

	<b>No.</b>	<b>Dimension</b>	<b>5th percentile [cm]</b>	<b>50th percentile [cm]</b>	<b>95th percentile [cm]</b>
<i>Female</i>	420	Hand length	15,8	17,2	18,7
<i>Male</i>			17,9	19,3	20,6
<i>Female</i>	381	Forearm - Hand length	37,3	41,7	44,6
<i>Male</i>			Not Available	Not Available	Not Available
<i>Female</i>	369	Forearm circumference, relaxed	19,9	22,0	24,1
<i>Male</i>			27,4	30,1	32,7

This application requires that the dimensions of the orthosis are chosen to be, as general as possible, so that most of people can use it. Therefore, the percentiles were strategically chosen for contemplating most of people from both genres.

In the case of the forearm's circumference, the data from of 95<sup>th</sup> percentile of men was considered, with a value of 327 mm in a relaxed condition, and therefore the calculated diameter of the forearm is 104, 09 mm. In this way, women population was included and even the man with the biggest forearm within the 95% of people is going to be able to wear it.

In the case of the length of the muscles' support, which is going to be worn on the forearm, the 50<sup>th</sup> percentile of the forearm-hand length, was contemplated as well as the 95<sup>th</sup> percentile of the hand's length. In other words, by considering that dimension, 50% of the people that are contemplated in the 95% of hand length are being enabled to use the brace. Both measurements were based on the women data, since they weren't completely available for males.

Finally, the forearm length was calculated with the subtraction of both features and the result is 230 mm.

The device was thought to be manufactured by 3D printing, that way, the features could be more customizable and the use of complex geometries such as roundness could make the structure suitable to be worn on the forearm.

From this point on, some concepts were developed, and are explained below.

### *Concept1*

The first concept for the PAM's support is illustrated with the sketch of Figure 4-29-Left. The main idea was to treat the muscle as a linear actuator with  $\text{Ø}18\text{mm}$  (inflated muscle), supported by a threaded attachment on the back side of the muscle.



**Figure 4-29.** Rough sketches of concepts 1 and 2.

### *Concept 2.*

The second concept is depicted in Figure 4-29 Right. This concept is similar than Concept 1, but one side of the muscle is attached to an extra piece which is used for tendon attachment and also as a slider in a T-shape slot.

Both concepts 1 and 2 are controversial, given that they are treating the muscles as linear actuators where there are surfaces in contact, which turn out to be opposite to one on the biggest

advantages of the use of PAM's in comparison with simple cylinders: the lack of friction within surfaces.

*Concept 3.*

The final and chosen concept was aimed to overcome an identified problem about the lack of comfort, if both muscles and springs were going to be placed on different sides of the forearm (such as depicted in the sketch of the Figure 4-12).

For that reason, this new concept includes both the muscles and springs in the same structure, over a curved shape that will fit in the forearm. The new sketch is presented in Figure 4-30, to use both actuators outside the forearm.

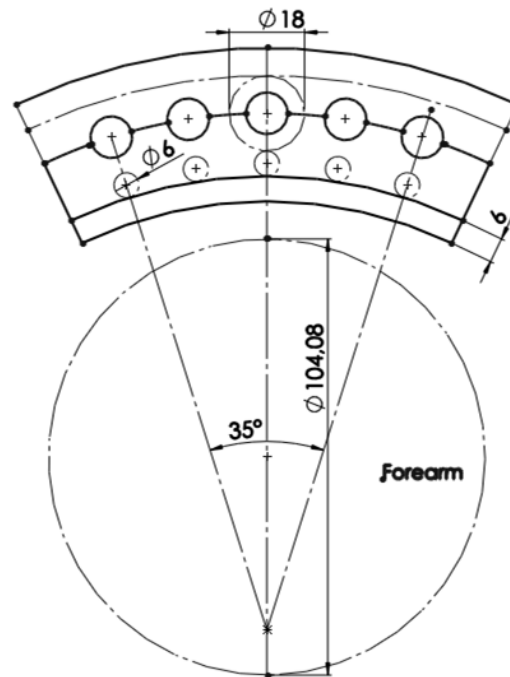


**Figure 4-30.** Rough sketch with some measurements for concept 3 of muscles' support.

As it can be seen in Figure 4-30, both the springs ( $\text{Ø } 6 \text{ mm}$ ) and inflated muscles ( $\text{Ø } 18 \text{ mm}$ ) diameters were contemplated in the design, as well as the forearm diameter. The final design consisted in three 3D printed parts.

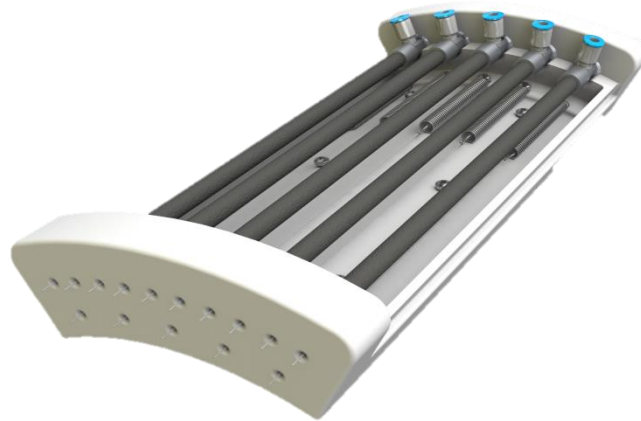


**Figure 4-31.** Part1. Final support structure for the actuators.

The part 1 (presented in. Figure 4-31), where the muscles and the springs are fixed, is 232 mm long (matching the anthropometric data of the forearm's length) and it is 38,81 mm tall.

In this structure, the springs are placed under the muscles.

The chosen material for the prototyping was Polyamide 12 (PA2200), because this is a type of plastic with good mechanical characteristics, and it is suitable for the contact with human tissue [50] which is ideal for the application.

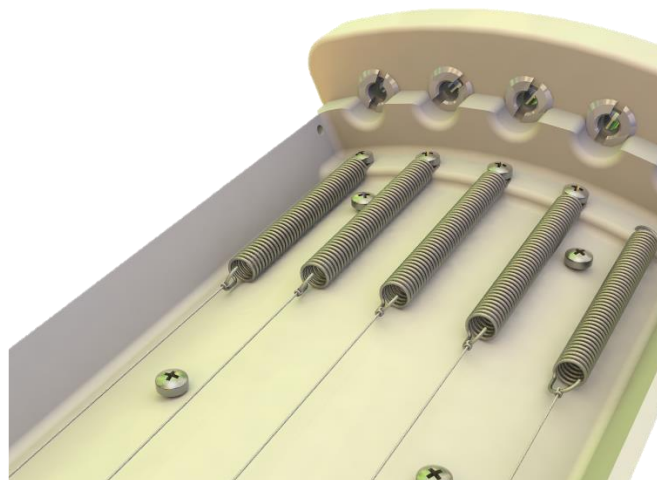


**Figure 4-32.** Attachment of the springs and muscles.

The springs are supported on the back of the structure with thermoplastic screws A2 3x8, as it is illustrated in Figure 4-32, while the muscles are attached with the use of metal screw inserts for enhancing the support into the structure. Also, the thread inserts can be manipulated for obtaining the desired orientation of the muscles in the structure.

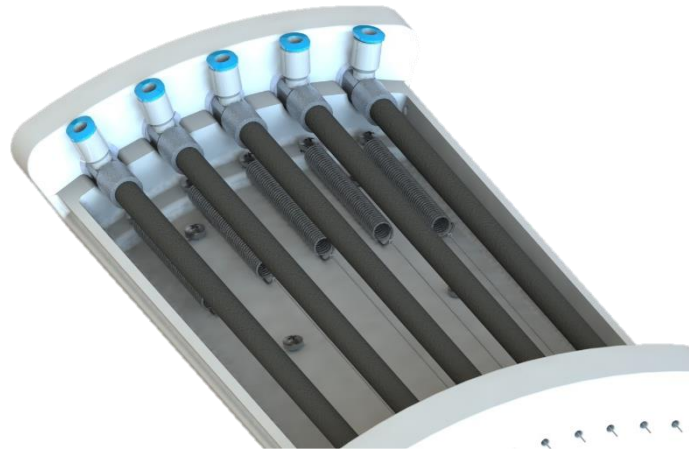


**Figure 4-33.** Inclusion of the fittings in the structure.

The Figure 4-33 illustrates, that the height of the device contemplates the height of the fittings QSM-B-M3-3-I-20, used for the artificial muscles tubing connection.

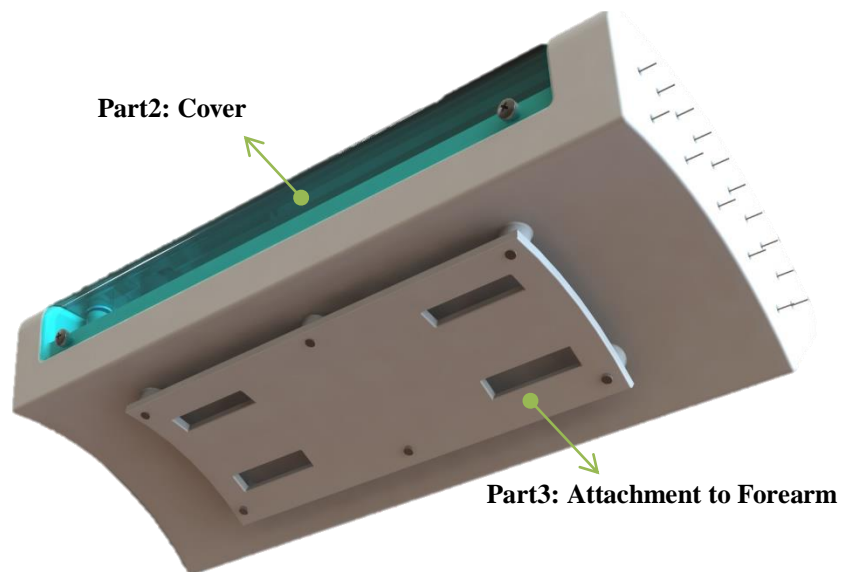


**Figure 4-34.** Concept 3. Muscles support structure.

On the other hand, Figure 4-34 shows the integration of the Part 2 and Part 3 corresponding to the cover of the frame and the attachment of device with straps to the forearm, respectively.

The part 3 is attached to the part 1 with 6 thermoplastics screws PT A2 3x14, while the part 2 is attached using 4 PT A2 3x8. Both of them are easily separable from the main frame. The part 2 was planned to be transparent, so that the user could observe when the muscles move. Also, part 2 contemplates the proper holes for placing the fittings and for plugging the tubes from outside the structure.

Regarding the slots where the artificial tendons pass through, Figure 4-35 shows the selected configuration. All the holes are  $\varnothing$  2 mm with fillets, so the tendons can move freely within them. Every edge of the slots is smoothed down for a better excursion of the tendons.



**Figure 4-35.** Tendons slots.

About the tendons connection, the springs are going to be attached to one thread of tendon. Whereas the muscles are going to be attached to 2 threads of tendon, for having more stability as well as avoiding any sharp edges that could cut the tendons.

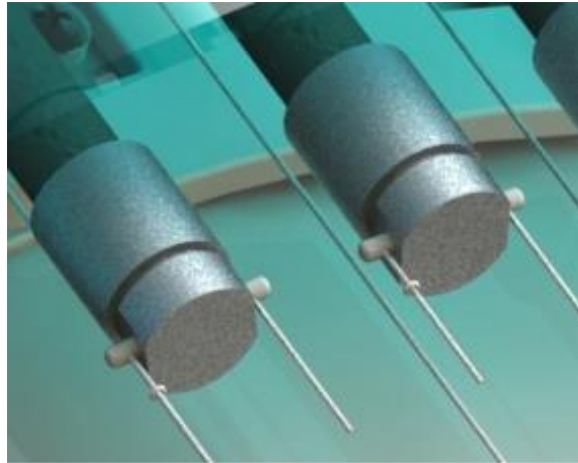


**Figure 4-36.** Tendons attachment to the muscle.

As it is depicted in Figure 4-36, the tendons are attached to the muscle using a press fitted connection of a  $\text{Ø}1,5 \times 12$  mm metallic pin, by doing this, there is not going to be any relative displacement between the tendon and the muscle and therefore the force is transmitted properly. Moreover, a knot is made on one side of the connection, where it can be easily detached in case of giving maintenance.

Now, considering these 3 components: muscle-tendon-pin, the Figure 4-36 can be related with Figure 4-35, where there is a cavity for securing the end of the muscle during its extension. The actuator is going to be guided by the symmetric tension of the two threads of the tendon into the cavity every time it deflates. By doing this, there is no necessity of surfaces in contact like in the first two concepts.

Additionally, the soft nature of the artificial muscles, makes possible to bend them during the assembly process, which is useful after attaching the tendons and then the muscles can placed manually to their resting position into the cavity.

For fixing the support structure to the forearm, a couple of Velcro straps were selected.

Finally, all the parts can be easily distinguished in the exploded view of Figure 4-37.

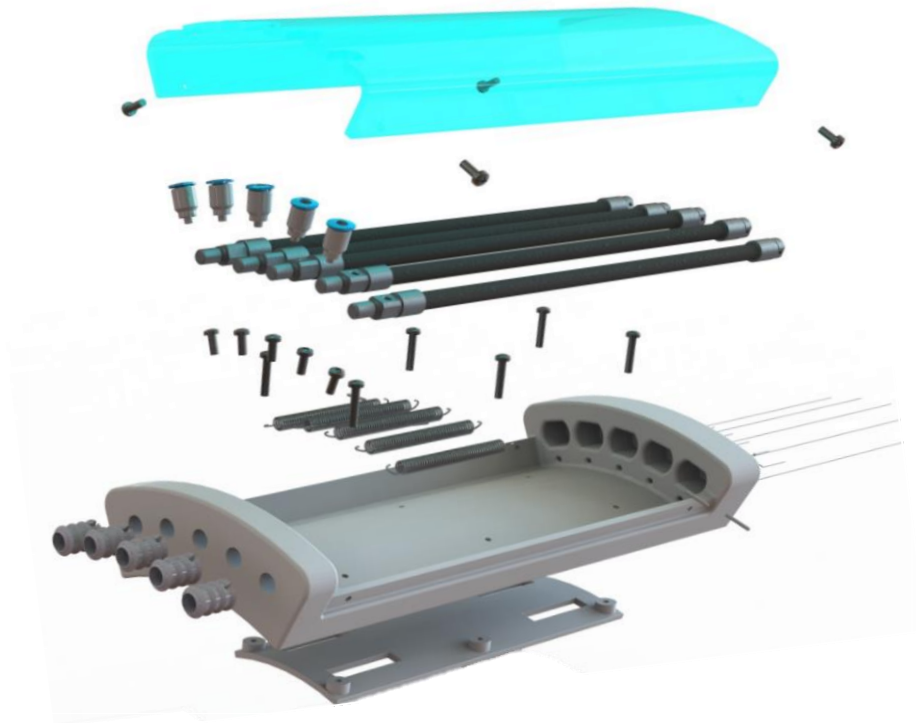


**Figure 4-37.** Exploded view of the actuators support structure.

#### 4.5.2. Finite Element Analysis

As part of the mechanical design, a FEA (Finite Element Analysis) was performed over the support structure of the actuators. An analysis of static forces analysis under Von Mises Criterion was realized, given that the PA2200 is a ductile material with a yield strength of 103,6 MPa.

A high quality solid standard mesh was performed in a simplified model of the whole assembly (without fillets), as it is depicted in Figure 4-38, with 93113 nodes and 57882 domain elements.

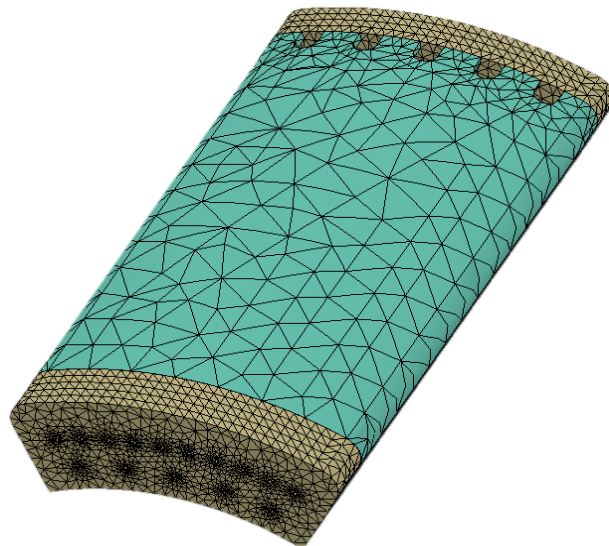


**Figure 4-38.** Mesh of the support structure of the actuators.

On a first study, ten forces of 100 N were axially applied in the specific points that anchor the actuators, whereas the opposite side of the structure was assumed to be a rigid surface, with the intention of inducing the greatest bending moment over the structure. The results of the simulation are shown in Figure 4-39.

With a total of 1000N, the structure does not experiment any visible deformation in a true scale. The greatest stress (2,9 MPa) is focused on the holey side of the cover (part 2), and the minimum stress is experimented on the widest walls.

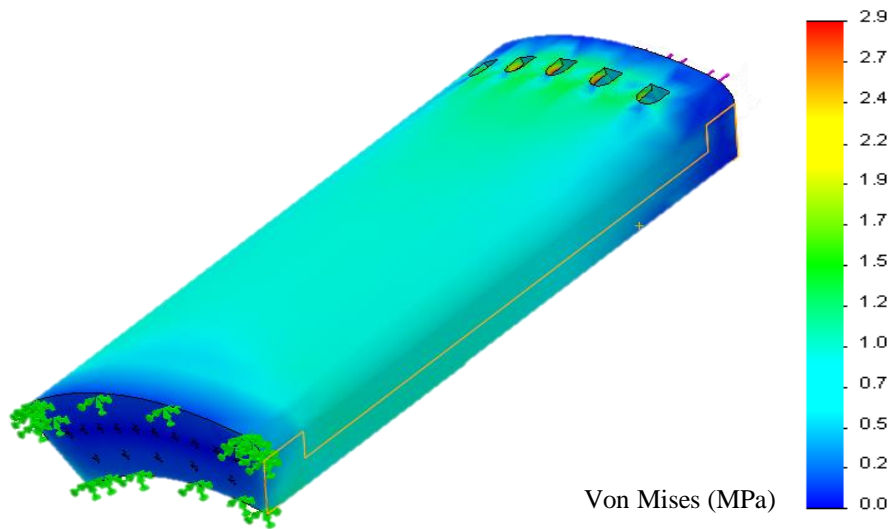


**Figure 4-39.** Von Mises stress study 1.

Regarding the factor of safety of the structure, a plot was generated and it is shown in Figure 4-40. The predominant FOS within the whole structure turns out to be 35 as a minimum value. This means that with 1000 N of axially applied force, the structure is not going to fail according to Von Mises criterion.

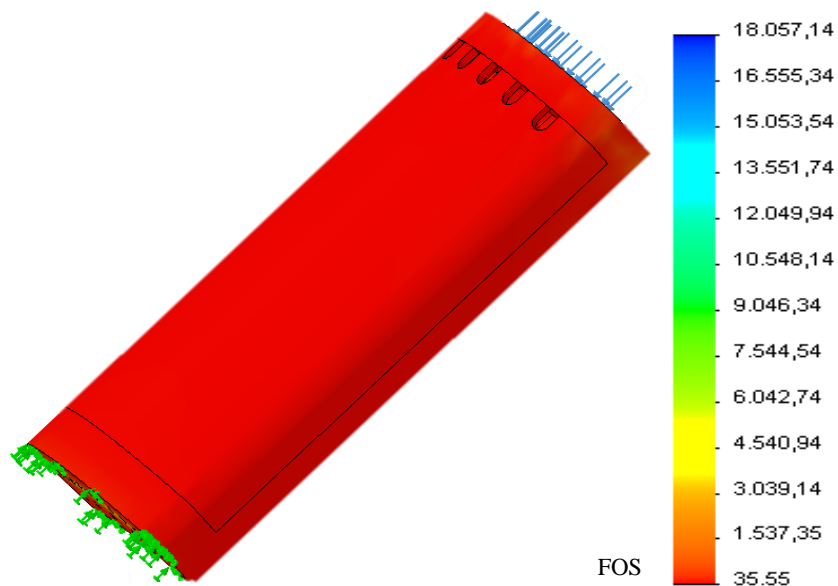


**Figure 4-40.** Factor of Safety study 1.

On the other hand, in a second study, 100N were applied in the direction normal to the 6 surfaces of the cover. The results are depicted in Figure 4-41

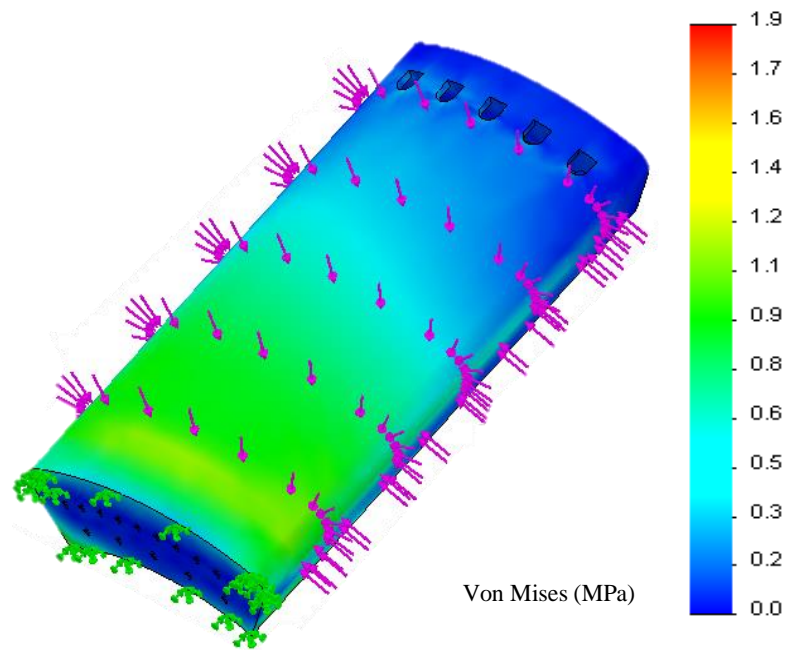


**Figure 4-41.** Von Mises stress study 2.

As it can be seen in the Von Mises stress plot of study 2, the greatest stress turned out to be 1,9 MPa in the zones near to the fixed boundary surface. On the other hand, the lowest stress is focused on the widest walls. This high resistance is product of the curved shape of the part 2 (cover), which particularly gives it more stability, because the lack of stress concentrators.

Finally, no strain is visible under a true scale.

For checking the FOS, the plot is presented in Figure 4-42

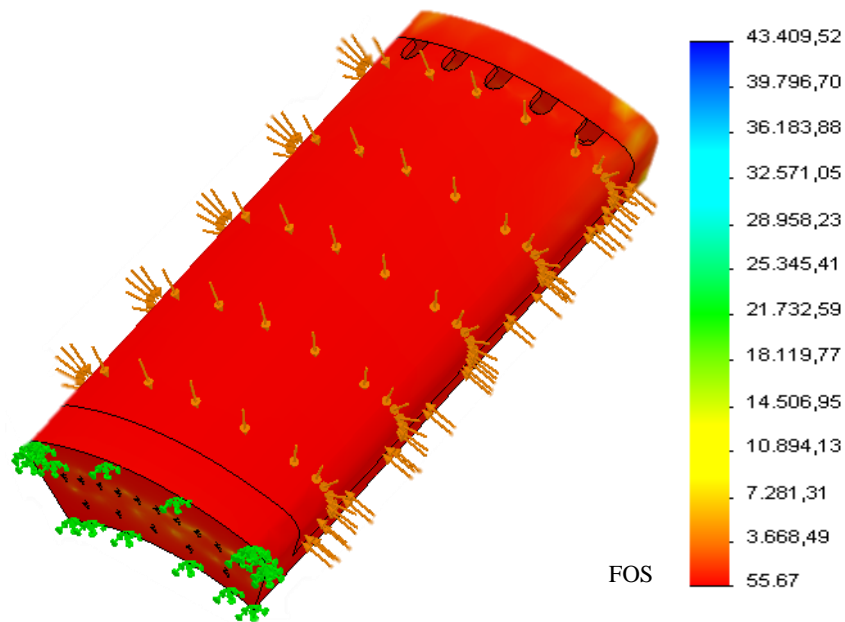


**Figure 4-42.** Factor of Safety study 2.

The overall factor of safety turned out to be 55, which means that under the total of 600N applied in the direction normal to the surfaces of the cover, the actuators support structure won't fail according to Von Mises criterion.

With this, it is verified that the mechanical design is correct.

#### **4.6. Tendons Layout in the Glove**

Since the support structure for the actuators was designed to include both muscles and springs on the same housing (so the comfort and easiness to wear were enhanced), then the glove required certain modifications for being able to work properly with the actuation system.

The tendons within the glove were planned to be placed inside the glove, leaving the outer surface for the electronic layout of the sensors and indicators.

Now that the sensory system assures that the finger do not lose their bending programmed path, it is possible to manipulate the tendons by curving the straight trajectories and then route them strategically, so that their terminals can be placed on the dorsal side of the hand (such as depicted in Figure 4-43), because at the end, what it does matter is the change of length in the excursion of the tendons.

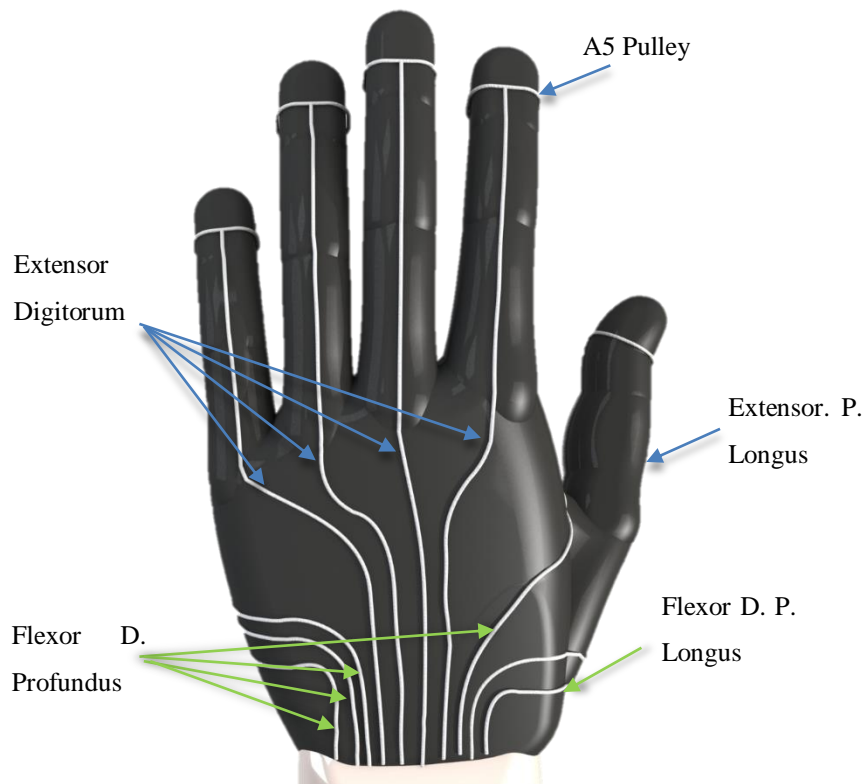


**Figure 4-43.** Dorsal side. Tendon-Pulleys layout of the glove.

As it can be appreciated in Figure 4-43, the tendons coexist in the dorsal side of the hand. A piece of artificial tendon is rolled over the Distal Phalanx to serve as an A5 Pulley that has to be placed as far from the DIP as possible to increase the momentum over it when the force is exerted, but not too far from it, so the pulley is still able to serve as a ring who can conduct the finger through its path.

Regarding the palmar side, the tendons were placed to follow the creases of the hand, since the creases normally follow the normal stresses imposed by the movements of the hand [13]. By doing this, the tendons wouldn't interfere with the natural motion of the palm and fingers. This resemblance can be addressed in Figure 4-44.

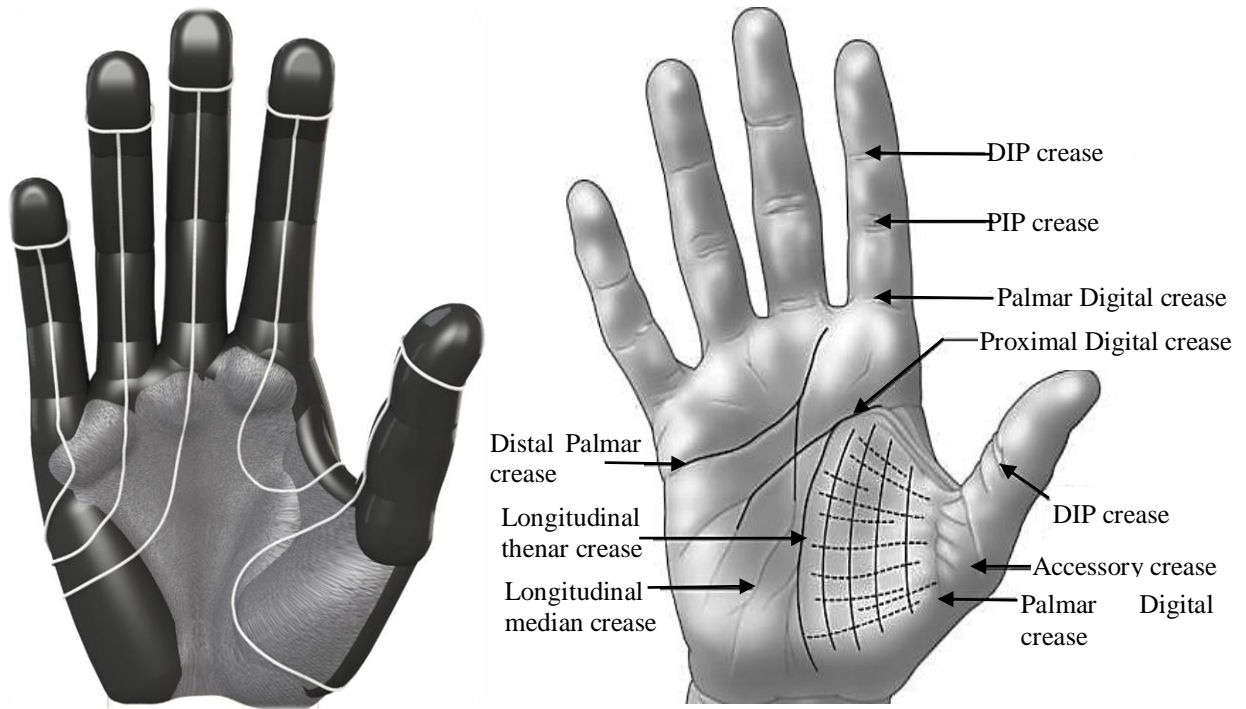


**Figure 4-44.** Palmar side. Tendon-Pulleys layout of the glove.

Thus, the tendon of the Flexor Pollicis Longus of the Thumb, is going to be routed over the Longitudinal Thenar crease, the FDP's of both the Index and the Middle fingers are going to be routed along the Proximal Digital Crease, and finally the FDP's of both Ring and Little fingers are going to be routed in a path close to the Distal Palmar crease.

For the implementation of the testing model, a size 8 glove<sup>13</sup> was chosen for the application.

<sup>13</sup> KCL 0665 08 Handschuh GemoMech® Nitril, Polyamid, Polyurethan Größe 8, Conrad, Germany



**Figure 4-45.** “Tendon - Layer” of the glove.

As it can be appreciated in Figure 4-45, the glove was planned to be used conversely than the conventional way (the elastic rubber-like surface is placed in the palmar side of the hand). So, by placing now that surface on the dorsal side of the hand, there is an extra force that will complement the action of the springs as antagonists in the restitution of the fingers position.

The whole mechanical system, regarding the actuation system and the orthosis, is shown in Figure 4-46.



**Figure 4-46.** Mechanical system of the project.

## **4.7. Electronics Design**

This section is aimed to show the details regarding the electronic system. The design of the electrical layer of the glove is presented, as well as the electronic control of the valve, the signal conditioning of the sensors and the selection of the power supply. It concludes with an overall description of the electronic circuit.

### **4.7.1. Electrical Layout of the Glove**

The final electronic configuration over the glove is depicted in Figure 4-47

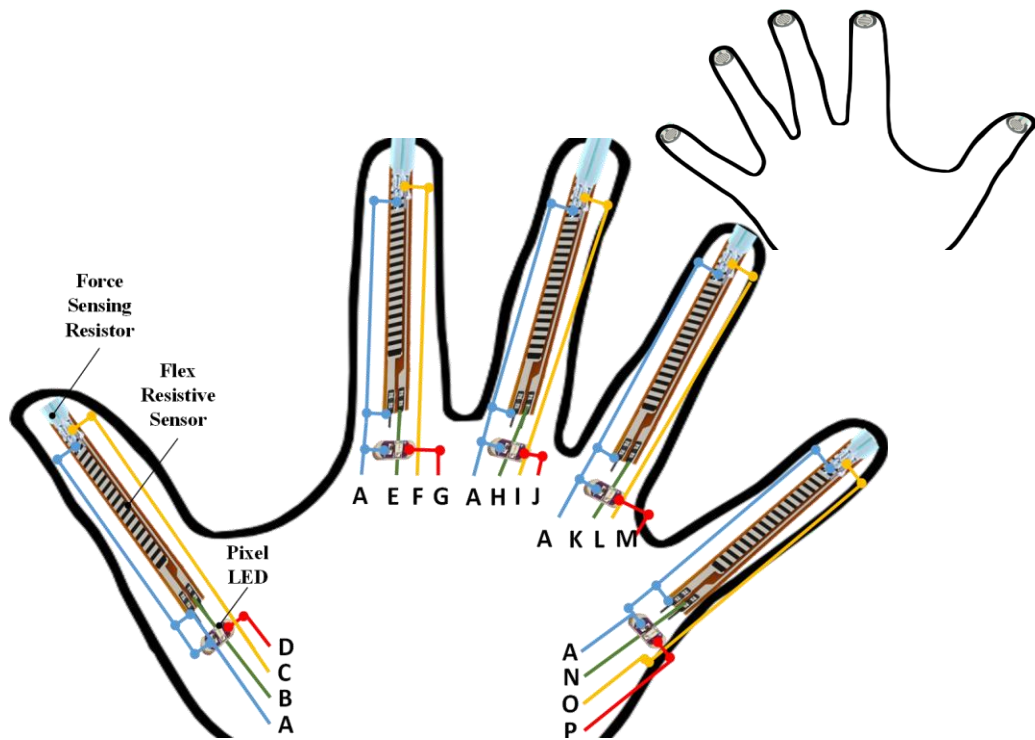


**Figure 4-47.** Electric layout of the glove. The connections are explained in Table 4-6.

Besides the sensors and Flora Pixels connections, just ground (GND) is integrated in the glove, this with the intention to avoid any contact between  $V_{cc}$  and GND within the glove. All the 16 wires were planned to be connected to the main electronic circuit with the use of a Ribbon Crimp Connector<sup>14</sup> and a Ribbon Cable, the connections are detailed in Table 4-6.

**Table 4-6.** List of electrical connections of the visual indicators and sensors in the glove

Letter	Connection	Letter	Connection
A	Ground (0V)	I	FSR3
B	FlxRS1	J	LED3
C	FSR1	K	FlxRS4
D	LED1	L	FSR4
E	FlxRS2	M	LED4
F	FSR2	N	FlxRS5
G	LED2	O	FSR5
H	FlxRS3	P	LED5

<sup>14</sup> Ribbon Crimp Connector - 10-pin (2x5, Female) - PRT-10650, Tinkersoup.de, Berlin, Germany

As can be inferred, this part of the project is related with textiles. For this thesis, the implementation of the electronics system within the glove of the testing model is going to be developed using conventional methods. However, it is important to highlight the availability of cutting edge technologies for textile integrations that are conducted by the Fraunhofer IZM<sup>15</sup>

#### 4.7.2. Controller

The controller was chosen, both to retrieve the signals from the sensors and to perform the main control over the orthosis. The system should have 5 PWM outputs and 10 analog inputs, so that the 5 VEAA valves and the 10 sensors are contemplated. In the case of the LED's, they are connected to the same PWM outputs to indicate the muscles activation.

The selected controller was **AtMega32U4** integrated in an Arduino Micro Board. The list of features of this board can be found in Table 4-7.

**Table 4-7.** List of relevant features of the Arduino Micro board. [51]

<b>Feature</b>	<b>Description</b>
<i>Microcontroller</i>	ATmega32u4
<i>Operating Voltage</i>	5V
<i>Input Voltage (recommended)</i>	7-12V
<i>Input Voltage (limits)</i>	6-20V
<i>Digital I/O Pins</i>	20
<i>PWM Channels</i>	7
<i>Analog Input Channels</i>	12
<i>DC Current per I/O Pin</i>	40 mA

This board was ideal because of its minimum size and the capacity of the microcontroller to manage the required number of inputs and outputs. These outstanding features can be appreciated in Figure 4-48.

---

<sup>15</sup> Texlab, Fraunhofer IZM.

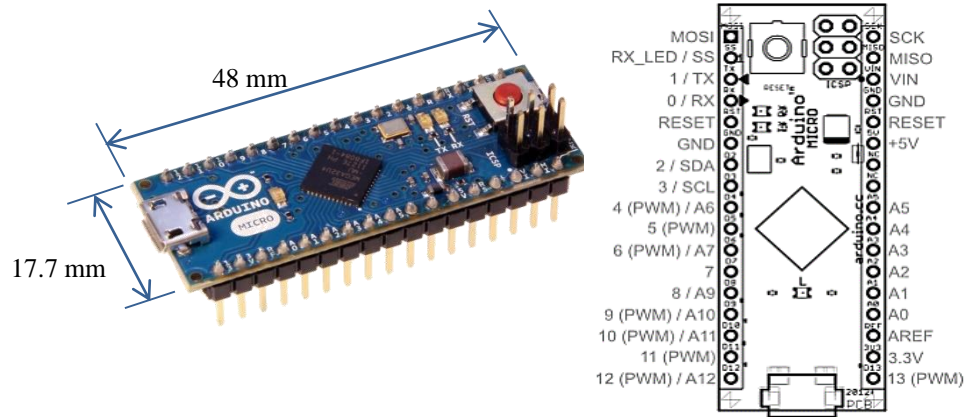


**Figure 4-48.** Dimensions and Pin out of the Arduino Micro. [51]

The pins 3, 5, 6, 9, 10, 11 and 13 can be used as 8-bit PWM outputs, which is ideal for the application.

### 4.7.3. VEEA 3/3 Piezo Valves.

The electronic circuit related with the high power interface and control of the piezoelectric valves is illustrated in the annex *Electronic Control of the VEAA 3/3 Piezo-valves* in Figure B-1. This circuit was developed by Festo, for testing the suitability of the valve in its laboratory.

It works with a single 5V PWM control signal for both the pressure and release side of the valve. The step up DC-DC conversion (blue dotted square in Figure B-1.) is done from a 9V-20mA source to 300V-600μA, representing 180 mW that are enough to feed the 5 valves.

The final behavior of the valve is illustrated in Figure 4-49. It can be inferred that when the analog signal ( $U_e$ ) reaches 2,5V (50% duty cycle of a 5V PWM) the valve is in the middle closed position, and the muscle holds its level of contraction. Under 2,5 V, the muscle deflates and over 2,5 V the muscle inflates.

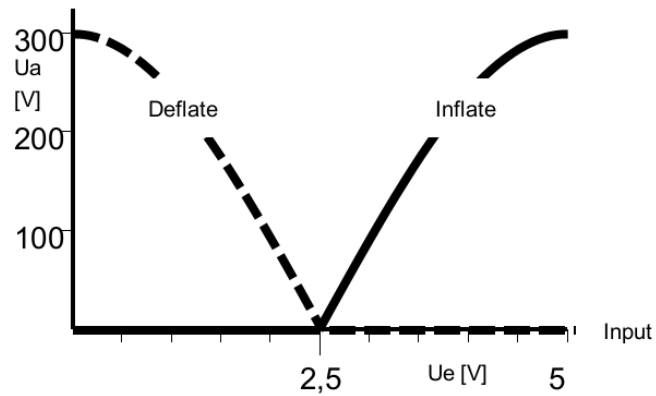


**Figure 4-49.** Behavior of the Valve according to the Control signal and the Power conversion<sup>16</sup>.

#### 4.7.4. Signal Conditioning

Once the valves, sensors and controller were chosen, then the interface between the sensors and the controller had to be realized.

For this task, is first important to highlight the electrical characteristics of the analog inputs of the ADC of the microcontroller. The Atmega32U4 has an input impedance of 10K $\Omega$  and it can handles up to 40mA [51].

##### 4.7.4.1. Signal Conditioning of the Flex Sensors

The datasheet of the Flex Sensors (See [B.3.2](#)) established that the maximum range of resistance goes from 25 k $\Omega$  to 125 k $\Omega$ . However, to have a wider span resolution, the range of values were experimentally determined by wearing the sensor on the glove and therefore using different levels of flexion possible with each finger. This characterization can be appreciated in *Chapter 6 Section 2*.

According to the information from the sensing characterization, a value of 60 k $\Omega$  was found to be the maximum bending resistance when wearing the sensor on the glove.

<sup>16</sup> Taken from the design of Dipl. Ing. Hannes Wirtl. Festo PiezoValves Division

The first simple configuration of measuring the flexion is a voltage divider between the sensor and one pull up resistor, as it can be depicted in Figure 4-50.

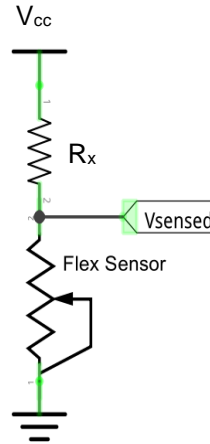


**Figure 4-50.** Basic configuration of the Flex Sensor measurement.

The idea is to select a proper pull-up resistance value for the maximum span of the sensor, requiring minimum forward amplification. The best way to do this, is to consider the resistance of both maximum bending and flat positions of the sensor and establish the following function:

$$s(R_x) = \frac{V_{cc} \cdot R_{f \max}}{R_{f \max} + R_x} - \frac{V_{cc} \cdot R_{f \min}}{R_{f \min} + R_x}$$

(4-6)

The equation (4-6) treats the span as a difference between the maximum and the minimum voltage of the sensor under the limits of its measurements. span (s) is presented as a function of  $R_x$ , the pull up resistor of the voltage divider.  $R_{f \max}$  and  $R_{f \min}$  are the maximum and minimum values of the flex resistive sensor respectively.  $V_{cc}$  is voltage used to feed the system (e.g. TTL 5V)

The value of  $R_x$  is calculated by optimizing the equation (5 3):

$$\frac{ds}{dR_x} = V_{cc} \left( \frac{60k\Omega}{(R_x + 60k\Omega)^2} - \frac{25k\Omega}{(R_x + 125k\Omega)^2} \right) = 0$$

(4-7)

A program in matlab was implemented for solving Equation (4-7).

```
syms R;
s=5*60/(60+R)-5*25/(25+R);
ds=diff (s,R);
Rvalues=eval (solve (ds,R));
Rideal=max (Rvalues); % Choose the positive value
display (strcat ('The ideal value of R is: ', num2str (Rideal,5), ' kOhms'));
```

The solution of equation (4-7) is {38,73 kΩ, -38,73 kΩ}. So, the selected resistor for a maximum span had to be approached to 38,73 kΩ.

For approaching to a proper value, the relationship between the sensor output span and the pull up resistance is plotted in Matlab.

```
graph=eplot (s, [0,65]);
ylabel ('Span Width (Volts)');
xlabel ('Value of R (kOhms)');
hold on
plot (Rideal, subs (s,R,Rideal), 'r*');
```

The result is depicted in Figure 4-51. In the range of values near the found solution (red asterisk), the voltage span is approximately 1,05V.

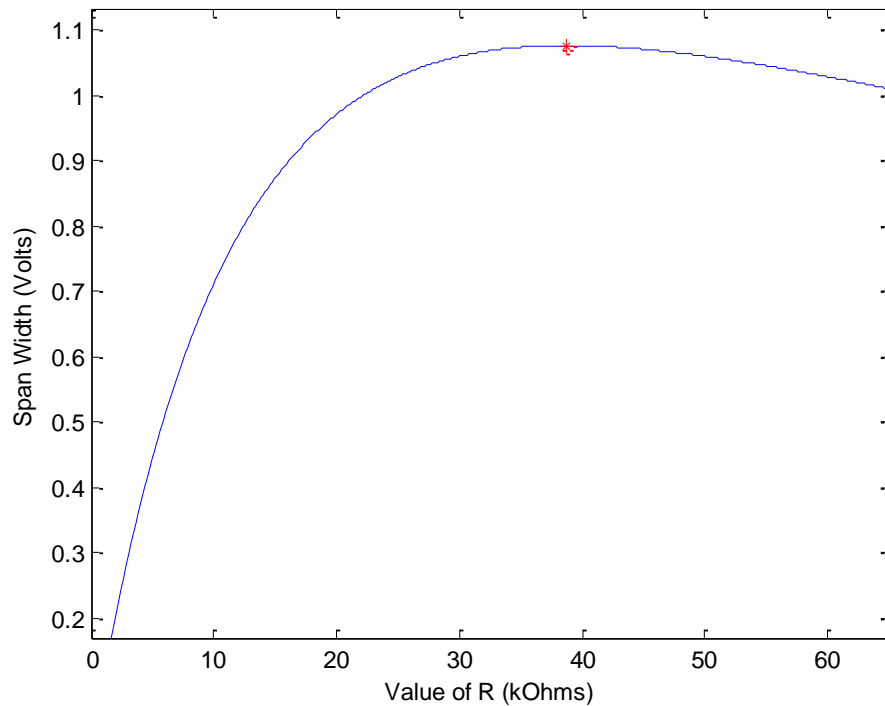


**Figure 4-51.** Span Width (Volts) vs Pull up Resistance (k $\Omega$ )

As it is observed in the Figure 4-51, if a commercial value of 39 k $\Omega$  is selected as the pull up resistance, there is not going to be any significant difference in the width of the output span of the sensor; hence, that value was chosen.

By calculating the voltage division, the span limits of the sensor turn out to be: 1,9531 V and 3,0303V. However, there is an inconvenient since that span doesn't exactly match with the ADC input span which is from 0 to 5V. Thus, it is necessary to condition the signal with an offset level and amplification for using the entire ADC range.

Figure 4-52 illustrates the span mismatch and the result after the level shifting.

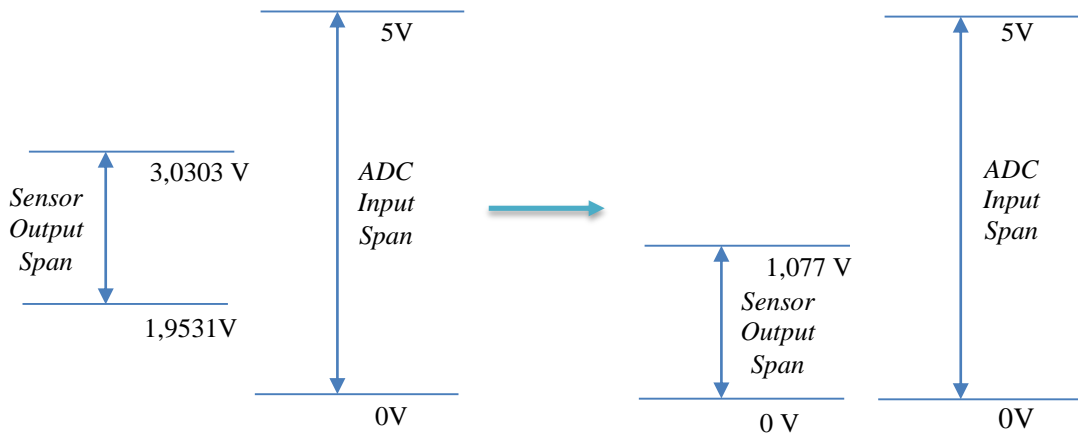


**Figure 4-52.** Spans mismatch and level shifting correction.

The lowest value from the sensor (1,9531V) is going to be considered as a voltage reference ( $V_{ref}$ ) to perform the level shifting through a subtraction operation. Using voltage division and an arrangement of commercial resistors the  $V_{ref}$  is approached with a practical reference value ( $V_{ref-p}$ ) by Equation (4-8).

$$V_{ref-p} = 5 \cdot \left[ \frac{100k\Omega}{100k + (150k\Omega + 6,2k\Omega)} \right] = 1,9516V$$

(4-8)

After doing this, the limits of the span regarding the practical offset level ( $V_{ref-p}$ ) are:  $V_{min} = 1,5$  mV and  $V_{max} = 1,0787$  V.

Then is time to amplify the signal to match the upper limit of the ADC input span. The spans mismatch and the required modification are illustrated in Figure 4-53.

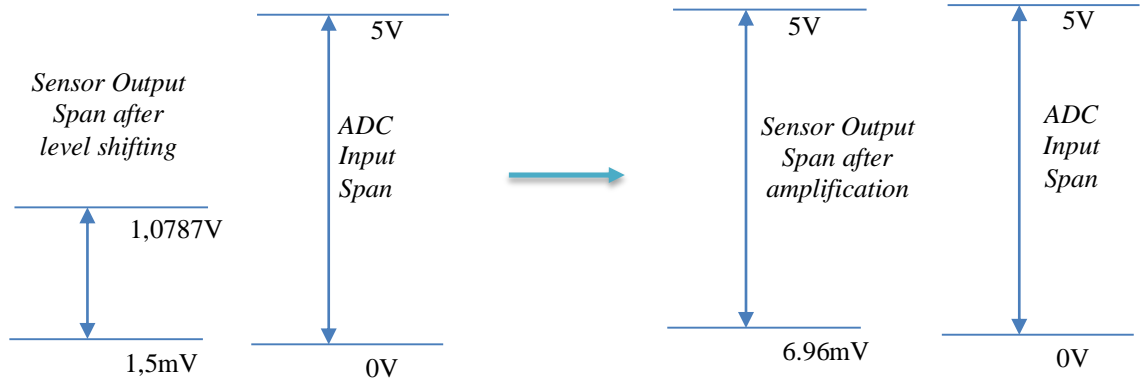


**Figure 4-53.** Spans mismatch and required amplification.

Regarding the amplification (Figure 4-53), the required gain as a relation between the desired upper limit (5V) and  $V_{\max}$  is 4,6352.

For fulfilling the required amplification and level shifting, operational amplifiers were considered. However, the use of a simple differential amplifier was discarded because its transfer function is sensitive to changes in the source impedance of the inputs.

Thus, an arrangement with operational amplifiers was develop in an instrumentation differential amplifier which given its high impedance input, won't vary the gain of the amplification due to a change in the source impedance of the sensor. The implemented circuit is shown in Figure 4-54

The equation (4-9) shows the relationship between the input and the output in an instrumentation differential amplifier.  $R_f$  and  $R_g$  are illustrated in Figure 4-54, both resistors are responsible of the gain of the circuit, but it is usual to set the gain solely with  $R_g$ .

$$V_{out} = (V_{sense} - V_{ref}) \cdot \left[ \frac{2R_f}{R_g} + 1 \right]$$

(4-9)

The practical value of the gain of the circuit is calculated in equation (4-10).

$$A_G = \left[ \frac{2(100k)}{(51k\Omega + 3,9k\Omega)} + 1 \right] = 4,6430$$

(4-10)

Figure 4-54 represents the circuit and the configuration in LTSPICE for the simulation of the Flex Sensor signal conditioning.

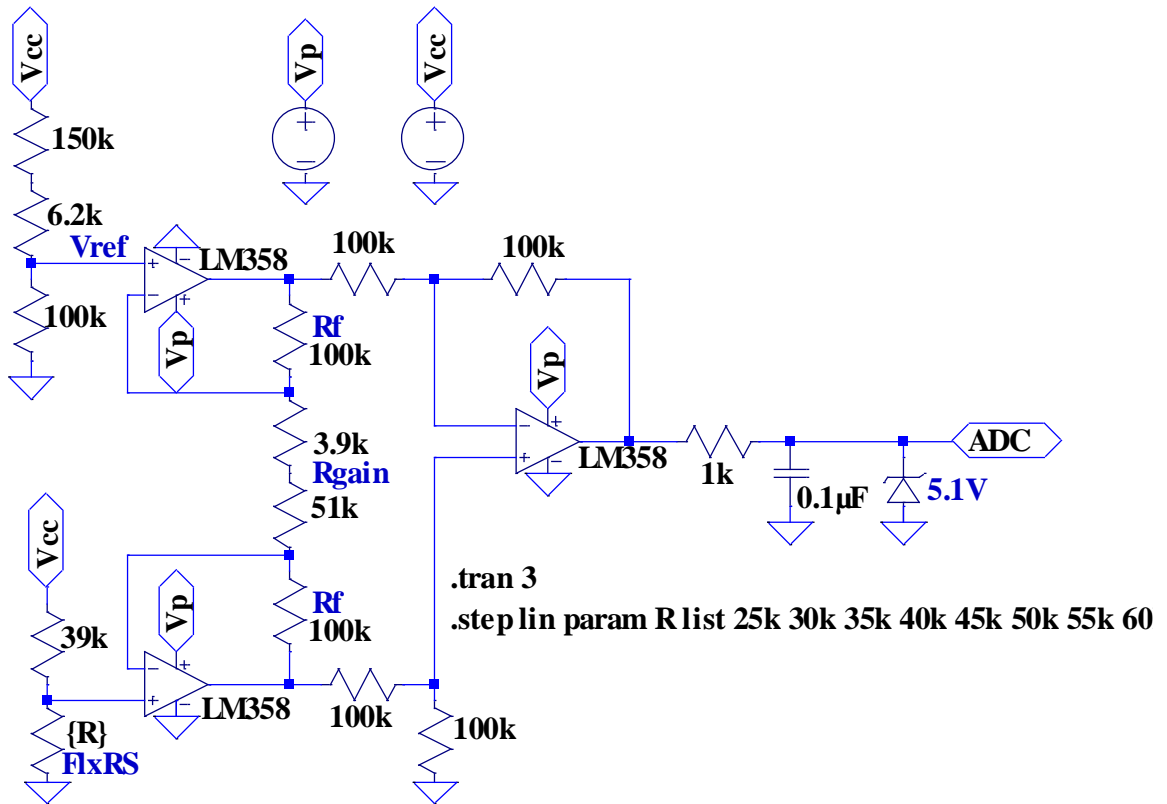


Figure 4-54. Signal conditioning of the Flex Resistive Sensor

To achieve better Common Mode Rejection Rate (CMRR) performance and also for simplifying the calculations, R1-R4 were selected as a set of 100 kΩ resistors, the equation of the differential amplifier is reduced as following.

With the gain calculated in equation (4-10), the final function between the input and output is presented in equation (4-11).  $V_{sense}$  is the sensor measurement and  $V_{out}$  is the output value of the conditioned signal.

$$V_{out} = (V_{sense} - 1,9516) \cdot 4,6430 \quad (4-11)$$

Besides the level shifting and the amplification, the signal also is filtered using a first order low pass filter at the end of the instrumentation differential amplifier. The cut off frequency is calculated in equation (4-12).

$$\frac{1}{2\pi \cdot 1k\Omega \cdot 0,1\mu F} = 1,6kHz \quad (4-12)$$

And finally to protect the ADC input from an overvoltage, a 5,1 V Zener diode is used for voltage regulation. The result of the simulation of the circuit presented in Figure 4-54 is shown in Figure 4-55. The flex sensor was simulated as a list of different resistance values from 25kΩ to 60kΩ.

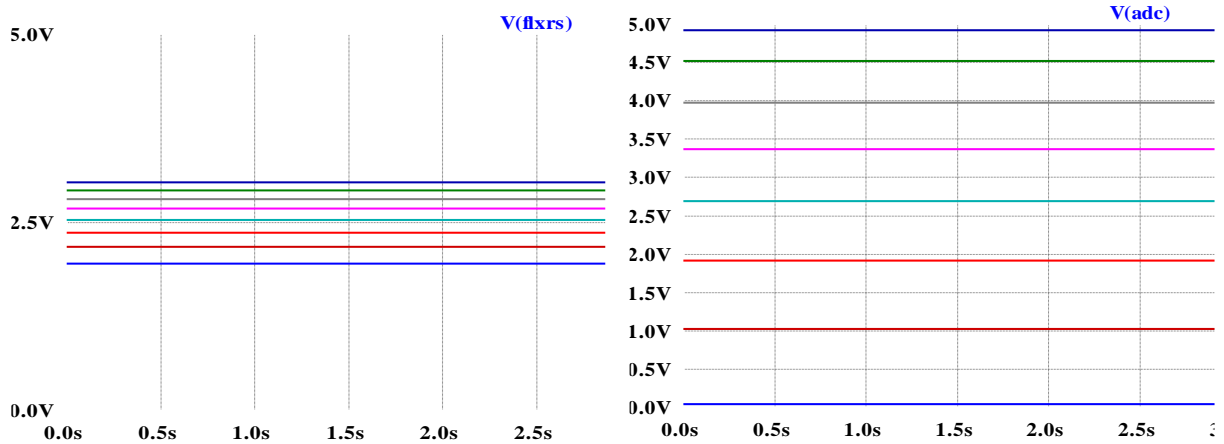


**Figure 4-55.** Simulation of the signal conditioning of the Flex Resistive Sensor

As it is depicted in the simulation, the measured signals from the sensor (left image) are distributed in the whole ADC span after the signal condition (right image).

Regarding the value of each bit from the ADC. The ADC of the Atmegau24 has a resolution of 10 bits, the voltage value of each bit is calculated in equation (4-13).

$$\frac{\text{Input}}{\text{Resolution}} = \frac{5}{2^{10} - 1} = 4,89 \frac{mV}{bit} \quad (4-13)$$

Thus, the total lost bits (LB) in the whole span are calculated in equation (4-14).

$$LB = 6,96mV \cdot \frac{1bit}{4,89mV} = 2 \quad (4-14)$$

This means that, after the signal conditioning, there is going to be a loss of just 4 bits out of 1024.

#### 4.7.4.2. Signal Conditioning of the Force Sensing Resistors.

According to the datasheet of the Force Sensing Resistor (See B.3.3), the resistance in the sensors varies from several Megaohms to few ohms. For this matter, to have a wider range of sensing in relation with the force exerted, the manufacturer recommends the configuration shown in the left image of Figure 4-56

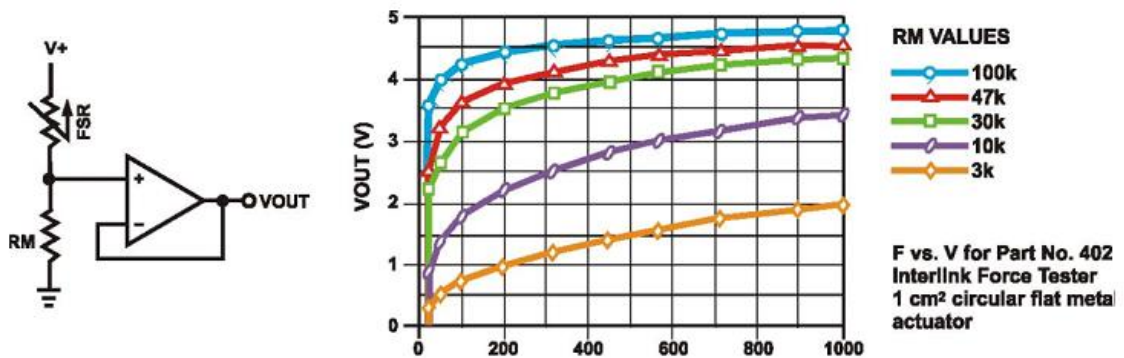
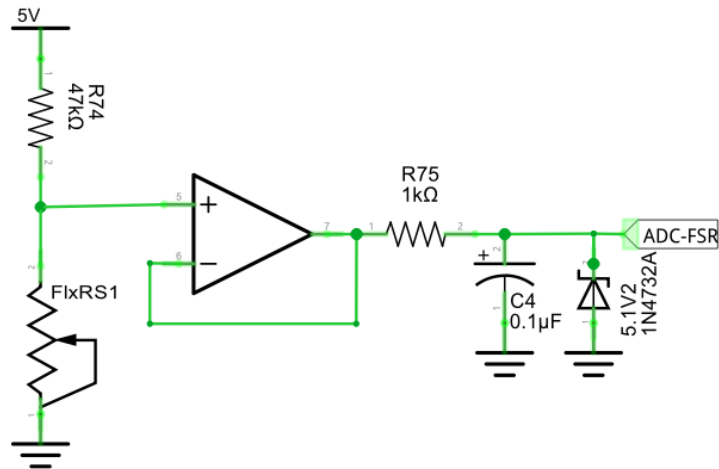


Figure 4-56. Application Information of the Force Resistive Sensor. [52]

However, the recommended configuration is not entirely suitable for the application, since the sensor is connected to a pull down resistor, which then would require a  $V_{cc}$  connection into the glove, fact that, as explained before, wanted to be avoided to simplify the implementation.

Thus, the configuration was changed as presented in Figure 4-57, where the sensor is used in a voltage divider with a pull up resistor. This only means that the signal from the sensor should be interpreted conversely; for example, the maximum output voltage is reached when the finger is not actuated.

The picture from the right in Figure 4-57 is still relevant to find the appropriate resistor value to achieve a good span of resistance within the operative forces. And then, a pull up resistor of  $47k\Omega$  was chosen.



**Figure 4-57.** Implemented configuration for conditioning of the Force Sensing Resistor.

Also, the signal was conditioned with a filter and a Zener diode as voltage regulator, like in the case of the flex resistive sensors.

#### 4.7.5. Power Supply

The power consumption of the valves turn out to be 180 mW, drawing 20 mA, according to the experimental data retrieved from Festo and presented in Figure B-1. Moreover, the system would draw 20mA per each Lillypad Pixel (*See B.3.4*).

The impedance decoupling of the Op. Amp provokes that the sensory system doesn't draw any extra significant current.

Therefore an off-the-shelf 9.6V 550mAh power supply<sup>17</sup> is good enough for the application, with it, the device can operate continuously for more than 4 hours.

<sup>17</sup> 9 V Block-Akku Li-Ion Conrad energy 6LR61 500 mAh 7.2 V 1 St., Conrad, Germany

### 4.7.6. Overall Electronic Circuit

The overall electronic interface can be depicted in both Figure 4-58, where the sensors, indicators and controller are shown, and Figure 4-59, where the signal conditioning of the sensors is shown. FlxRS stands for the connection with the Flex Resistive Sensor and FSR is the connection of the Force Sensing Resistor, whereas ADC-FlxRS is the conditioned signal for the flex sensor, and ADC-FSR, the conditioned signal for the force sensor.

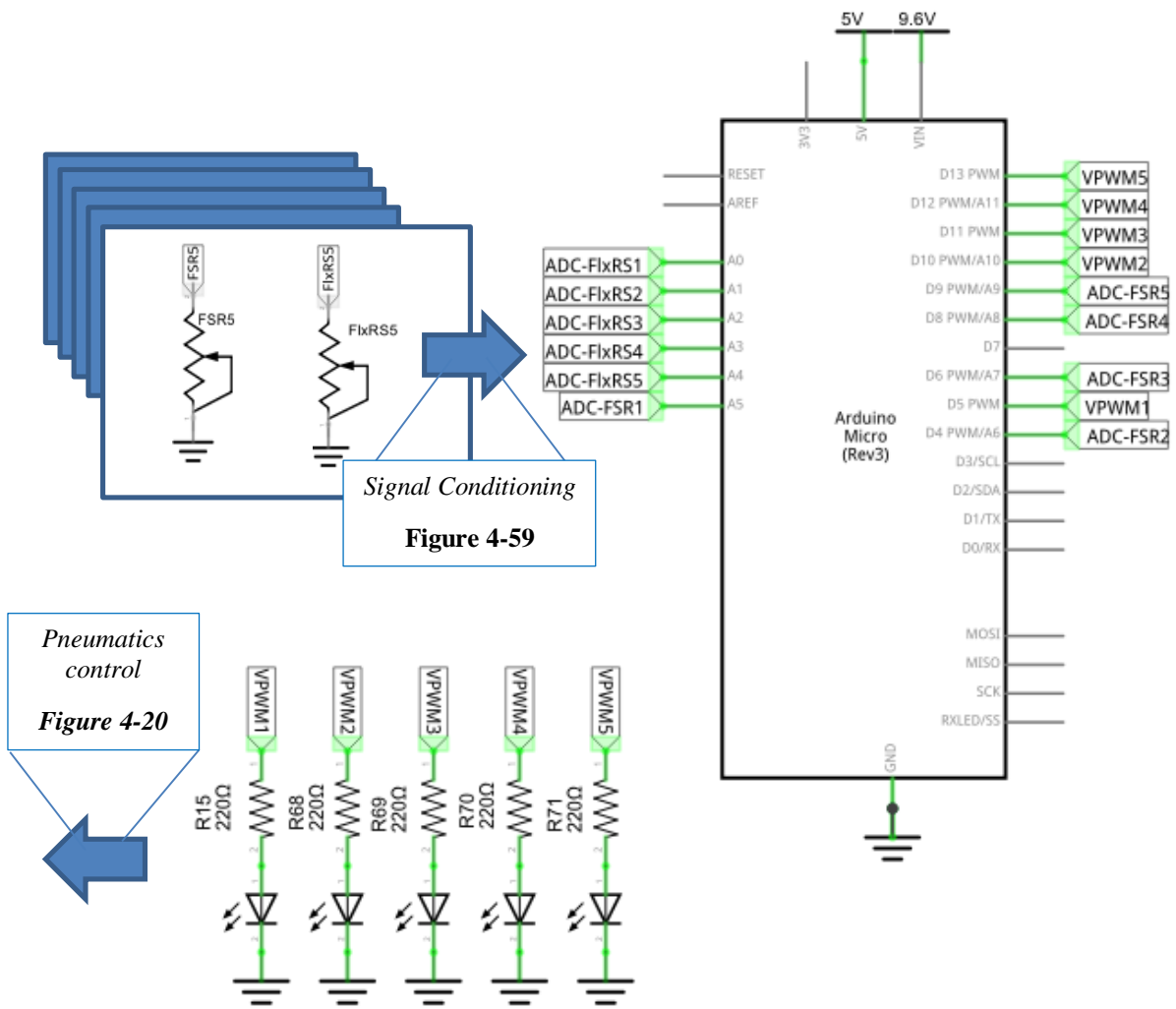
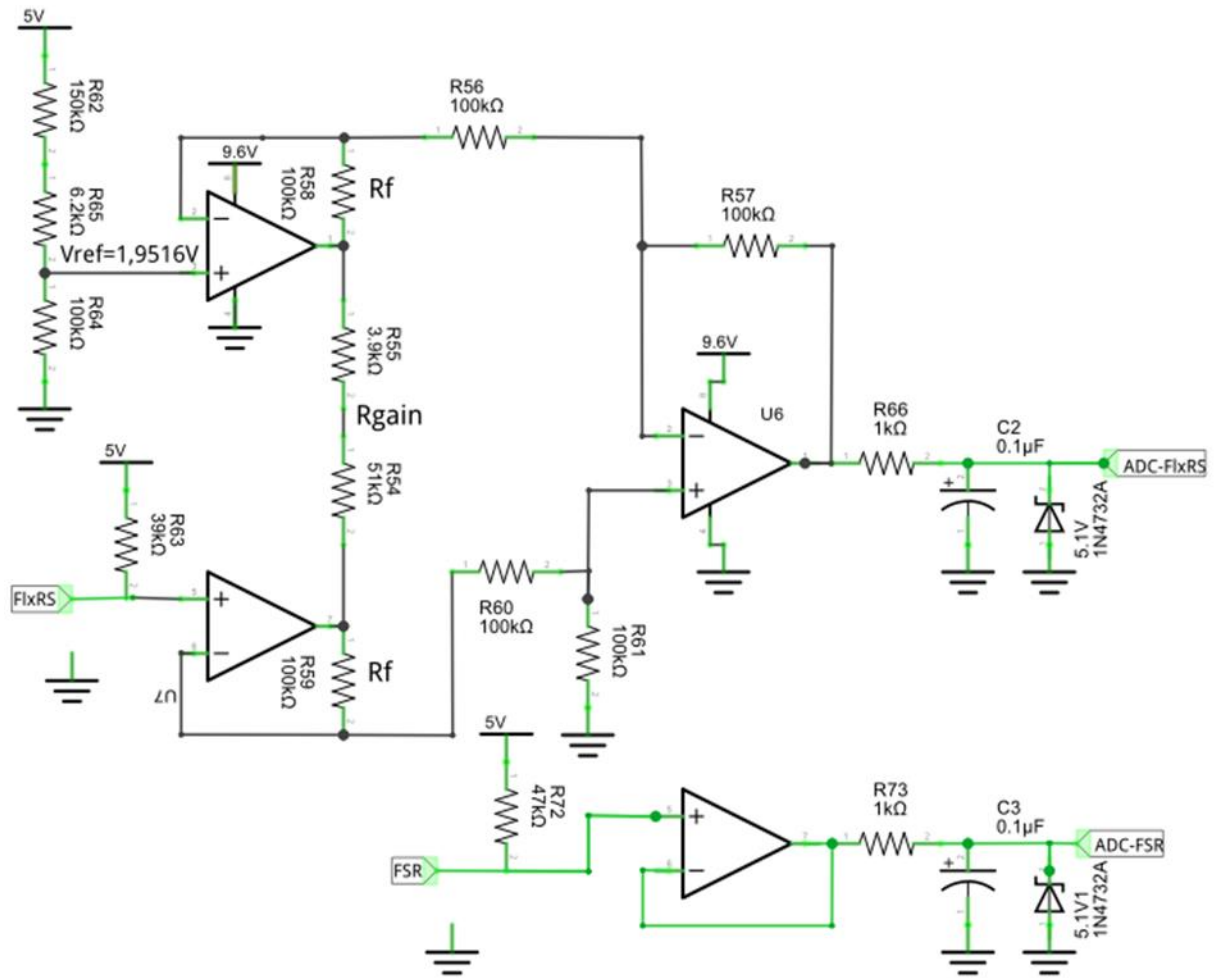


Figure 4-58. Overall Electronic Design - Part 1. .

VPWM stands for Valve-PWM. That signal is connected to both the LED indicator and the Piezo-Valve in parallel configuration.



**Figure 4-59.** Overall Electronic Design - Part 2. Signal conditioning per each pair of sensors (Flex-Force).

As it is shown in Figure 4-59, per each pair of force-flex sensors it is required to use two single supplied operational amplifiers, such as the LM358.

## Chapter 5. Control Strategy

This chapter is aimed to establish the principles for a first control approach and make the orthosis ready for further laboratory tests.

### 5.1. Inputs and Outputs

The system can be described as a combination of 10 inputs, 5 of them corresponding to the Force Sensing Resistors and 5 for the Flex Resistive Sensors. On the other hand, the outputs of the system are 5 signals for both controlling the valves and feeding the indicators. Figure 5-1 illustrates the system.

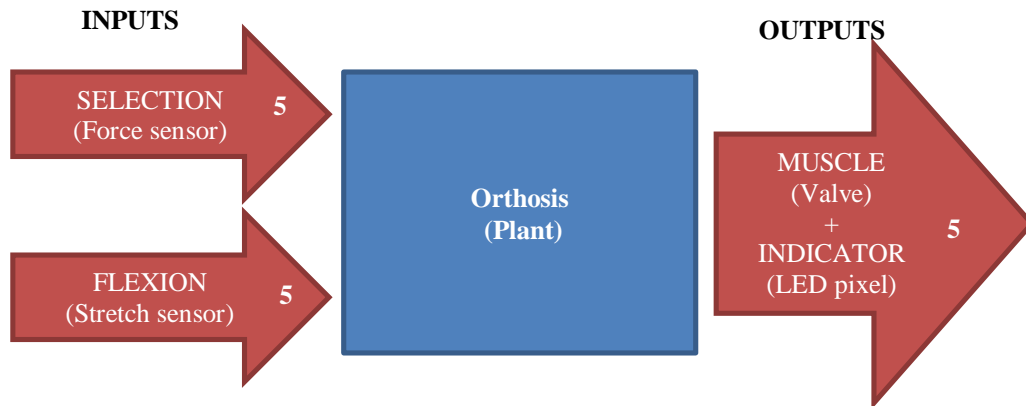


**Figure 5-1.** Inputs and Outputs of the System.

This system can be identified as a Multiple Input – Multiple Output System. However, the fingers are actuated one by one and therefore the system can be simplified as Single Input Single Output. (SISO)

It is very important to highlight that to derivate an analytical description model of the entire control system is impractical because of highly nonlinear properties of the real mechanism, starting with the nonlinear behavior of the PAM's and ending with the complex and non parameterizable interaction between the soft Orthosis and the human body.

Thus, the most practical thing to do, for a first approach of control, is to consider the system as a classical black box, and implement experimental tuning controllers, instead of finding complicated mathematical models. The bottom up approach would start first with a feed-forward controller and then with a feedback proportional (P) controller.

## 5.2. Concept 1. Feed Forward Control

The first concept would be the implementation of a feed forward control, by calculating the amount of time required for performing the desired motion with a predefined PWM duty cycle as illustrated in Figure 6-2.

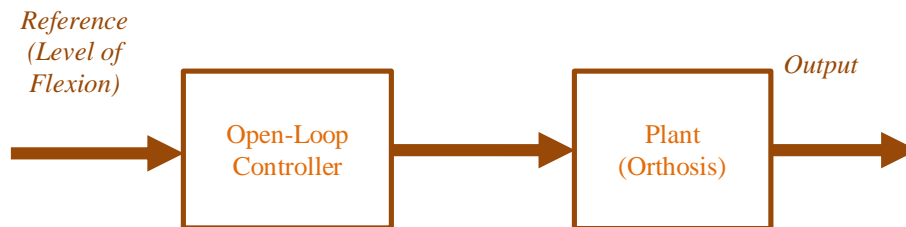


**Figure 5-2.** Feed-forward Controller

The time of the valve operation can be easily calculated by studying the behavior of the system with PWM duty cycle changes, and then measuring the values from the outputs (flex sensors)

However, it should be said that this approach is not likely to be sufficient for the successful control of the orthosis for two reasons. The first reason is that the motion would be clearly affected by the position of the wrist and therefore there is going to be a variation in the necessary time depending on the hand orientation. The second reason is about the possible leakage of air from the valves which would, as well, cause an imprecise final position of the finger. Thus, the feed-forward control is just recommended as an experimental tool for determining the behavior of the system under changes in the PWM duty cycle.

### 5.3. Concept 2. Proportional (P) Feedback Control.

The second concept would take advantage of the flex sensor as signal for feedback control. As it is shown in Figure 5-3, the reference is the desired level of flexion, the control signal is PWM and the output is the actual flexion of the finger.

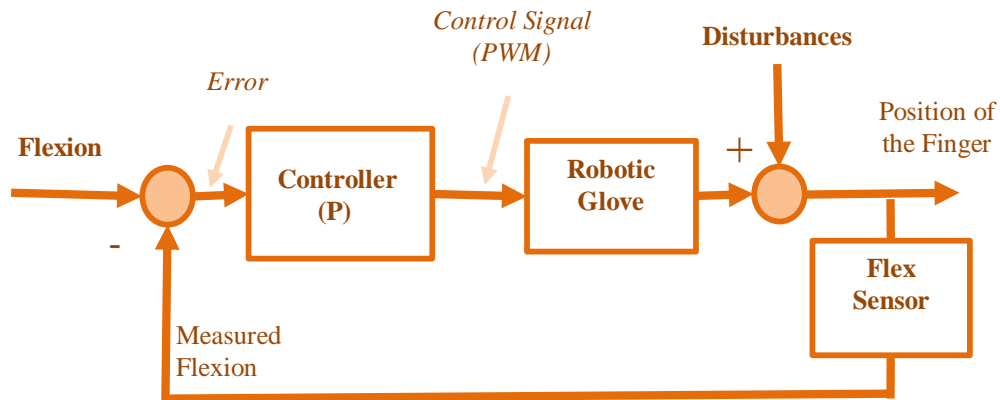


**Figure 5-3.** Feed-back P Controller

The feedback proportional controller (P) dynamically contracts or releases the artificial muscles by operating the 3/3 piezo valves with PWM. As depicted in Figure 5-3 the control loop is tuned by the proportional gain,  $k_p$ , which is the ratio of PWM duty-cycle and level of flexion error. Even though the duty-cycle increases as the error increases, it cannot exceed 100% due to the nature of PWM control. The choice of  $k_p$  impacts the settling time, overshoot, and steady state error.

The PWM duty-cycle per each valve is determined by the following rule:

$$d_c = e \cdot k_p + 0,5 \tag{5-1}$$

In Equation (5-1),  $d_c$  is the duty cycle,  $k_p$  is the proportional gain of the controller and  $e$  is the error for the level of flexion.

It is very important to highlight that, in case of performing a rehabilitation exercise, the control loop would just be turned on as long as the finger is moving to the desired position, and afterwards, the system would wait certain time to then return the finger to its original resting condition, with the same PWM/error rate ( $KP$ ). An example of this type of behavior, with 5s of delay, is shown in Figure 5-4. There, the cycle starts and ends in a subtask from the main loop of the controller.

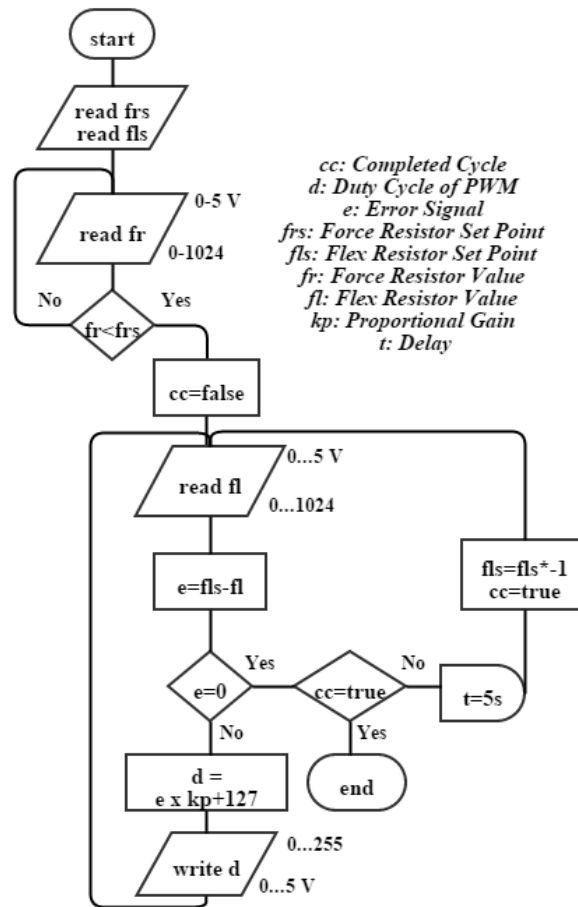


**Figure 5-4.** Flow Diagram of the Movement of One Finger in Rehabilitation

As explained in the section of the valves selection, the great advantage of using a piezo valve, is that the frequency has no limitation regarding the mechanical response time of the valve as in the case of the solenoid valves, so the frequency of operation can be set as high as possible.

Finally the overall control system architecture is presented in Figure 5-5.

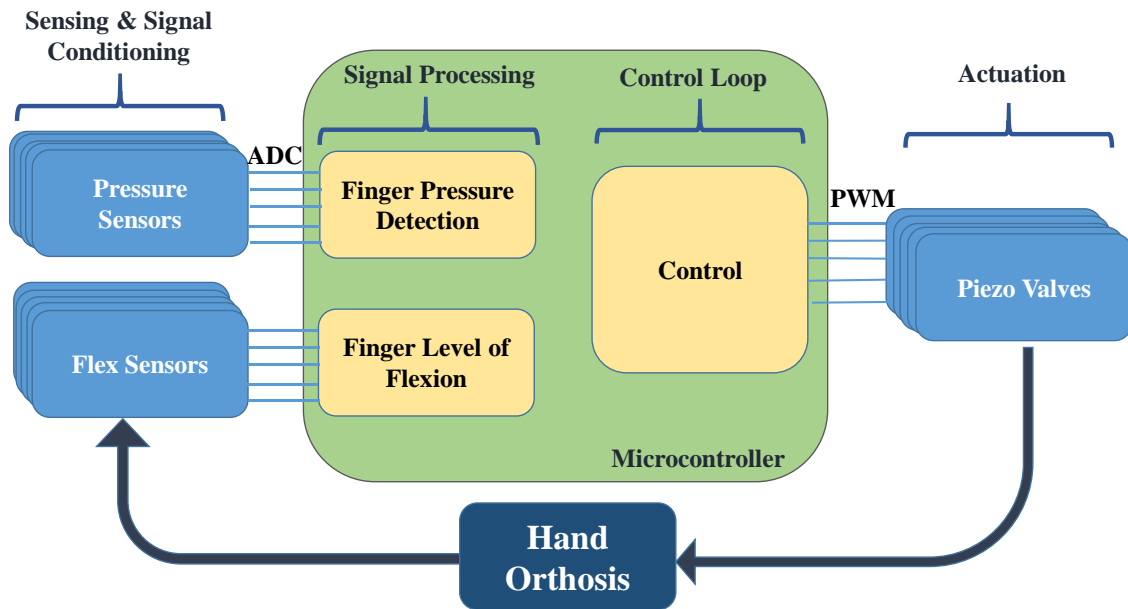


**Figure 5-5.** Control System Architecture

## Chapter 6. Assembly

This chapter is aimed to show the fulfillment of the objective regarding the assembly of the testing model. In this part the methodology of construction is presented as well as the characterization of the sensing and actuation systems.

### 6.1. Methodology

The first step of the assembly was focused on the glove. As planned, the tendon layout was going to be inside the glove. The tendons were fixed to the glove using common cotton threads that form a sheath for the tendons. The attachment was made in the middle section of the distal interphalangeal joint with a ring elaborated with the same Dyneema Wires, and from that point, the tendon was routed as planned in the design. The first stage of the assembly is depicted in Figure 6-1.



**Figure 6-1.** First Stage in the Assembly Process

The tendons were placed in pairs of threads that will be used afterwards for the attachment with the artificial muscle. The glove is used conversely (with the rubber side on the dorsal part of the hand) to enhance the finger restoration force and increase the easiness of implementation of the electronic layer of the glove.



**Figure 6-2.** Assembly of the Tendon Layout of the Glove

Figure 6-2 illustrates the mechanical tendon layout of the glove, as it can be seen, the other side of the glove is free to set up the sensors and the connection wires. The LEDs were sewn close to the MCP joints. On the other hand, the flex sensors and the force sensors were attached with permanent glue to the rubber side of the glove, as it is depicted in Figure 6-3.



**Figure 6-3.** Assembly of the Electronic Layout of the Glove

Moreover, the female Ribbon connector is attached close to the wrist with some stitches of Dyneema rope. The final configuration of the electronic layer of both sides of the hand is depicted in Figure 6-4.



**Figure 6-4.** Electronic Layer of the Glove



The threaded inserts were screwed in to the holes of the back side of the mechanical support where the muscles are attached, they can be easily twisted to adjust the final orientation of the fittings in the cover of the housing. The springs were firmly placed with the use of the m3x8 screws, to be aligned with the openings of the tendons. As it is highlighted in the blue circle of Figure 6-5, the terminals of the tendons were secured with the use of Ø1 mm cylinder springs.

Then, after screwing the muscles into the thread inserts, they were folded and manually placed within the cavities, as illustrated by the green circle of the Figure 6-5.

The pneumatic connections were realized with QSM-B-M3-3-I-20 fittings for No.3 tubing

Then, a dimensional verification was performed with the muscles to verify the inflation behavior. As expected, the outer diameter of the muscle comply the 17,7 mm. (last picture in Figure 6-5 ).

The Figure 6-6 illustrates the glove-support interface for the testing model. The tendons were planned to be connected to the muscles when contracted.

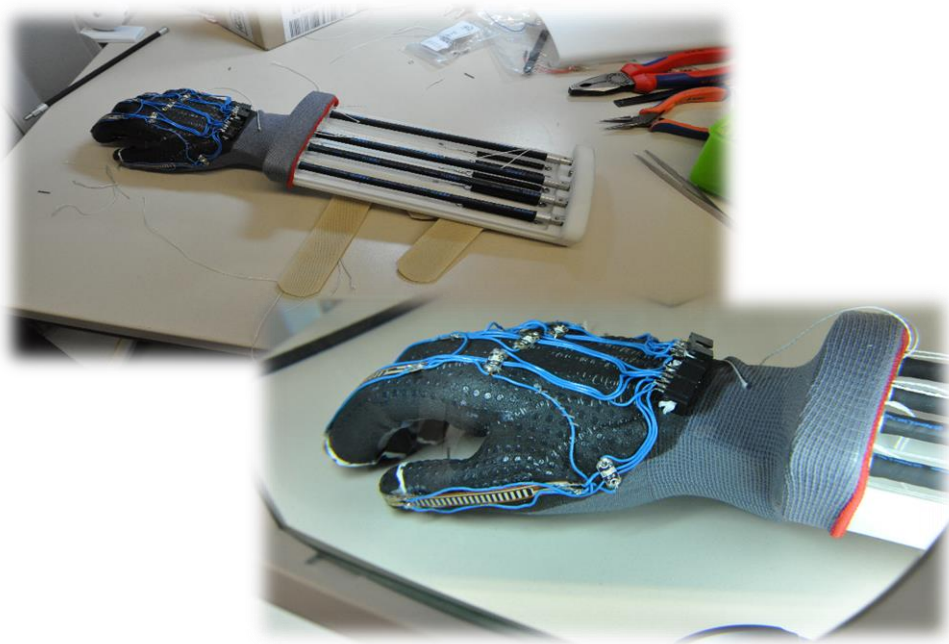


**Figure 6-6.** Glove-Support Interface

Then, the electronic circuit was planned to be mounted on a breadboard since it is a testing model. Figure 6-7 is depicting the configuration considering one valve, to be able to perform tests over the control cycle of one finger.

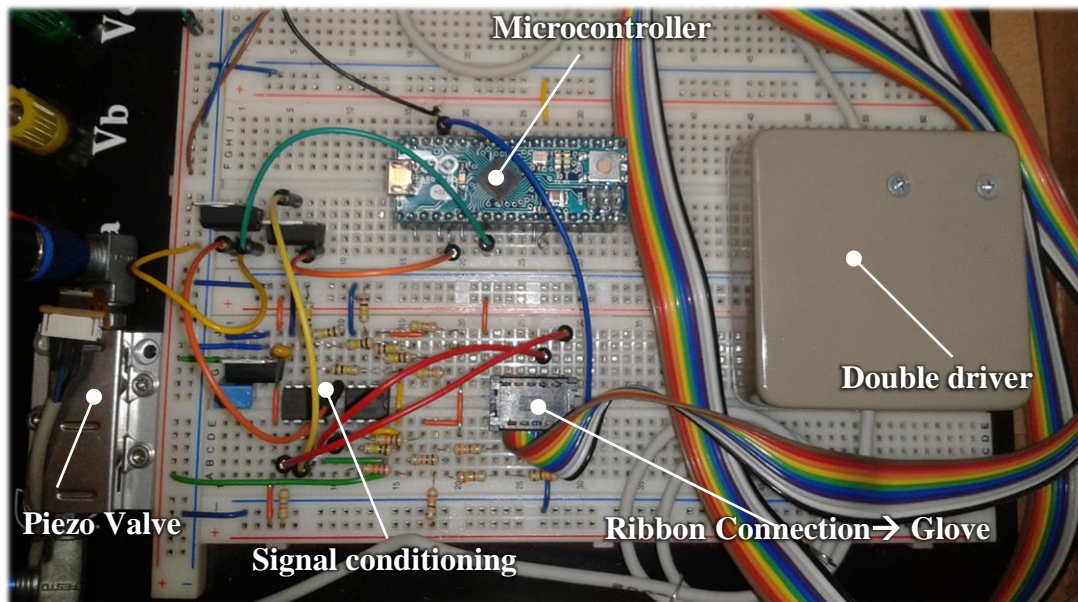


**Figure 6-7.** Breadboard Connections for the Testing with One Valve.

The final configuration of the testing model is presented in Figure 6-8.

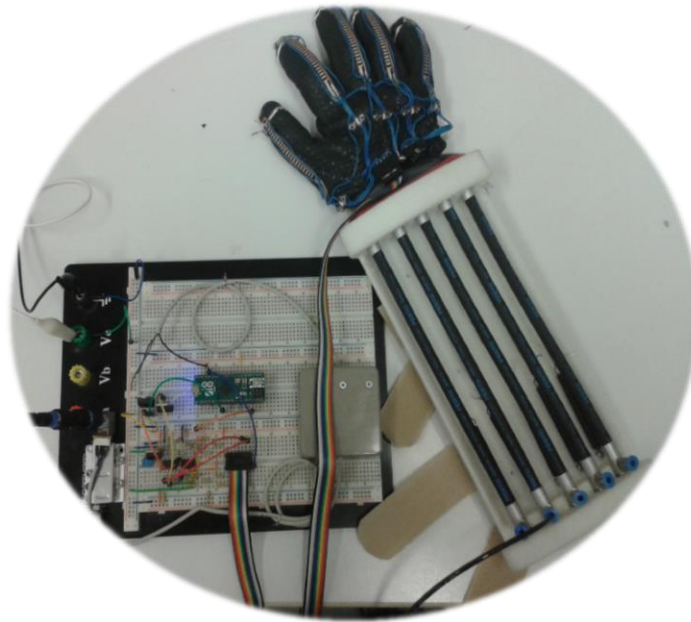


**Figure 6-8.** Assembly of the Testing Model.

After the assembly, an uncontrolled contraction of the muscles was performed to verify that all the muscles fit within the orthosis as presented in Figure 6-9

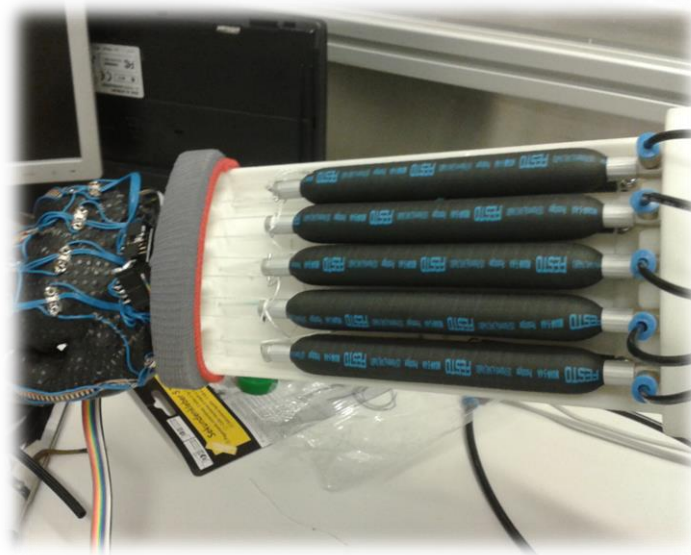


**Figure 6-9.** Test of inflation of the Muscles.

With the cover, the final appearance of prototype is depicted in Figure 6-10.



**Figure 6-10.** Final appearance of the Prototype.

## **6.2. Characterization**

This section aims to the characterization of the subparts of the testing model. This characterization is divided in actuation and sensing.

### **6.2.1. Actuation**

An experiment was conducted in Festo to assess the behavior of a muscle with 150mm MXAM 15° membrane with a piezo valve, as it can be appreciated in Figure B-2 from *Annex B.2*. In this experiment, the valve was feed with a 300V step signal for three different input pressures (2, 4 and 6 bar). The output pressure of the valve, as well as the stroke of the muscle, was measured. These results were given to the author of this thesis to be analyzed.

Now, by analyzing the behavior of the system, the muscle-valve response, with an input pressure of 6 bar and a step signal of 300V, is over damped. As it can be inferred, the system has two different time constants, one of 1,2 s for inflation and about 2,5 s for deflation.

Considering both time constants, every cycle of movement would last 3,7 s, which translates in a frequency of movement of 16,22 cycles per minute.

According to the *FR3 Frequency of movement*, the system should work with a maximum frequency of movement of 10 cycles per minute. This only means that for fulfilling that functional requirement, the speed of motion and thus the frequency of movement should be varied with the use of PWM signal that operates the flow proportional valve.

With the presented results and the analysis presented above, the functionality of the piezo-electric valve and the artificial muscle is validated.

### 6.2.2. Sensing Characterization

Figure 6-11 shows the characterization of resistance of the sensor according to the level of flexion of the finger. This experiment was realized wearing the glove in a healthy hand and emulating the ranges of motion of per each finger and measuring the resistance with a digital multimeter.

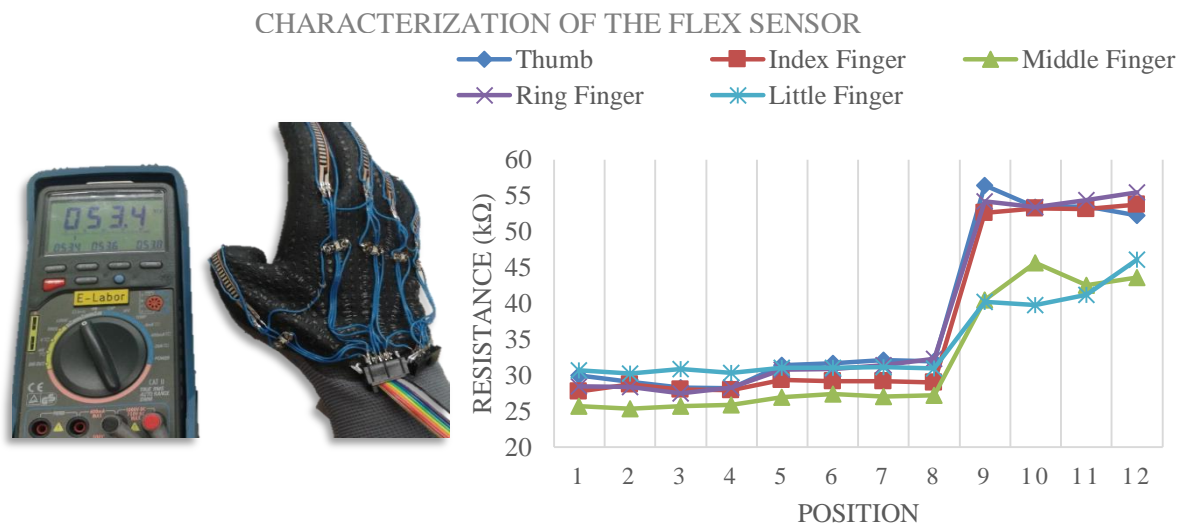


**Figure 6-11.** Characterization of the flex sensor

The maximum level of resistance among the fingers was 56,4 k $\Omega$ , thus a value of 60 k $\Omega$  was taken into account as an operative maximum value of the sensor for the signal conditioning.

On the other hand, regarding the finger pressure sensing, the FSR pressure sensors were characterized in order to determine the threshold value for the finger intention of movement. Using the microcontroller, data was sent to the computer via serial USB (CDC) port, and therefore the values were recorded after the ADC conversion.

It can be appreciated in Figure 6-12, that the average threshold value was set at the bit 350, any value less than that (which means more force, given the inverted configuration) is considered as an external fingertip pressure for intention of finger movement. This threshold limit value can be easily modified by the user.



**Figure 6-12.** Characterization of the force sensor

### 6.3. Findings

The first finding was about how stable is the support structure of the actuators, even when it lies on a vertical position, such as depicted in Figure 6-13. This is explained due to the complex geometry used in the conception and design, and it also represents another clear advantage of using rapid prototyping.



**Figure 6-13.** High stability of the structure.

On the other hand, there is a very important finding regarding the use of a glove as a hand orthosis. The glove was actuated without a control system to study the behavior of the orthosis in a real hand, instead of a SOMSO Hand as in the prior work.

Given that the hand is being used as the mechanical support of the motion, the level of fitness of the glove over the hand has a direct influence in the performance of the orthosis.

The identified limitation is that since the fabric of the glove is stretchable, the tendon always pulls the fabric away from the finger, causing a bow that provokes that the excursion of the tendons is not directly translated to finger motion.

A similar phenomenon occurs in the human hand when one of the pulleys is broken, and is called “bowstringing effect”. This is illustrated in Figure 6-14.

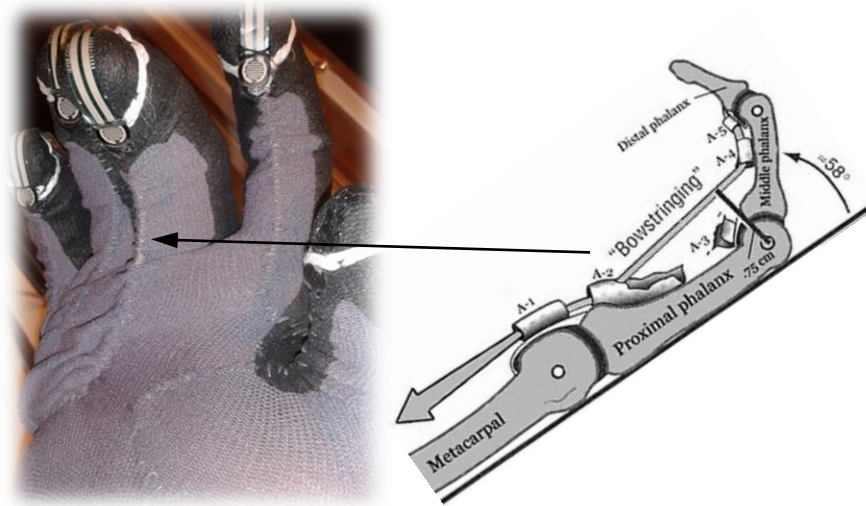


**Figure 6-14.** Bowstringing Effect in the orthosis. Right Image [18]

The bowstringing effect certainly decreases the angle of the middle phalanx during the pulling of the tendon, justified only by the absence of a pulley in the PIP. This fact explains that the bending of the finger requires always more strain from the flexors. It is provoked by the morphology of the flexor connection and the contraction level of the fabric. Thus, a solution is conceptualized in Figure 6-15.

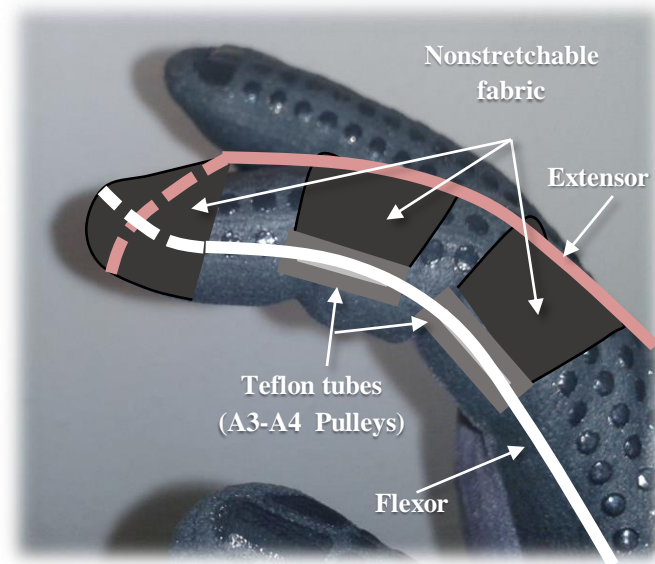


**Figure 6-15.** Solution to Bowstringing Effect. Right Image [18]

The solution is aimed into the use of non-stretchable fabric on the dorsal side of the glove, sewn with Teflon tubes resembling the A4 and A3 pulleys that would allow a symmetric 2 thread tendon to be routed along the sides of the finger and a non-stretchable thimble (“A5 pulley”) to assure the fixing to the finger.

Another finding was that despite orthosis was easy to wear and take off, some of the tendons exerted certain pressure over the skin in the metacarpophalangeal joints. This fact compromises the *NFR.3 Comfort of wearing*; nevertheless, with the use of cutting edge technologies for textiles<sup>18</sup>, the solution to this functional requirement can be enhanced, and this represents part of future work.

<sup>18</sup> Such as TITV (Institut für Spezialtextilien und flexible Materialien)

## **Chapter 7. Conclusions and Outlook.**

1. The main contribution of this thesis is the design of a mechatronic system, based on human kinesiology, to actuate a soft orthosis using the tendon driven mechanism. From the mechanical design, electronics and pneumatics, a testing model was elaborated for further experiments as a first approach of a wearable device.
2. The real complex mechanism of the human hand is simplified taking advantage of the coupled function between the interphalangeal joints. On the other hand, the orthosis uses the patient's hand for supporting the motion, since there are no rigid links.
3. The housing of the actuation system was elaborated using anthropometric data that would enable most of population to wear this device. Moreover, designing for rapid prototyping enhances the overall shape, improving the ergonomics and the static mechanical behavior due to the stability of tailor made complex geometries.
4. A Finite Element Analysis was performed over the mechanical structure applying several hundreds of newtons in the most critical places of the structure, getting factors of safety of more than 35.
5. The limitation of the non parameterizable dynamics that the human hand-soft orthosis represents is depleted with the use of sensors that resemble the human somatosensory system to measure the finger level of flexion. Also, these sensors make the system controllable, having a direct repercussion in the safety of use.
6. A new variable to measure was introduced using force sensors to fulfill the human interface requirements by selecting intuitively which finger should move. These sensors can be used in the future to perform complex dexterity control.
7. The best actuation method was found to be the use of Pneumatic Artificial Muscles that have several advantages in force, stroke and operability characteristics in comparison with other types of artificial muscles such as the Nitinol.

8. The use of Piezo Electric 3/3 valves represents great advantages in energy efficiency, weight, portability, and reduces complexity in the control architecture.
9. The sensory system enables a plurality of future applications for records tracking, assessment of the patient's dexterity recovery, and more complex rehabilitation program exercises.
10. LED Pixels were integrated in the glove along with the sensors in an electronic layer that enables a human interface and reinforces the patient efforts of motion of their fingers through visual feedback.
11. A proportional controller (P) was conceptualized to be the best first approach for controlling the fingers motion, using the finger level of flexion as a controlled variable.
12. The final bio inspired nature of the project can be appreciated in Figure 7-1

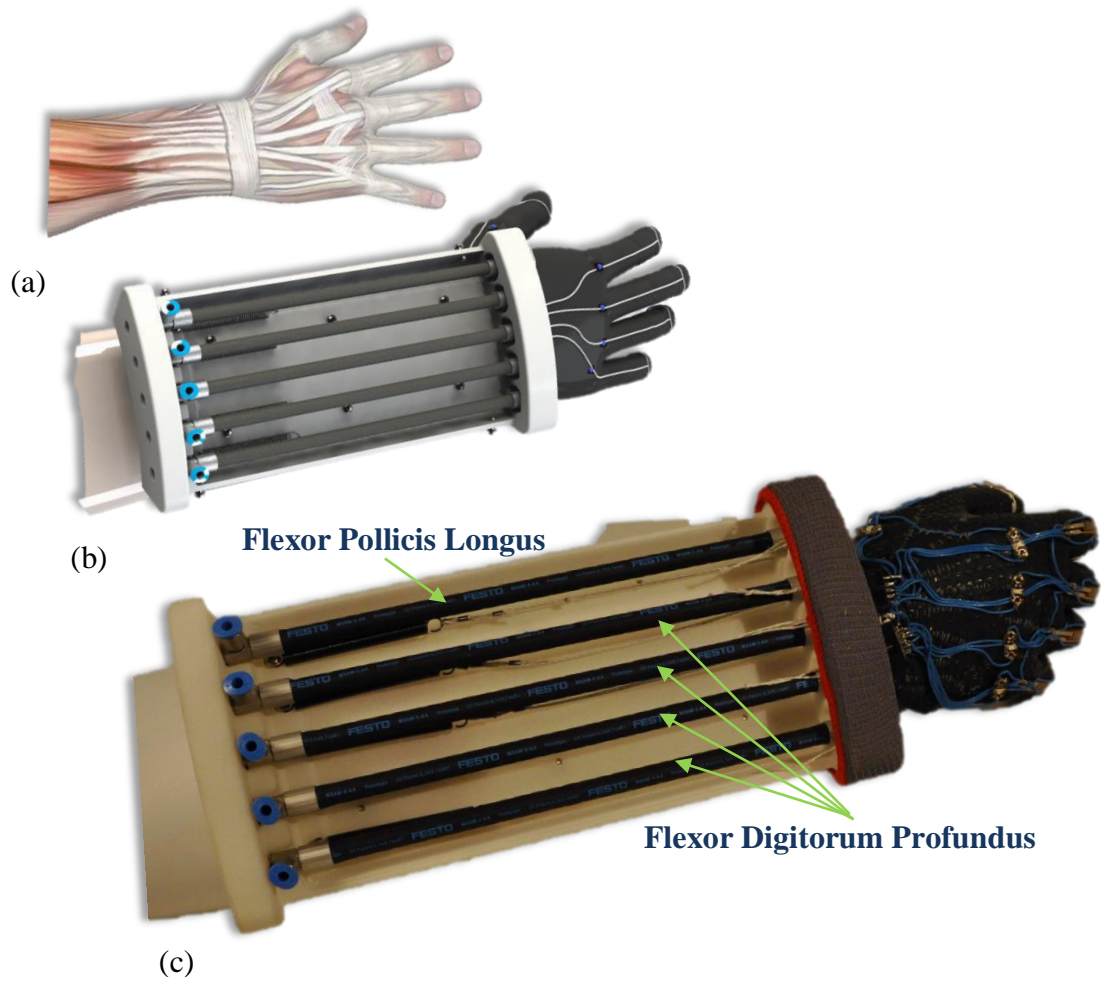


**Figure 7-1.** Conception, Design and Prototype of Bio-inspired Active Soft Orthotic Device. (a) Hand Muscle Anatomy. (b) Design Concept. (c) Actual Prototype.

### *Future Work*

Some steps that need to be addressed in the future are:

1. To perform tests over the assembled model, study the behavior of the entire system using feed forward control and use that information to implement the proportional feedback controller.
2. The solution of the bowstringing effect needs to be implemented to enhance the characteristics of the testing model.
3. It is necessary to use cutting edge technologies for electronics integration of the sensors within the glove and, therefore, increase the comfort of wearing and enhance the electrical safety.
4. After the prototyping, an embedded electronic system should be developed.
5. The requirements were validated during the design; however, the requirement of weight has to be confirmed in the future when the manifold of the valves and the electronic hardware are integrated in the device, meanwhile, the current structure is made of lightweight materials that greatly contributes to the fulfillment of the requirement.
6. Different scenarios have to be found about the use of the orthosis in rehabilitation exercises. Also it is required an assessment of the system effectiveness as a power assistive device in real patients.
7. Develop a computer interface to easily program training exercises.

## List of References

- [1] K. A. Zimmermann, "Muscular System: Facts, Functions & Diseases," 04 February 2014. [Online]. Available: <http://www.livescience.com/26854-muscular-system-facts-functions-diseases.html>. [Accessed 16 July 2014].
- [2] S. Soekadar, Interviewee, *Reha-Device für gelähmte Hände*. [Interview]. September 2014.
- [3] D. J. E. n. J. L. a. C. S. C. Reinkensmeyer, "'Robotics, motor learning, and neurologic recovery,'" *Annual Review of Biomedical Engineering*, , vol. 6, pp. 497-525, 2004.
- [4] E. Taub, N. Miller, T. Novack, E. Cook and W. Fleming, "'Technique to improve chronic motor deficit after stroke,'" *Archives of Physical Medicine and Rehabilitation*, vol. 74, no. 4, pp. 347-354, 1993.
- [5] P. Heo, M. G. Gwan g, S.-. j. Lee, K. Rhee and J. Kim, "Current Hand Exoskeleton Technologies for Rehabilitation and Assistive Engineering," *INTERNATIONAL JOURNAL OF PRECISION ENGINEERING AND MANUFACTURING*, vol. 13, pp. 807-824, 2012.
- [6] University of Loma Linda, "Orthosis," [Online]. Available: <http://lomalindahealth.org/east-campus/our-services/rehabilitation/programs-and-divisions/orthotics-and-prosthetics/orthotics/index.page?>. [Accessed 17 July 2014].
- [7] Fraunhofer IPA, "Biomechatronic Systems," [Online]. Available: [http://www.ipa.fraunhofer.de/Biomechatronic\\_Systems.83.0.html?&L=2](http://www.ipa.fraunhofer.de/Biomechatronic_Systems.83.0.html?&L=2). [Accessed 16 October 2014].
- [8] R. Lincoln, "The Fluidic Muscle: A 'New' Development," 2002. [Online]. Available: <http://www.ijme.us/issues/spring%202002/articles/fluid%20muscle.dco.htm>. [Accessed 21 July 2014].

- [9] 5starsengineering, «Concurrent Engineering,» 20 October 2013. [En línea]. Available: <http://5starsengineering.blogspot.de/>. [Último acceso: 21 July 2014].
- [10] Y. Rai, "Body Movements," 16 April 2013. [Online]. Available: <http://www.meritnation.com/ask-answer/question/i-don-t-understand-what-is-gliding-joint/science/4540302>. [Accessed 1 October 2014].
- [11] A. Lluch, «Intrinsic causes of stiffness of the interphalangeal joints,» de *Joint Stiffness of the Upper Limb*, Taylor & Francis, 1997, pp. 259-264.
- [12] The Physiology of the Joints - Volume I: Upper Limb, 5th ed., Churchill Livingstone, 1982.
- [13] M. Tuncay Duruöz, Hand Function: A Practical Guide to Assessment, Istanbul, Turkey: Springer, 2014.
- [14] C. L. Taylor and R. J. Schwarz, "The anatomy and mechanics of the human hand," *Artificial Limbs*, vol. II, no. 2, pp. 22-35, 1955.
- [15] D. Q. Thomas, «Muscles of the Wrist and Fingers,» [En línea]. Available: <http://www.castonline.ilstu.edu/Thomas/181/Muscles%20of%20the%20Wrist%20and%20fingers%20DT.pdf>. [Último acceso: 14 September 2014].
- [16] D. Elliot and D. A. McGrouther, "The excursions of the long extensor tendons of the hand," *The Journal of Hand Surgery: British & European Volume*, vol. XI, no. 1, pp. 77-80, 1986.
- [17] T. J. Armstrong y D. B. Chaffin, «An investigation of the relationship between displacements of the finger and wrist joints and the extrinsic finger flexor tendons,» *Journal of Biomechanics*, vol. XI, nº 3, pp. 119-128, 1978.
- [18] D. A. Neumann, Kinesiology of the Musculoskeletal System: Foundations for Rehabilitation, St. Louis: Mosby, 2002.

- [19] A. Chiri, F. Giovacchini, N. Vitiello, E. Cattin, S. Roccella, F. Vecchi y M. C. Carrozza, «HANDEXOS: Towards an exoskeleton device for the rehabilitation of the hand,» *IEEE/RSJ International Conference on Intelligent Robots and Systems*, pp. 1106-1111, 2009.
- [20] A. Wege and G. Hommel, "Development and control of a hand exoskeleton for rehabilitation of hand injuries," *IEEE/RSJ International Conference on Intelligent Robots and Systems*, pp. 3046-3051, 2005.
- [21] Y. Hasegawa, Y. Mikami, K. Watanabe and Y. Sankai, "Five-fingered assistive hand with mechanical compliance of human finger," *IEEE International Conference on Robotics and Automation*, pp. 718-724, 2008.
- [22] H. K. In, K.-J. Cho, K. R. Kim y B. S. Lee, «Jointless structure and under-actuation mechanism for compact hand exoskeleton,» *IEEE International Conference on Rehabilitation Robotics.*, pp. 1-6, 2011.
- [23] B. L. Shields, J. A. Main, S. W. Peterson y A. M. Strauss, «An anthropomorphic hand exoskeleton to prevent astronaut hand fatigue during extravehicular activities,» *IEEE Transactions on Systems, Man and Cybernetics, Part A: Systems and Humans.*, vol. V, nº 5, pp. 668-673, 1997.
- [24] D. Trivedi, C. D. Rahn, W. M. Kier and I. D. Walker, "Soft robotics: Biological inspiration, state of the art, and future research," *Applied Bionics and Biomechanics*, vol. V, no. 3, pp. 99-117, 2008.
- [25] E. Bojan, "Entwicklung eines mit Festo-Muskeln angetriebenen Handschuhs für den Einsatz bei der Rehabilitation nach Handlähmungen oder zur Kraftverstärkung in der Produktion," September, 30, 2013.
- [26] N. Petroff, K. D. Reisinger y P. A. C. Mason, «Fuzzy-Control of a Hand Orthosis for Restoring Tip Pinch, Lateral Pinch, and Cylindrical Prehensions to Patients with Elbow

- Flexion Intact,» *IEEE transactions on neural systems and rehabilitation engineering*, vol. IX, n° 2, pp. 225-231, 2001.
- [27] A. Hollister and D. Giurintano, "Thumb movements, motions, and moments.," *Journal of Hand Therapy*, vol. VIII, no. 2, pp. 106-114, 1992.
- [28] T. Imaeda, K. An y W. Cooney, «Functional anatomy and biomechanics of the thumb,» *Hand Clinics*, vol. VIII, n° 1, pp. 9-15, 1992.
- [29] A. Barr y J. Bear-Lehman, «Biomechanics of the wrist and the hand,» de *Basic Biomechanics of the Musculoskeletal System*, Lippincott Williams & Wilkins, 2001, pp. 358-387.
- [30] Y. ., C. Q. a. K. C. Yasumuro, «3D modeling of human hand with motion constraints,» *Proc. Int. Conf. Recent Advances 3-D Digital Imaging Modeling*, pp. 275-282, 1997.
- [31] CNX Anatomy and Physiology , «Interactions of Skeletal Muscles in the Body,» 04 September 2014. [En línea]. Available: [http://cnx.org/contents/14fb4ad7-39a1-4eee-ab6e-3ef2482e3e22@7.1:74/Anatomy\\_&\\_Physiology](http://cnx.org/contents/14fb4ad7-39a1-4eee-ab6e-3ef2482e3e22@7.1:74/Anatomy_&_Physiology). [Último acceso: 1 October 2014].
- [32] McGill Molson Medical Informatics Project, "Agonist - Antagonist Muscles," 6 October 2008. [Online]. Available: <https://www.mededportal.org/icollaborative/resource/1424>. [Accessed 1 October 2014].
- [33] B. Ivo, "Modellbildung und Regelung," Berlin, 2010.
- [34] S. M. Mirvakili, " Niobium Nanowire Yarns and Their Application as Artificial Muscle," Vancouver, 2013.
- [35] D. Stoeckel, «The Shape Memory Effect – Phenomenon, Alloys and Applications,» *Shape Memory Alloys for Power Systems*, 1995.
- [36] D. Stockel, «Shape Memory Actuators Improve Car Performance,» *Springs Vol.31*, May 1992.

- [37] DINALLOY, Inc., «Flexinol® Actuator Wire Technical and Design Data,» 2014. [En línea]. Available: <http://www.dynalloy.com/TechDataWire.php>. [Último acceso: 1 August 2014].
- [38] F. Daerden y D. Lefeber, «Pneumatic Artificial Muscles: actuators for robotics and automation,» Brussels.
- [39] FESTO, "Fluidic Muscle DSMP/MAS," May 2013. [Online]. Available: [http://www.festo.com/cat/en-us\\_us/search?query=DMSP](http://www.festo.com/cat/en-us_us/search?query=DMSP). [Accessed 21 July 2014].
- [40] K. Brabham, M. Marr y A. L. P. Smith, «Artificial Muscle,» 2012. [En línea]. Available: [www.ee.pdx.edu/~mperkows/CLASS.../ArtificialMusclePresentation.ppt](http://www.ee.pdx.edu/~mperkows/CLASS.../ArtificialMusclePresentation.ppt). [Último acceso: 20 October 2014].
- [41] N. Tsagarakis y D. G. Caldwell, «Development and Control of a ‘Soft-Actuated’ Exoskeleton for Use,» *Autonomous Robots*, nº 15, p. 21–33, 2003.
- [42] Festo AG & Co. KG, *Vereinbarung über die Gewährleistung und Haftung für zu Testzwecken/gemeinsamer Entwicklung überlassen Prototyp-Produkten*, Esslingen, 2014.
- [43] MISUMI, "Extension Springs - Standard Lengths," [Online]. Available: <http://www.misumi-europe.com/shop-uk/eu/ItemDetail/10300266030.html>. [Accessed 10 August 2013].
- [44] Dyneema, «Product Technologies,» [En línea]. Available: <http://www.dyneema.com/emea/product-technologies.aspx#sthash.3wGUyQEs.dpuf>. [Último acceso: 15 October 2014].
- [45] Asco Valvet, «Solenoid Valves,» *Engineering Information*, pp. 463-488, 2014.
- [46] FESTO, «Piezo valves in medical technology and laboratory automation,» 2011. [En línea]. Available: <https://www.google.de/url?sa=t&rct=j&q=&esrc=s&source=web&cd=1&cad=rja&uact>

=8&ved=0CDQQFjAA&url=http%3A%2F%2Fwww.festo.com%2Fnet%2Fen-in\_in%2FSupportPortal%2FDownloads%2F251418&ei=kc1QVOSNLMnxaKf3gPgM&usg=AFQjCNFG8AkDn2rDtLFscNbKz1s1Fs\_mhA&sig2=g51eXixA19. [Último acceso: 23 September 2014].

- [47] J. Rantala y J. Raisamo, «Tactile sensing & feedback,» Finland, 2011.
- [48] M. Grusin, "Flex Sensor 2.2" - Small Retail," 09 August 2011 . [Online]. Available: <https://www.sparkfun.com/tutorials/270>. [Accessed 23 July 2014].
- [49] N. A. a. S. Administration, «Anthropometry and Biomechanics,» de *Man-Systems Integration Standards*, vol. I.
- [50] lasersintering.com, «Available Laser Sintering Materials,» 2014. [En línea]. Available: <http://www.lasersintering.com/sls-material.php>. [Último acceso: 22 September 2014].
- [51] Arduino, «Arduino Micro,» [En línea]. Available: <http://arduino.cc/en/Main/arduinoBoardMicro>. [Último acceso: 15 September 2014].
- [52] Interlink Electronics. Inc, «FSR 400 Datasheet,» [En línea]. Available: <http://dlnmh9ip6v2uc.cloudfront.net/datasheets/Sensors/ForceFlex/2010-10-26-DataSheet-FSR400-Layout2.pdf>. [Último acceso: 12 September 2014].
- [53] Houghton Mifflin Company, «The American Heritage® Dictionary of the English Language,» 2009. [En línea]. Available: <http://www.thefreedictionary.com/radius>. [Último acceso: 10 September 2014].
- [54] Encyclopedia Britannica, Inc, "muscles of the forearm: posterior view," 2008. [Online]. Available: <http://www.britannica.com/EBchecked/media/121138/Muscles-of-the-forearm>. [Accessed 21 July 2014].

- [55] M. Iwak, Hasegawa, Yasuhisa y Y. Sankai, «Study on wearable system for daily life support using McKibben pneumatic artificial muscle,» *The 2010 IEEE/RSJ International Conference on*, pp. 3760-3675, 18 October 2010.
- [56] McGovern and Bill, "CPM Helps Patients Regain Motion Before Strength," [Online]. Available: <http://www.arthroscopy.com/sp06004.htm>. [Accessed 14 October 2014].
- [57] Saunders, "Dorland's Medical Dictionary for Health Consumers," 2007. [Online]. Available: <http://medical-dictionary.thefreedictionary.com/Ulnar>. [Accessed 10 September 2014].
- [58] «Gelenke Zeichnung01.jpg,» 24 September 2005. [En línea]. Available: [http://commons.wikimedia.org/wiki/File:Gelenke\\_Zeichnung01.jpg](http://commons.wikimedia.org/wiki/File:Gelenke_Zeichnung01.jpg). [Último acceso: 1 October 2014].
- [59] Houghton Mifflin Company, The American Heritage® Dictionary of the English Language, Fourth ed., Houghton Mifflin Company, 2009.
- [60] Walkabout.com, "Sizing: Gloves," [Online]. Available: [http://www.walkabout.com/shop/size\\_glove.asp](http://www.walkabout.com/shop/size_glove.asp). [Accessed 1 October 2014].
- [61] P. Ingraham, «Massage Therapy for Tennis Elbow and Wrist Pain,» 2012. [En línea]. Available: <http://saveyourself.ca/articles/spot-05-forearm-extensors.php>. [Último acceso: 1 October 2014].
- [62] K. Corcoran, «Give yourself a hand,» 13 November 2012. [En línea]. Available: [http://anatomy4fitness.blogspot.de/2012\\_11\\_01\\_archive.html](http://anatomy4fitness.blogspot.de/2012_11_01_archive.html). [Último acceso: 10 October 2014].
- [63] K. An, L. Askew and E. Chao, "Biomechanics and functional assessment of upper extremities," in *Ergonomics/Human Factors III*, North-Holland., Elsevier Science Publishers, B.V., 1986.

- [64] N. Tsagarakis y D. Caldwell, «Development and Control of a ‘Soft-Actuated’ Exoskeleton for Use in Physiotherapy and Training,» *Autonomous Robots*, nº 15, p. 21–33, 2003.
- [65] E. B. Brokaw, I. Black, R. J. Holley and P. S. Lum, "Hand Spring Operated Movement Enhancer (HandSOME): A Portable, Passive Hand Exoskeleton for Stroke Rehabilitation," *IEEE Transactions on Neural Systems and Rehabilitation Engineering*, vol. IX, no. 4, pp. 391-399, 2011.
- [66] M. DiCicco, L. Lucas y Y. Matsuoka, «Comparison of control strategies for an EMG controlled orthotic exoskeleton for the hand,» *IEEE International Conference on Robotics and Automation*, vol. II, pp. 1622-1627, 2004.
- [67] M. L. Newport, «Early Repair of Extensor Tendon Injuries,» de *Hand Surgery 1st Edition*, Lippincott Williams & Wilkins, 2004, p. 738.
- [68] S. Ueki, H. Kawasaki, S. Ito, Y. Nishimoto, M. Abe, T. Aoki, Y. Ishigure, T. Ojika and T. Mouri, "Development of a Hand-Assist Robot With Multi-Degrees-of-Freedom for Rehabilitation Therapy," *IEEE/ASME Transactions on Mechatronics*, vol. XVII, no. 1, pp. 136-146, 2012..
- [69] ganfyd.org, "Flexor digitorum superficialis," 25 December 2007. [Online]. Available: [http://www.ganfyd.org/index.php?title=Flexor\\_digitorum\\_superficialis](http://www.ganfyd.org/index.php?title=Flexor_digitorum_superficialis). [Accessed 1 October 2014].
- [70] H. F. Gray, *Anatomy of the Human Body*, Twentieth ed., Philadelphia and New York: Lea & Febiger, 1918.
- [71] F. J. R. Johansson R, «Coding and use of tactile signals from the fingertips in object manipulation tasks,» *Nature Reviews / Neuroscience*, pp. 345-359, 2009.

## **A. Appendixes**

### **A.1. Glossary**

All the terms are taken from: [53].

*Carpal:* A bone of the *carpus*.

*Carpus:* The group of eight bones forming the joint between the forearm and the hand. Also called wrist.

*Intrinsic:* situated within or peculiar to a part.

*Kinesiology:* the branch of physiology that studies the mechanics and anatomy in relation to human movement

*Radial:* related to the side of to the radius, which is a bone extending from the elbow to the wrist on the same side to the thumb in humans

*Ulnar:* related to the side of to the Ulna, which is a bone extending from the elbow to the wrist on the side opposite to the thumb in humans.

*Volar Plate:* A tough ligamentous band bridging the volar aspect of the proximal interphalangeal joint in fingers II-V and opposing hyperextension. Rupture of the volar plate due to injury or disease permits recurrent hyperextension and can lead to swan-neck deformity.

## A.2. Used Equations

$$\theta_{DIP} = \frac{2}{3} \cdot \theta_{PIP} \quad (4-1)$$

$$V = \frac{\pi}{4} (18mm)^2 \cdot 177mm = 4,5041 \times 10^{-5} m^3 \quad (4-2)$$

$$n = \frac{6bar \cdot [4,5041 \times 10^{-5} m^3]}{(273,15 + 20)K \cdot 8,3144621(75) \cdot 10^{-5} m^3 \cdot bar \cdot K \cdot mol^{-1}} = 1,10875 \times 10^{-2} mol \quad (4-3)$$

$$m_{CO_2} = 1,10875 \times 10^{-2} mol \cdot \frac{44,01 g}{mol} = 0,4880 g \quad (4-4)$$

$$m_{air} = 1,10875 \times 10^{-2} mol \cdot \frac{28,9645 g}{mol} = 0,32114 g \quad (4-5)$$

$$s(R_x) = \frac{V_{cc} \cdot R_f \max}{R_f \max + R_x} - \frac{V_{cc} \cdot R_f \min}{R_f \min + R_x} \quad (4-6)$$

$$\frac{ds}{dR_x} = V_{cc} \left( \frac{60k\Omega}{(R_x + 60k\Omega)^2} - \frac{25k\Omega}{(R_x + 125k\Omega)^2} \right) = 0 \quad (4-7)$$

$$V_{ref-p} = 5 \cdot \left[ \frac{100k\Omega}{100k + (150k\Omega + 6,2k\Omega)} \right] = 1,9516V \quad (4-8)$$

$$V_{out} = (V_{sense} - V_{ref}) \cdot \left[ \frac{2R_f}{R_g} + 1 \right] \quad (4-9)$$

$$A_G = \left[ \frac{2(100k)}{(51k\Omega + 3,9k\Omega)} + 1 \right] = 4,6430 \quad (4-10)$$

$$V_{out} = (V_{sense} - 1,9516) \cdot 4,6430 \quad (4-11)$$

$$\frac{1}{2\pi \cdot 1k\Omega \cdot 0,1\mu F} = 1,6kHz \quad (4-12)$$

$$\frac{\text{Input}}{\text{Resolution}} = \frac{5}{2^{10} - 1} = 4,89 \frac{mV}{bit} \quad (4-13)$$

$$LB = 6,96mV \cdot \frac{1bit}{4,89mV} = 2 \quad (4-14)$$

$$d_c = e \cdot kp + 0,5 \quad (5-1)$$

$$V_{pressure} = 5 - V_{release} \quad (B-1)$$

## **B. Annexes**

### **B.1. Electronic Control of the VEAA 3/3 Piezo-valves**

As it can be seen in the black dotted square in Figure B-1, regarding the power interface, a push pull configuration driver is use for controlling each side of the valve.

A second order low pass RC filter (green dotted square in Figure B-1) is used as a Digital to Analog Converter (DAC) with the PWM signal. The cut off frequency is 159Hz.

Two operational amplifiers are used in order to isolate the impedances between the controller and the valve. One of those operational amplifiers has a reference value of 5V for achieving the complementary signal for simultaneously operate the exhausting and pressure side of the valve.

The mathematical function of such Op.Amp (red dotted square in Figure B-1), for the complementary control of the push pull drivers of both sides of the valve is presented in Equation (B-1), where  $V_{pressure}$  is the input of the pressure side and  $V_{release}$  is the filtrated and low impedance signal from the first Op. Amp for the release side.

$$V_{pressure} = 5 - V_{release}$$

**(B-1)**

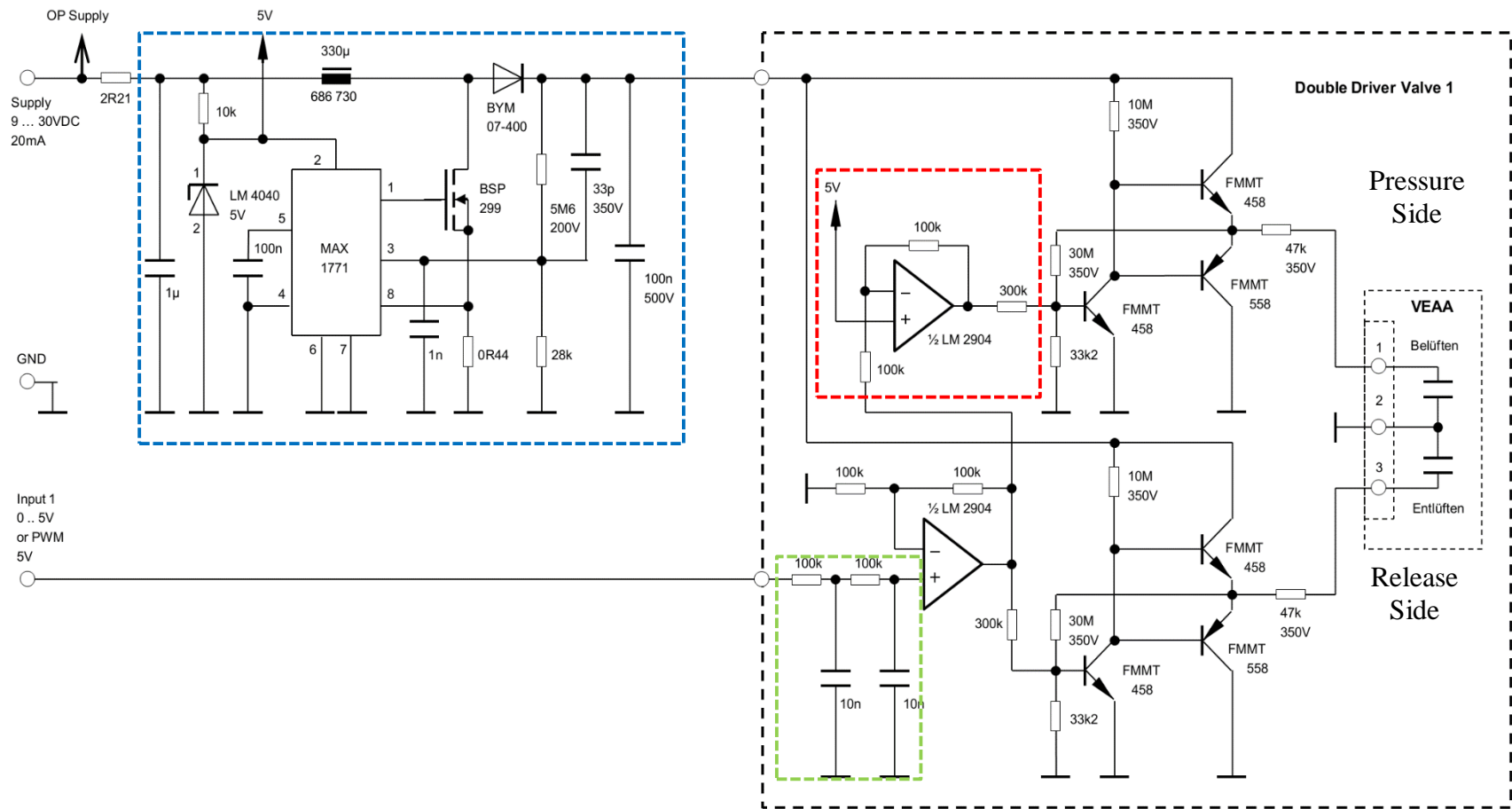


**Figure B-1.** VEAA 5 Way Control Circuit. Developed by Dipl. Ing. Hannes Wirtl, Festo Piezo Valves Division

## B.2. Characterization of the Valve-Muscle System.

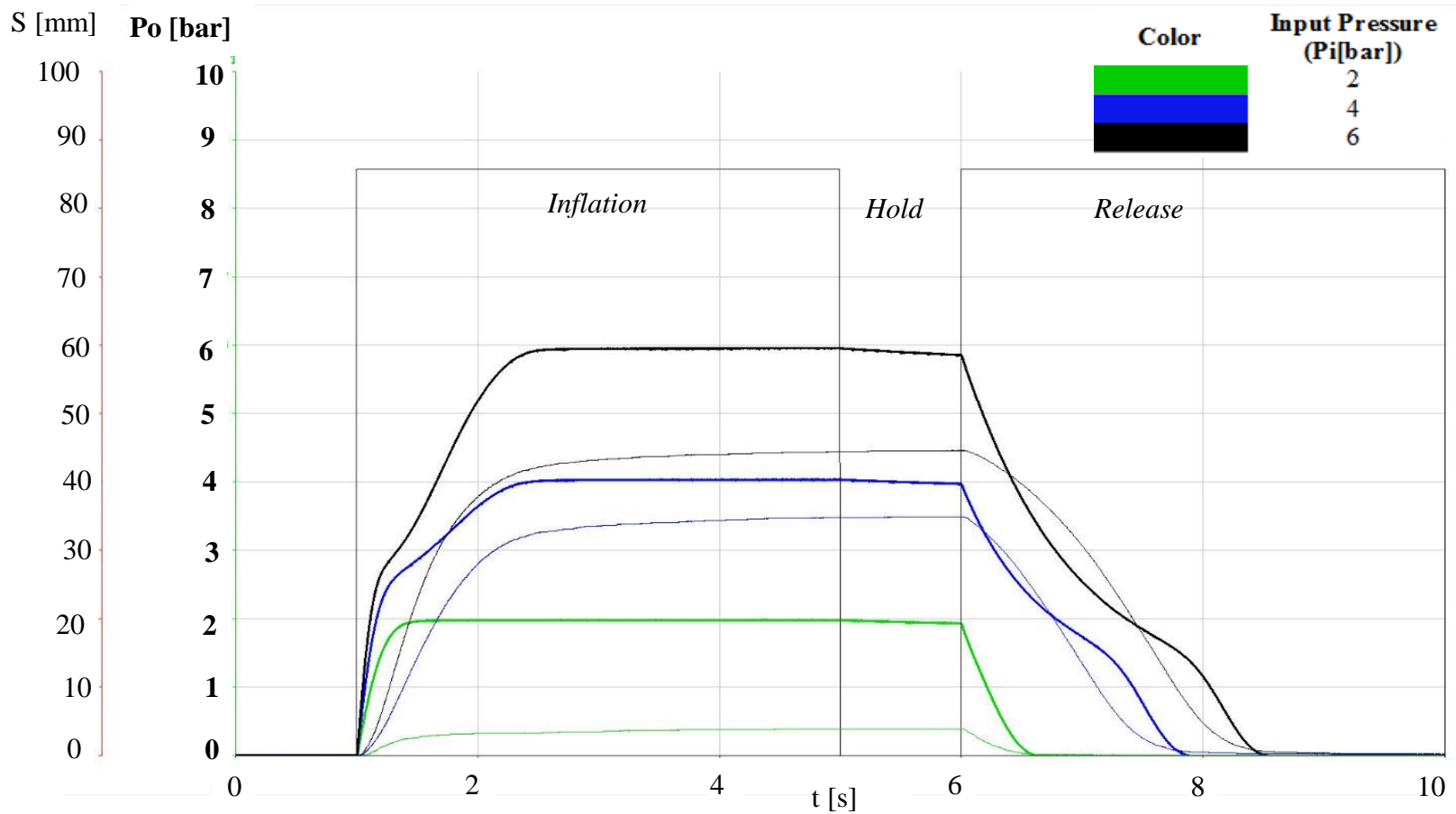


**Figure B-2.** Output Pressure ( $P_o$ ) and Muscle Stroke ( $S$ ) for Different Input Pressures ( $P_i$ )<sup>19</sup>. Experiment conducted in Festo Ag & Co.

<sup>19</sup> Bold lines are for  $P_o$  and normal lines are for  $S$ .

## B.3. Components Datasheets

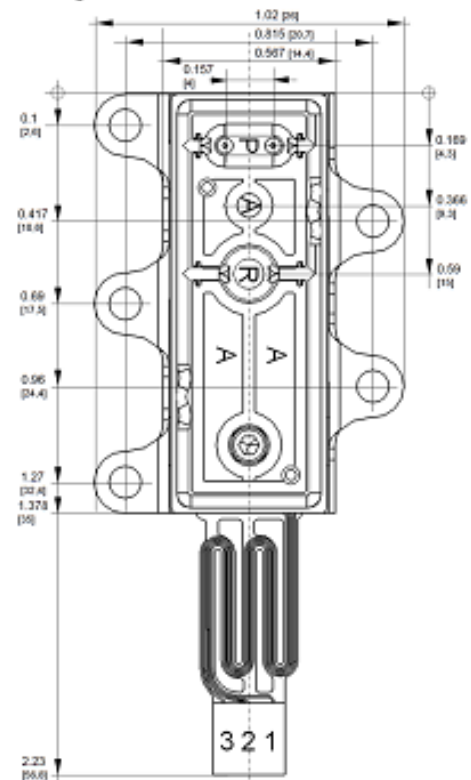
### B.3.1. Piezoelectric Flow Proportional Valve

#### Specification VEAA

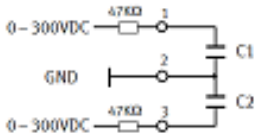
General data	Value
Valve principle	Piezo bender - soft sealing
Valve function	3/3way closed middle position proportional flow valve
Connection	Flange
Operating temperature	41°F ... 104°F (5°C ... 40°C)
Storage temperature	-4°F ... 158°F (-20°C ... 70°C)
Response time	< 5ms @ 10% input pressure
Service life	>10mio cycles

Pneumatic data	Value
Media	Air, Oxygen, inert gases
Input pressure	-14psig ..175psig,
Nominal width	P-side 0,3mm; R-Side 0,3mm
Flow	3/3way Pressure side [P → A]: 15lpm@160psi 8,5lpm@87psi  Exhaust side: [A → R]: 11lpm@160psi 7,5lpm@87psi  (see diagram)
Leakage	< 0,6l/h @ 100psig

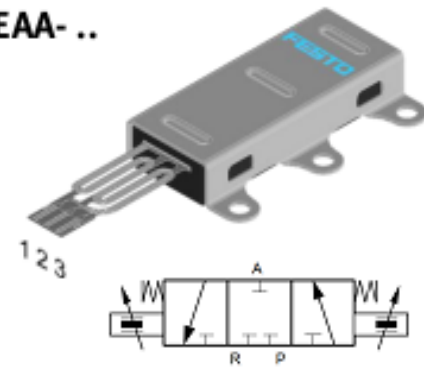
VEAA- ..



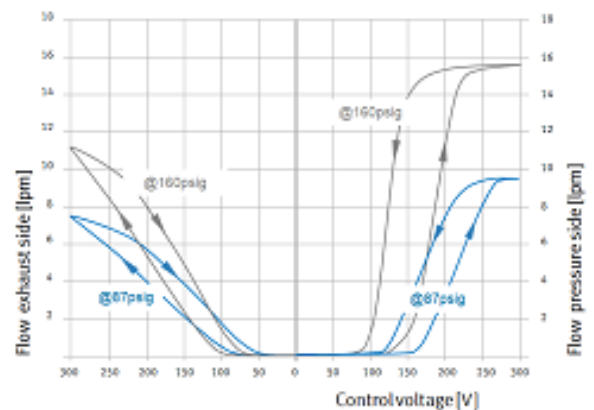
### Specification VEMC

Electrical data	Value
Operation voltage	0 ... 300VDC in serial with a 47KΩ resistor
Permitted charge current	5,5mA typical - 10mA max.
Capacitance	23nF ± 20% (typical) each side
Switching energy	< 4mWs
Contacts	Pin1 = Pressure side Pin2 = GND Pin3 = Exhaust side
Interface	ZIF connection: 3-pin, 2 mm pitch → plug to be used: 1 mm pitch, 5-pin  

VEAA- ..



Mechanical data	Value
Body material	PZT carbon fibre reinforced ceramics, Polyarylamide, Polyimid, NBR, Epoxy, stainless steel, gold, Acrylated Urethane glue, PUR varnish, Oxygen grease
Dimensions	Valve body: Height: 0,27in / 7mm Width: 0,567in / 14,4mm Length: 1,378in / 35mm
Weight	4g (60gr) without plug and manifold
Mounting	M2,5 screws
Footprint	See dimensional sketch



### B.3.2. Flex Sensor 5.9cm



## FLEX SENSOR FS

*Special Edition Length*

### Features

- Angle Displacement Measurement
- Bends and Flexes physically with motion device
- Possible Uses
  - Robotics
  - Gaming (Virtual Motion)
  - Medical Devices
  - Computer Peripherals
  - Musical Instruments
  - Physical Therapy
- Simple Construction
- Low Profile

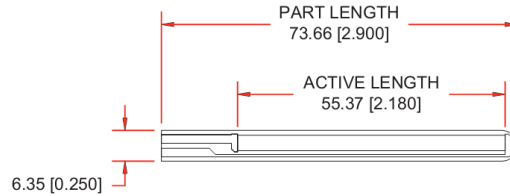
### Mechanical Specifications

- Life Cycle: >1 million
- Height:  $\leq 0.43\text{mm}$  (0.017")
- Temperature Range:  $-35^{\circ}\text{C}$  to  $+80^{\circ}\text{C}$

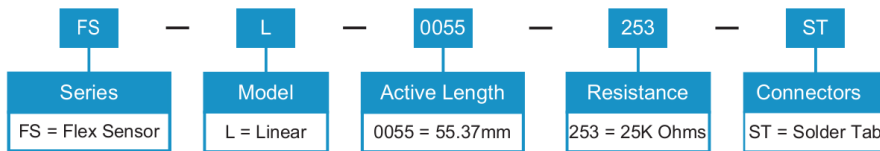
### Electrical Specifications

- Flat Resistance: 25K Ohms
- Resistance Tolerance:  $\pm 30\%$
- Bend Resistance Range: 45K to 125K Ohms (depending on bend radius)
- Power Rating : 0.50 Watts continuous. 1 Watt Peak

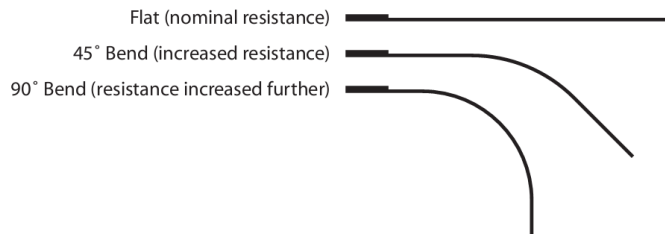
### Dimensional Diagram - Stock Flex Sensor



### How to Order - Stock Flex Sensor



### How It Works



## B.3.3 Force Sensor

#### Features and Benefits

- Actuation Force as low as 0.1N and sensitivity range to 10N.
- Easily customizable to a wide range of sizes
- Highly Repeatable Force Reading; As low as 2% of initial reading with repeatable actuation system
- Cost effective
- Ultra thin; 0.35mm
- Robust; up to 10M actuations
- Simple and easy to integrate

#### Industry Segments

- Game controllers
- Musical instruments
- Medical device controls
- Remote controls
- Navigation Electronics
- Industrial HMI
- Automotive Panels
- Consumer Electronics

#### Description

Interlink Electronics FSR™ 400 series is part of the single zone Force Sensing Resistor™ family. Force Sensing Resistors, or FSRs, are robust polymer thick film (PTF) devices that exhibit a decrease in resistance with increase in force applied to the surface of the sensor. This force sensitivity is optimized for use in human touch control of electronic devices such as automotive electronics, medical systems, and in industrial and robotics applications.

The standard 400 sensor is a round sensor 7.62mm in diameter. Custom sensors can be manufactured in sizes ranging from 5mm to over 600mm. Female connector and short tail versions can also be ordered.



Figure 1 - Typical Force Curve

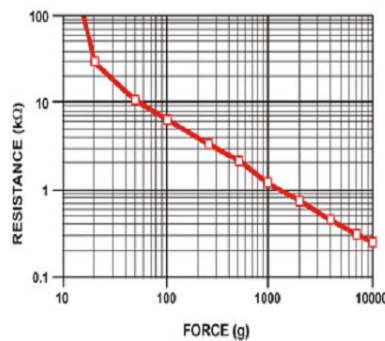
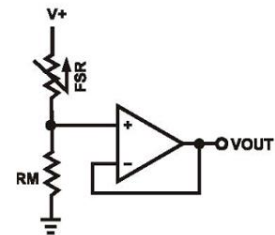


Figure 2 - Typical Schematic



Interlink Electronics - Sensor Technologies

## Applications

### Detect & qualify press

Sense whether a touch is accidental or intended by reading force

### Use force for UI feedback

Detect more or less user force to make a more intuitive interface

### Enhance tool safety

Differentiate a grip from a touch as a safety lock

### Find centroid of force

Use multiple sensors to determine centroid of force

### Detect presence, position, or motion

Of a person or patient in a bed, chair, or medical device

### Detect liquid blockage

Detect tube or pump occlusion or blockage by measuring back pressure

### Detect proper tube positioning

### Many other force measurement applications

## Device Characteristics

Feature	Condition	Value*	Notes
Actuation Force		0.1 Newtons	
Force Sensitivity Range		0.1 - 10.0 <sup>2</sup> Newtons	
Force Repeatability <sup>3</sup>	(Single part)	± 2%	
Force Resolution <sup>3</sup>		continuous	
Force Repeatability <sup>3</sup>	(Part to Part)	±6%	
Non-Actuated Resistance		10M W	
Size		7.62mm diameter	
Thickness Range		0.2 - 1.25 mm	
Stand-Off Resistance		>10M ohms	Unloaded, unbent
Switch Travel	(Typical)	0.05 mm	Depends on design
Hysteresis <sup>3</sup>		+10%	$(R_{F+} - R_{F-})/R_{F+}$
Device Rise Time		<3 microseconds	measured w/steel ball
Long Term Drift		<5% per log <sub>10</sub> (time)	35 days test, 1kg load
Temp Operating Range	(Recommended)	-30 - +70 °C	
Number of Actuations	(Life time)	10 Million tested	Without failure

\* Specifications are derived from measurements taken at 1000 grams, and are given as one standard deviation / mean, unless otherwise noted.

1. Max Actuation force can be modified in custom sensors.
2. Force Range can be increased in custom sensors. Interlink Electronics have designed and manufactured sensors with operating force larger than 50Kg.
3. Force sensitivity dependent on mechanics, and resolution depends on measurement electronics.

### B.3.4 Lilypad Blue Pixel



YETDA INDUSTRY LTD.

### Technical Data Sheet

MODEL NO : S150ANB4-H

1206Package 3.2\*1.6mm Chip LEDs

Features :

- Package in 8mm tape on 7" diameter reel
- Compatible with automatic placement equipment
- Compatible with reflow solder process

Applications :

- Indicators
- Automotive : backlighting in dashboard and switch
- Backlight for LCD

Dice material	Emitted color	Lens Color
InGaN	Blue	Water Clear

Electrical/Optical Characteristics(Ta=25°C)

Parameter	Symbol	Condition	Min	Typ.	Max	Unit
Luminous Intensity	Iv	IF=20mA		250		md
Dominant Wavelength	$\lambda_D$	IF=20mA		470		nm
Peak Emission Wavelength	$\lambda_p$	IF=20mA		472		nm
Viewing Angle	$2\theta_{1/2}$	IF=20mA		130		Deg
Forward Voltage	Vf	IF=20mA		3.2	3.8	V
Reverse Current	IR	VR=5V			10	$\mu A$

Absolute Maximum Ratings(Ta=25°C)

Parameter	Symbol	Maximum	Unit
Power Dissipation	Pd	78	mW
Peak Forward Current (1/10 Duty Cycle 0.1ms Pulse Width)	IF(Peak)	100	mA
Continuous Forward Current	IF	30	mA
Reverse Voltage	VR	5	V
Derating Linear From 25°C		0.3	mW/°C
Operating Temperature Range	Topr	-30 to +80	°C
Storage Temperature Range	Tstg	-40 to +90	°C

20090727



## **B.4. Project Datasheet**

### **Student information:**

**Name:** Jacob Hernández Sánchez

**Passport ID:** 3 0463 0119

**Matr.-Nr. ITCR:** 201054413

**Address:** 25 m N and 50 m W from the NW side of Fello Meza Stadium, Cartago, Costa Rica.

**Cellphone:** (+506)85339896/(+506)88655348/ (+49)152202379141

**Email:** jacob.hernandez@ipa.fraunhofer.de

### **Project Details:**

**Name of the Project:** “Bio-inspired Mechatronic Design for the Actuation of a Soft Orthosis for Rehabilitation and Assistance of Hands”

#### ***Institute Info:***

**Name:** Fraunhofer Institute for Manufacturing Engineering and Automation (Fraunhofer IPA)

**Main Activity:** Applied Sciences Research and Development.

**Exact Address:** Nobelstr. 12. 70569 Stuttgart. Germany

### **Supervisors Data:**

**Name:** Dr.ner.nat. Oliver Schwarz

**Position:** Group Leader

**Department:** Biomechatronic Systems

**Major:** MBA **Academic Degree:** Dr.rer.net

**Tel:** + 49 711 970-3754

**Email:** Oliver.Schwarz@ipa.fraunhofer.de

**Name:** Dipl.-Ing. Conrad Hochberg

**Position:** Research Fellow

**Department:** Biomechatronic Systems

**Major:** Mechanical Engineer **Academic Degree:** Diplom (equivalent to Master's)

**Tel:** +49 711 970-3713

**Email:** [conrad.hochberg@ipa.fraunhofer.de](mailto:conrad.hochberg@ipa.fraunhofer.de)